Functional characterization of Modified Vaccinia Virus Ankara-encoded anti-apoptotic proteins

Dissertation

zur Erlangung des Grades

“Doktor der Naturwissenschaften”

am Fachbereich Biologie

der Johannes Gutenberg-Universität Mainz

Markus Lantermann

geboren in Groß-Gerau

Mainz, April 2009

Danksagungen

An erster Stelle möchte ich mich bei [redacted] für die Ermöglichung und Begutachtung dieser Dissertation bedanken.

Ich danke Herrn [redacted] für die Möglichkeit der Anfertigung meiner Dissertation in seiner Forschungsgruppe am Paul-Ehrlich-Institut, für die wissenschaftliche Unterstützung sowie vieler Tipps und Anregungen, die er mir in den letzten Jahren zukommen ließ. Natürlich bedanke ich mich auch für die Begutachtung dieser Arbeit.

Frau [redacted] danke ich für die Betreuung und die kritische Auseinandersetzung mit meiner Arbeit, die mich oft zu neuen Sichtweisen diverser Problemstellungen führte.

Frau [redacted] sei gedankt für ihren kritischen und weiterführenden Blick auf meine Arbeit und ihre Unterstützung wann immer ich sie brauchte.

Nicht genug danken kann ich [redacted] für zahllose bereichernde Gespräche, Ideen und Kritik. Danke dass du immer da warst, wenn ich mal Hilfe gebraucht habe.

Danke an alle Kollegen der Abteilung Virologie des Paul-Ehrlich-Instituts für ihre fachliche Hilfe und eine kurzweilige Zeit: [redacted]

Der größte Dank gilt meiner Familie und meiner [redacted] ohne deren Liebe, Verständnis und Unterstützung ich meinen bisherigen Weg nicht so hätte beschreiten können, wie er hinter mir liegt.

Contents

Contents	I
Abbreviations	VI
1 Summary	**1**
2 Introduction	**3**
2.1 Poxviruses	**3**
2.1.1 Taxonomy of the *poxviridae*	3
2.1.2 Structure and genomic organization	4
2.1.3 Viral life cycle	5
2.2 Modified Vaccinia Virus Ankara	**8**
2.2.1 Generation of MVA	8
2.2.2 Genome structure and viral gene expression profile	8
2.3 MVA-induced immune responses	**9**
2.4 MVA-encoded inhibitors of apoptosis	**10**
2.4.1 Apoptotic pathways	11
2.4.2 Vaccinia virus anti-apoptotic protein F1	12
2.4.3 The structural bcl-2 homologue N1	13
2.5 MVA-encoded immunoregulatory gene functions	**15**
2.5.1 The interferon-resistance gene E3L as immune regulator	15
2.6 Aim of the thesis	**17**
3 Materials	**19**
3.1 Chemicals	**19**
3.2 Biochemicals	**20**
3.3 Anesthesia	**21**
3.4 Buffers and solutions	**21**
3.5 Kits	**24**
3.6 Enzymes	**24**
3.7 Synthetic oligonucleotides (Primers)	**25**

3.8 Synthetic oligonucleotides (siRNA) 26
3.9 Plasmids 27
3.10 Synthetic peptides 27
3.11 Antibodies 27
3.12 Flourescent dyes 29
3.13 Viruses 29
3.14 Cell lines 30
3.15 Bacteria 30
3.16 Animals 30
3.17 Media 31
3.18 Consumables 32
3.19 Laboratory equipment 33

4 Methods 35
4.1 Cloning procedures using *Escherichia coli* 35
4.1.1 Transformation of plasmid-DNA into competent *E. coli* 35
4.1.2 Plasmid purification from *E. coli* for analytical purpose (Mini-prep) 35
4.1.3 High yield plasmid purification from *E. coli* (Maxi-prep) 35
4.2 Cell culture 36
4.2.1 Cell culture conditions and cell split 36
4.2.2 Transient transfection of small interfering RNAs and plasmid DNA 36
4.3 Virological methods 37
4.3.1 *In vitro* virus infections 37
4.3.2 Generation of recombinant MVA 37
4.3.2.1 Infection and transfection of CEF cells 37
4.3.2.2 Transient host-range selection of recombinant virus clones on RK13 cells 38
4.3.2.3 Selection of K1L-free virus clones 38
4.3.2.4 Amplification and purification of virus clones 38
4.3.2.5 Virus titration 39
4.4 DNA analysis 39
4.4.1 DNA sequencing 39
4.4.2 Analytical gel electrophoresis 39
4.4.3 DNA purification from agarose gels 39

4.4.4 Restriction enzyme digestion 40
4.4.5 Determination of DNA concentration 40
4.4.6 Ligation 40
4.4.7 Preparation of DNA from vaccinia virus infected cells 40
4.4.8 Polymerase chain reaction (PCR) 41
4.5 RNA analysis 41
4.5.1 RNA-preparation 41
4.5.2 Determination of RNA concentration 42
4.5.3 RNA gel electrophoresis 42
4.5.4 Northern blot 42
4.5.5 Construction of DIG-labeled RNA-probes 43
4.5.6 Functional control of generated DIG-labeled RNA-probes 43
4.5.7 Hybridization of membrane-bound RNA with DIG-labeled RNA probes 44
4.5.8 Detection of RNA/RNA-hybrids 44
4.6 Protein analysis 45
4.6.1 Generation of vaccinia virus-specific antibodies 45
4.6.1.1 Anti-F1 antibody 45
4.6.1.2 Anti-N1 antibody 45
4.6.2 Immunostain of vaccinia virus-infected cells 45
4.6.3 Western blot 46
4.6.3.1 Preparation of cell lysates 46
4.6.3.2 Sodium dodecyl sulphate polyacrylamide gel electrophoresis (SDS-PAGE) 46
4.6.3.3 Wet-transfer of proteins 46
4.6.3.4 Immunodetection of proteins on PVDF membranes 47
4.6.3.5 Immunodetection of proteins on nitrocellulose membranes using the Li-Cor detection system 47
4.6.4.6 Stripping of PVDF and nitrocellulose membranes 48
4.6.4 [^{35}S]-metabolic labelling of proteins 48
4.6.5 FACS analysis of virus-induced apoptosis 48
4.6.6 β-galactosidase enzyme activity assay 49
4.6.6.1 Preparation of cell lysates 49
4.6.6.2 Determination of protein yield 49

4.6.6.3 β-galactosidase enzyme activity assay 50
4.7 *In vivo* and *ex vivo* analysis 50
4.7.1 Immunization of mice 50
4.7.2 Blood serum withdrawal 50
4.7.3 Determination of MVA-specific antibody titers 50
4.7.4 Quantification of vaccinia virus-specific T cell responses 51
4.7.4.1 Preparation of splenocytes 51
4.7.4.2 Determination of splenocyte cell count 51
4.7.4.3 Vaccinia virus-specific stimulation and staining of splenocytes 51
4.7.5 Analysis of protective capacity against a lethal ectromelia virus challenge 52
4.8 Statistical analysis 53

5 Results 54
5.1 Impact of the anti-apoptotic vaccinia virus protein F1 on MVA immunogenicity 54
5.1.1 Molecular characterization of MVAΔF1L 54
5.1.2 MVAΔF1L induces apoptosis in murine cells 56
5.1.3 Induction of humoral immune responses by MVAΔF1L 58
5.1.4 MVAΔF1L immunization effectively primes VACV-specific T-cell responses 59
5.1.5 Protective capacity of MVAΔF1L against lethal poxvirus infections 62
5.2 Functional characterization of the N1L open reading frame encoded by MVA 66
5.2.1 Generation and characterization of MVA variants encoding for different N1 proteins 66
5.2.1.1 Plasmids used for the generation of recombinant MVA with modified N1L ORF 66
5.2.1.2 Generation of MVAΔN1L 68
5.2.1.3 Generation of revertant viruses MVA-N1L$_{rev}$ and MVA-WRN1L$_{rev}$ 70
5.2.1.4 Growth analysis of recombinant MVA 73
5.2.1.5 Anti-apoptotic function of N1 75
5.2.1.6 N1L expression after viral infection 76

5.2.2 Expression of N1 variants after transfection 78
5.2.2.1 Construction of plasmids expressing N1 variants 78
5.2.2.2 Expression of N1 variants 79
5.3 Influence of the double-stranded RNA-binding protein E3 on the cellular RNA interference pathway 81
5.3.1 SiRNA-mediated downregulation of a vaccinia virus-encoded marker gene 81
5.3.1.1 Downregulation of lacZ-expression early after MVA-infection 81
5.3.1.2 Downregulation of lacZ-expression during late stages after infection 83
5.3.2 SiRNA-mediated gene knock-out of the E3L gene product induces phenotypic alterations in the MVA life cycle 86

6 Discussion 88
6.1 MVAΔF1L efficiently provides protective immunity against lethal orthopoxvirus challenge 88
6.2 The vaccinia virus N1 protein is presumably non-functional in MVA 91
6.3 The vaccinia virus double-stranded RNA-binding protein E3 does not interfere with siRNA-mediated gene silencing in mammalian cells 93
6.4 Concluding remarks – Outlook 95

7 Literature 96

Curriculum vitae – deleted in the electronical version

Erklärung 103

Abbreviations

APC	Antigen presenting cell
Bcl	B-cell lymphoma
BH3	B-cell lymphoma 2-homology domain 3
BHK	Baby hamster kidney
bp	Base pairs
BSA	Bovine serum albumin
CD	Cluster of differentiation
CEF	Chicken embryo fibroblast
CVA	Chorioallantois vaccinia virus Ankara
DNA	Deoxyribonucleic acid
dsDNA	Double-stranded DNA
e.g.	*Exempli gratia* – for example
ECTV	Ectromelia virus
ELISA	Enzyme linked immunosorbent assay
EV	Extracellular virion
FCS	Fetal calf serum
GFP	Green fluorescent protein
HEK	Hyman embryonic kidney
i.m.	intramuscular
i.n.	Intranasal
ICS	Intracellular cytokine stain
ITR	Inverted terminal repeat
IV	Immature virion
kb	Kilo base pairs
kDa	Kilo Dalton
KLH	Keyhole limpet hemocyanin
LD	Lethal dose
MEF	Murine embryonic fibroblast
MHC	Major histocompatibility complex
mRNA	Messenger RNA
MV	Mature virion
MVA	Modified vaccinia virus Ankara

n.s.	Not significant
ORF	Open reading frame
pAPC	Professional antigen presenting cell
PCR	Polymerase chain reaction
pfu	Plaque forming units
PKR	Protein kinase R
pNpp	p-nitrophenyl phosphate
PO	peroxidase
RISC	RNA-induced silencing complex
RK	Rabbit kidney
RNA	Ribonucleic acid
RNAi	RNA interference
rRNA	Ribosomal RNA
s.d	Standard deviation
SDS-PAGE	Sodium dodecyl sulphate polyacrylamide gel electrophoresis
SEM	Standard error of the mean
siRNA	Short interfering RNA
SPF	Specific pathogen free
WB	Western blot
WR	Vaccinia virus Western Reserve
WV	Wrapped virion

The most exciting phrase to hear in science, the one that heralds new discoveries, is not

“Eureka” (I found it) but “That´s funny…”

Isaac Asimov (1920 – 1992)

1 Summary

Candidate vaccines based on the highly attenuated orthopoxvirus strain MVA are tested against various infectious and cancer diseases and, more profound, vaccines based on wildtype and recombinant viruses have been found safe and immunogenic in clinical trials. Favourable properties of MVA vaccines such as replication deficiency, avirulence and immunostimulatory capacity with adjuvant activity have been early attributed to the particular genetic make-up of the MVA virus. Indeed, compared to conventional vaccine strains like Lister or Wyeth, MVA lacks many functional genes for potentially important regulators of virus-host interactions. However, some gene functions responsible for counteraction of cellular antiviral pathways are still conserved in the genome of MVA and the inhibition of apoptosis seems to be one important mechanism, the virus is still able to interact with.

Vaccinia viruses encode several proteins which prevent the induction of virus-induced apoptosis. The vaccinia virus anti-apoptotic protein F1 for example was shown to inhibit Bak and Bax activation, thereby counteracting the activation of the mitochondrial pathway of apoptosis in a highly effective manner. Another vaccinia virus protein, N1, which was implicated as a strong virulence factor *in vivo*, like F1 shows structural and functional similarity to members of the cellular anti-apoptotic bcl-2 family and was also shown to inhibit apoptosis. The vaccinia virus early protein E3 inhibits programmed cell death by binding to and sequestration of dsRNA molecules, normally inducing cellular antiviral pathways also driving the induction of apoptosis. All three anti-apoptotic genes were functionally analyzed during this work.

The vaccinia virus ORF F1L is highly conserved between different orthopoxvirus strains and is also encoded by MVA. In this work, the impact of the apoptosis-inhibiting protein F1 on MVA-induced immune responses was analyzed by examining vaccinia virus-specific T- and B-cell responses as well as protection against a lethal poxvirus challenge, using an MVA vaccine with a deleted F1L gene (MVAΔF1L). Immunization of C57BL/6 mice with MVAΔF1L leads to amounts of vaccinia virus-specific primary $CD8^+$ and $CD4^+$ T cell as well as antibody responses comparable to that of wild type MVA. Furthermore, immunization of C57BL/6 mice with MVA leads to protective immunity against a lethal orthopoxvirus challenge, independently of the presence of the anti-apoptotic protein F1.

The N1L gene in the genome of MVA shows an unnatural 3´ sequence caused by a genomic deletion during the MVA attenuation process. This mutation could possibly lead to unfunctionality due to an altered C-terminus in the protein. Here, the functionality of this ORF was analyzed in the background of viral infection as well as after transient transfection of plasmid-encoded N1L variants. It was found that the MVA-related N1L gene is efficiently transcribed in MVA-infected cells but the protein is rapidly degraded in a proteasome-dependent manner supporting the mean of a loss of N1 function in MVA-infected cells. In contrast, the natural WR-derived ORF was expressed into a stable protein. N1 proteins lacking one ore two distinct c-terminal domains were also only detectable in the presence of proteasome inhibition. Therefore, the natural 3´ sequence of the N1L ORF is fundamentally needed to generate a stable and functional N1 protein.

The dsRNA-binding activity of E3 could possibly lead to an inhibition of the cellular RNA interference pathway mediated by small dsRNA molecules (siRNA). During this work, it could be shown that expression of an MVA-encoded marker gene (β-galactosidase) can be efficiently inhibited by lacZ-specific siRNA independently of the presence of E3 protein. Both vaccinia virus early and late gene expression could be decreased by siRNA. Furthermore, downregulation of the expression of the E3L gene itself by siRNA in MVA-infected cells produced the phenotype of an E3L knock-out virus lacking late gene expression, which illustrates the possibility of siRNA as screening procedure for vaccinia virus gene function analysis.

The results obtained in this work contribute to the understanding of the complicated poxvirus-host network, especially concerning the role of virus-induced apoptosis. The findings can finally be beneficial for defining specificities of MVA as a vector vaccine candidate.

2 Introduction

2.1 Poxviruses

The *poxviridae* family consists of complex animal viruses with double-stranded DNA genomes, which are able to infect mammals, birds and insects. Several poxviruses have the ability to infect humans, mostly as zoonotic infections transmitted from animal hosts. The causative agent of the highly lethal human smallpox disease, the variola virus (*variola major*), is strictly restricted to the human species, a fact enabling the eradication of this eldest known infectious disease. Edward Jenner demonstrated in 1796 that scarification of the skin with poxviruses closely related to variola (members from the orthopoxvirus genus, e.g. cowpox virus or vaccinia virus – see chapter 2.1.1) leads to protection against the human smallpox disease. He called this method "vaccination", a term which is still used in our days to describe the immunization of animals and humans to protect them from distinct infectious diseases. In the year 1958 the *World Health Organization* initiated a global immunization program using cowpox virus and vaccinia virus, resulting in the eradication of the human smallpox disease as declared in 1980.

2.1.1 Taxonomy of the *poxviridae*

The poxvirus family is divided into the two sub-families *chordopoxvirinae* and *entomopoxvirinae,* based on vertebrates and insects as host organisms, respectively. They are further classified in eight (*chordopoxvirinae)* and three (*entomopoxvirinae)* genera, comprising several virus species (Table 2.1). The members within each genus are closely related genetically and show similarities in morphology and host tropism. Variola virus and vaccinia virus, both members of the orthopoxvirus genus, belong to the most extensively studied members of the poxvirus family.

Table 2.1: Taxonomy of the *poxviridae*

Sub-family	Genus	Virus species (examples)
Chordopoxvirinae	Orthopoxvirus	variola, vaccinia, ectromelia, cowpox, monkeypox, camelpox
	Parapoxvirus	pseudocowpox, orf, sealpox, bovine papular stomatitis
	Avipoxvirus	fowlpox, canarypox, pigeonpox, penguinpox, crowpox
	Capripoxvirus	goatpox, lumpy skin disease, sheeppox
	Leporipoxvirus	myxoma, rabbit fibroma, squirrel fibroma
	Suipoxvirus	swinepox
	Molluscipoxvirus	molluscum contagiosum
	Yatapoxvirus	tanapox, yaba monkey tumor
Entomopoxvirinae	Alphaentomopoxvirus Betaentomopoxvirus Gammaentomopoxvirus	poxviruses of beetles, butterflies, dipters and their larvae

Modified from Damon, 2007

2.1.2 Structure and genomic organization

Poxvirus virions are large compared to other known animal viruses. The brick-shaped virion particles are about 300 x 200 x 100 nm in size making them visible even under light microscopic conditions. Different infectious virion variants are produced during the viral life cycle (see chapter 2.1.3), distinguished mainly by the number and composition of the membranes surrounding the viral core, which contains the viral genome. Additionally, two prominent lateral bodies are found on both sides of the viral core.

The genome of poxviruses consists of a large double-stranded DNA (dsDNA) molecule of 130 000 to 300 000 base pairs (bp) encoding for about 150 to 200 genes, depending on the virus strain. Both ends of the viral genome are covalently closed, with identical sequences in reverse orientation on both sides, denoted as inverted terminal repeats (ITR, Figure 2.1C) (Garon et al., 1978). The ITRs can vary in length due to repetitions, deletions and different numbers of short tandem sequences in the different virus strains (Wittek and Moss, 1980).

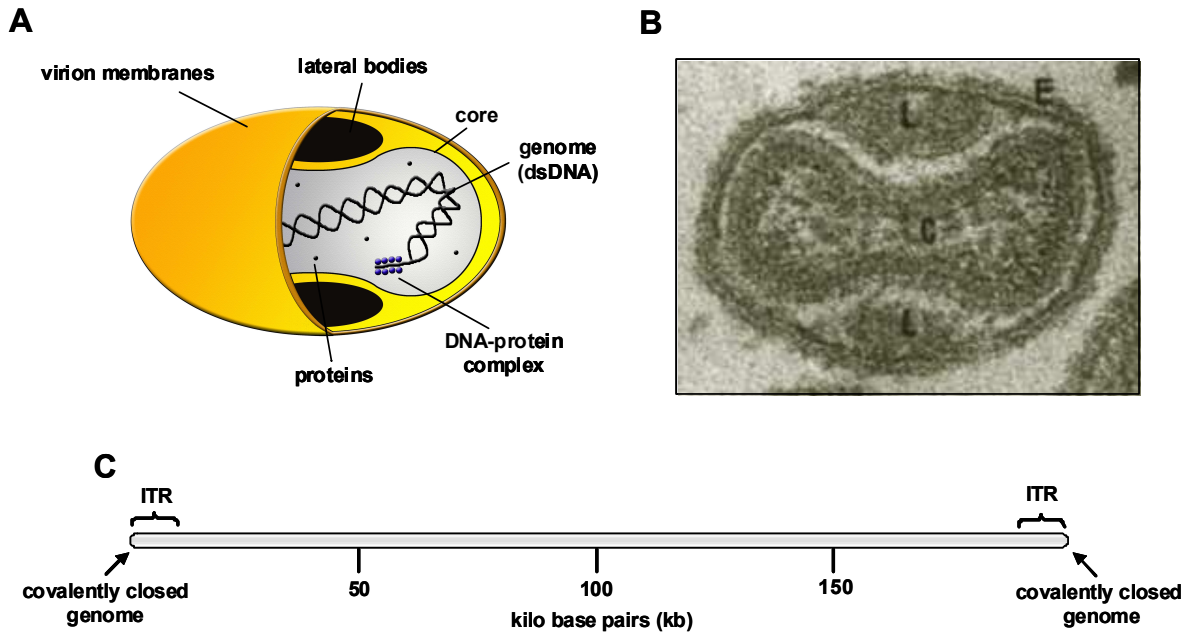

Figure 2.1: The structure of poxviruses. A Schematic view of an intracellular poxvirus virion. Detailled description in the text. **B** Electron micrograph of an intracellular vaccinia virus virion. C: core, L: lateral body, E: external membrane, from Pogo and Dales, 1969. **C** Schematic structure of the vaccinia virus genome. Both inverted terminal repeats at the covalently closed ends of the genome are shown. The size of the genome is denoted in kilo base pairs (kb) - modified from Baroudy et al., 1982.

The genome is mapped by digestion using the restriction endonuclease *Hin*dIII, which in the case of vaccinia virus leads to 16 DNA-fragments, termed alphabetically in regard of the size from A to P, with A being the biggest and P being the smallest fragment. The open reading frames in the fragments are numbered and the reading direction is designated by an R (rightwards) or L (leftwards). Another prominent characteristic of poxvirus genomes is the central localization of genes essential for viral replication and morphogenesis whereas genes encoding proteins responsible for virus-host-interactions and immunomodulation are often localized at the ends of the genome. The former genes are normally highly conserved in contrast to the latter ones, showing some heterogeneity in sequence between different poxvirus strains.

2.1.3 Viral life cycle

The poxvirus replication cycle is described here exemplified by the life cycle of vaccinia virus, the prototype member and most extensively characterized virus species among all orthopoxviridae (Moss, 2007).

Poxviruses replicate exclusively in the cytoplasm of the infected cell and the tightly regulated steps of the replication cycle are shown schematically in Figure 2.2.

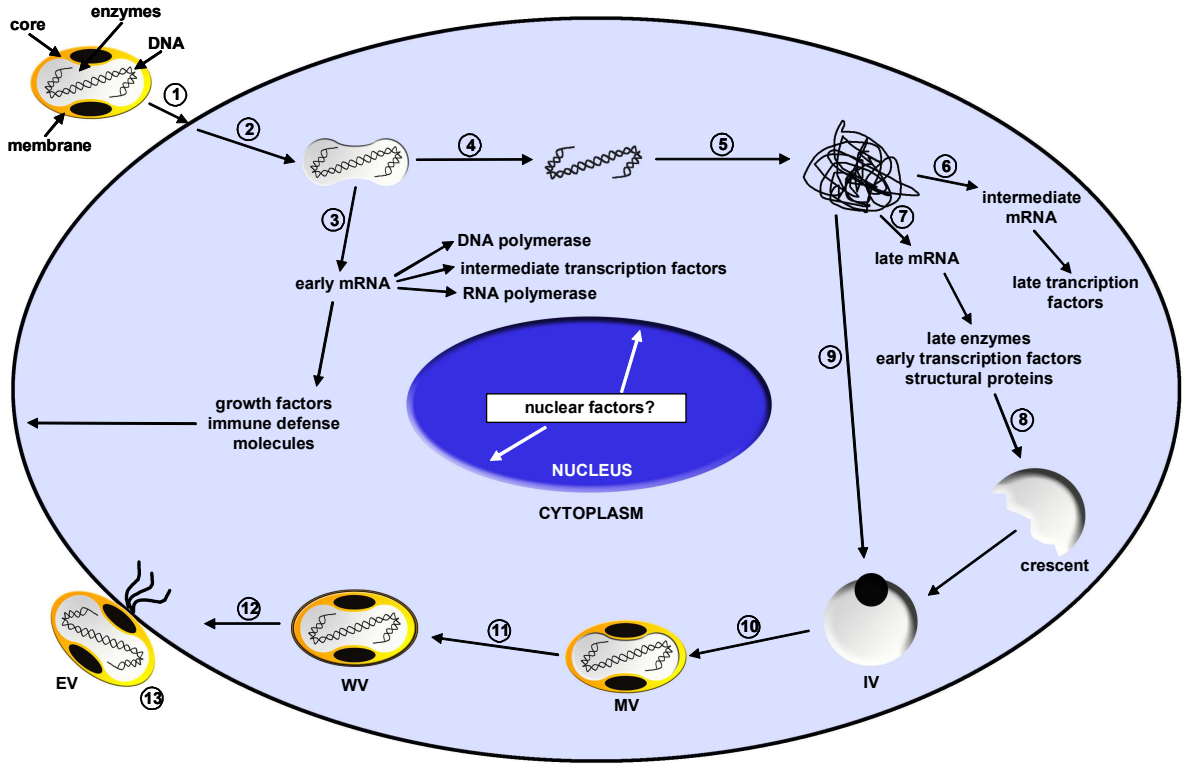

Figure 2.2: Replication cycle of the *poxviridae*. Schematic view of the vaccinia virus replication cycle. Detailed descriptions of single events are given in the text. IV: immature virion; MV: mature virion; WV: wrapped virion; EV: extracellular virion

The life cycle of vaccinia virus begins with the attachment of the virion particle to the cellular plasma membrane (1). Although the cellular receptor is not known precisely, the involvement of glycosaminoglycans for virus entry has been described under certain conditions (Carter et al., 2005). After attachment and fusion with the plasma membrane, the viral core is released into the cytoplasm of the host cell (2). At this step, the cascade-like gene expression pattern is initiated. Early gene expression starts within minutes after infection (3), very rapidly followed by the release of the viral DNA molecule (4). The poxvirus early gene class encodes gene products responsible for immune modulation, the viral RNA- and DNA-polymerase and transcription factors needed for the initiation of intermediate gene expression. After DNA replication (5), expression of the intermediate class of genes takes place, mainly encoding transcription factors for the late class of genes (6), which in turn encode structural gene products and enzymes needed for early transcription in a new infection round (7). During the

complete replication cycle, each gene class is responsible for initiating the expression of the upcoming class by encoding specific transcription factors. In return, the upcoming expression of one class is responsible for the transcriptional shutdown of the former class (Figure 2.3). The structural proteins finally assemble with discrete membrane structures (8), in which one DNA unit is packaged to form an immature virion (IV; 9). After a further maturation step, the first form of an infectious virion is built (10). This mature virion (MV) is wrapped in the trans-golgi network to gain additional membrane layers, then denoted as wrapped virion (WV; 11). WVs are then transported along the microtubule network towards the periphery of the cell (12), where fusion of the most outer viral envelope with the plasma membrane takes place. These extracellular virions (EV), now wrapped by two membrane layers, are either released from the cell or remain attached at the cell membrane (13). Attached EVs induce the polymerization of actin tails to expose the virion particles, which seems to be an efficient mechanism to infect neighbouring cells. Although the whole replication cycle takes place exclusively in the cytoplasm of infected cells, some nuclear and cytoplasmic cellular factors have already been described to be involved in transcription and morphogenesis.

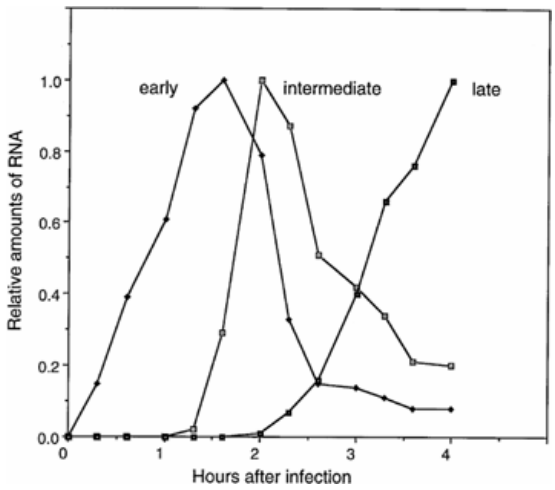

Figure 2.3: Cascade-like organization of poxvirus gene transcription. Relative amounts of viral mRNA derived from a typical early, intermediate and late gene, respectively, depicted against time after infection of HeLa cells with vaccinia virus. From Moss, 2007.

A further characteristic of the vaccinia virus life cycle represents the very rapid shut-off of host cell macromolecular synthesis. Very early after infection, the cellular protein synthesis ceases to background levels, the amount and timeline of which seems to be dependent on different viral factors as well as the infectious dose and type of cell.

2.2 Modified Vaccinia Virus Ankara

The highly attenuated vaccinia virus strain modified vaccinia virus Ankara (MVA) belongs to the orthopoxvirus genus of poxviruses and has been derived from a vaccine strain formerly used in turkey, which was renamed to chorioallantois vaccinia virus Ankara (CVA) after its transfer to Germany.
MVA was subsequently used as poxvirus vaccine in over 120 000 individuals without causing the side effects often recognized when immunization was performed with replication competent vaccinia virus strains, even in immunocompromised persons (Mayr et al., 1978). Due to its very good safety profile and immunogenicity (see chapter 2.3), MVA is now being developed as a third generation smallpox vaccine as well as vector vaccine against different infectious and cancer diseases (Frey et al., 2007; Hawkridge et al., 2008).

2.2.1 Generation of MVA

In order to develop a more attenuated vaccine strain for smallpox immunizations, the precursor of MVA, the CVA, was repeatedly passaged on chicken embryo fibroblasts (CEF) (Mayr et al., 1975). During over 570 passages in cell culture virus replication adapted to the chicken cells as host and the virus finally lost the ability to replicate in most cells of mammalian origin, including human cells (Meyer et al., 1991; Carroll and Moss, 1997). This attenuation was caused by extensive genomic alterations, resulting in the deletion of large parts of the viral genome and mutations of many genes not fundamentally needed for replication on CEF cells (see chapter 2.2.2).

2.2.2 Genome structure and viral gene expression profile

The genomic alterations found in MVA include six major deletions, several smaller ones and numerous point mutations, accounting for the loss of about 15% or 30 kb of genomic information compared to the parental CVA strain (208 kb in CVA compared to 178 kb in MVA – Figure 2.4 and Meyer et al. 1991). Many genes responsible for immunomodulation and host range, located mainly at the ends of the double-stranded DNA genome, were deleted

during this process, in contrast to genes essential for virus replication lying in the more conserved middle regions of the genome.

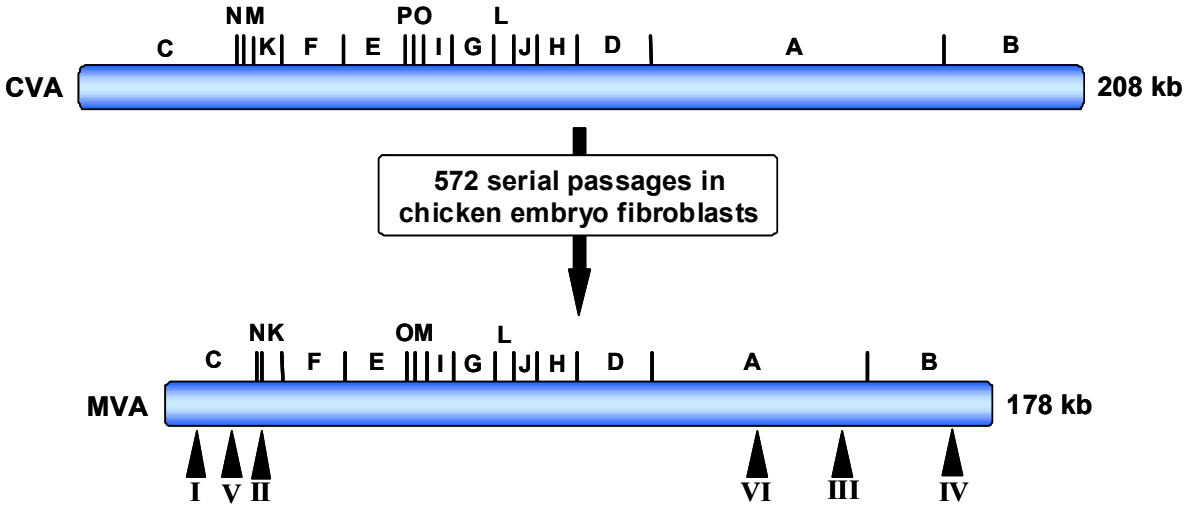

Figure 2.4: Attenuation process leading to MVA. Schematic view of the dsDNA genomes of the chorioallantois vaccinia virus Ankara (CVA; upper scheme) and the modified vaccinia virus Ankara (MVA; lower scheme). The *Hin*dIII nomenclature of both virus genomes is depicted above, the positions of the six major deletions I to VI in MVA are shown below the scheme.

Some viral genes encoding proteins responsible for the modulation of a antiviral immune response are still functionally maintained in the MVA genome (McFadden, 2005; Antoine et al., 1998). Despite the block in the viral life cycle at the step of virion morphogenesis, all gene classes are efficiently expressed during these abortive infections (Sutter and Moss, 1992), making MVA a preferable vector for recombinant gene expression. Moreover, MVA offers the possibility to analyze vaccinia virus gene functions under low biosafety conditions.

2.3 MVA-induced immune responses

Infection of mice with vaccinia virus induces humoral and cellular immune responses, both playing a role for the development of immunologic memory against orthopoxvirus infection (Xu et al., 2004). However, vaccinia virus encodes many gene functions responsible for subverting different aspects of the antiviral response (Smith, 1999). For example, the B19R gene function is responsible for the inhibition of a virus-induced cellular type I interferon response after vaccinia virus infection. Because of the deletion of this open reading frame

during the attenuation process, MVA induces type I interferon responses *in vivo* (Waibler et al., 2007), presumably supporting innate and adaptive immune responses (Stetson and Medzhitov, 2006). Furthermore, MVA immunization leads to the development of a robust and long term immunity against viral and recombinantly expressed antigens (Sutter and Staib, 2003; Drexler et al., 2004; Perez-Jimenez et al., 2006).

MVA is being developed as a third generation smallpox vaccine and has been demonstrated very recently to be highly effective as therapeutic vaccine against a lethal ectromelia virus (ECTV) challenge in several mouse infection models. This protective capacity was even shown to be superior over standard vaccinia virus vaccine strains like Elstree (Samuelsson et al., 2008; Paran et al., 2009).

The stimulation of cytotoxic T cells by MVA occurs by direct presentation of antigens as well as by indirect presentation via the cross presentation pathway (Gasteiger et al., 2007; Liu et al., 2008). In particular, T cell priming seems to be dependent on the latter mechanism (Gasteiger et al., 2007). Cross presentation of vaccinia virus-encoded antigens requires the uptake of exogenous antigen by a subset of dendritic cells, for example from virus-infected cells undergoing apoptosis (Fonteneau et al., 2003). After uptake of apoptotic bodies, viral antigens are processed by these professional antigen presenting cells, finally leading to the MHC class I-dependent presentation of antigenic peptides on the cell surface to cytotoxic $CD8^+$ T cells (Ackerman and Cresswell, 2004; Monu and Trombetta, 2007). In addition to the induction of an effective adaptive cellular immune response, MVA immunization initiates a humoral immune response by inducing the production of long-lived antibody titers, directed against prominent virion surface antigens (Cosma et al., 2004).

2.4 MVA-encoded inhibitors of apoptosis

Programmed cell death, or apoptosis, is an important cellular mechanism of self-destruction with roles in development, tissue homeostasis and elimination of virus-infected cells (Hengartner, 2000). For efficient replication, numerous viruses have therefore developed molecules to subvert the induction of apoptosis. MVA also encodes some anti-apoptotic proteins responsible for inhibition of key components within the cellular apoptotic cascade (Taylor and Barry, 2006).

2.4.1 Apoptotic pathways

The initiation of apoptosis is very tightly regulated by different intracellular inducers and inhibitors of apoptosis, normally arranged in a very sensitive balance. Pro-apoptotic signals of diverse origin trigger the induction of at least one apoptotic signal transduction pathway, finally leading to the death of the cell (Taylor et al., 2008). A schematic view of the intracellular apoptotic events is given in Figure 2.5.

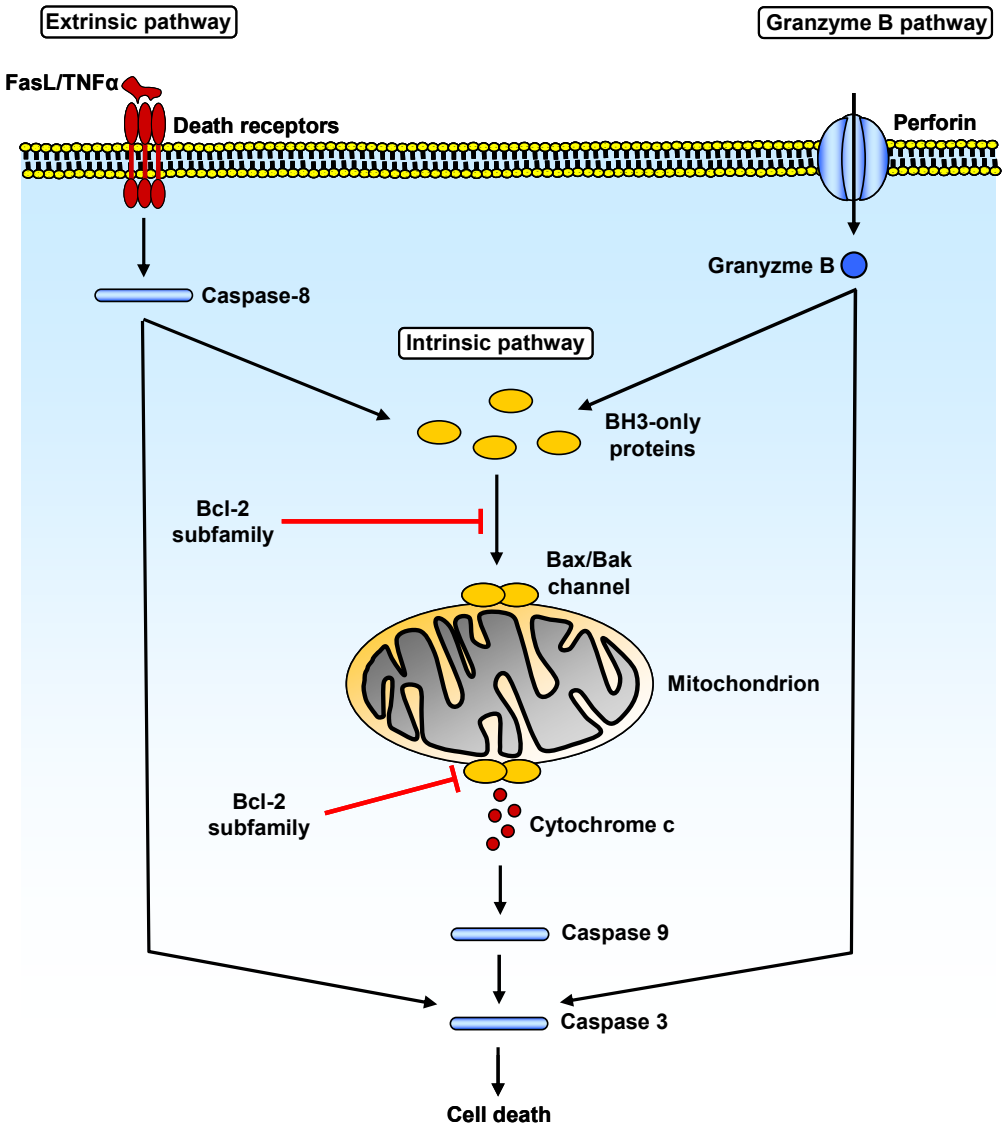

Figure 2.5: Schematic view of apoptotic signal transduction pathways. Detailed description of the apoptotic events are given in the text.

So far, there are three different apoptotic pathways known, distinguished mainly by the inducing pro-apoptotic signal (Figure 2.5). All pathways are able to converge at different points, finally leading to the activation of the main effector protease caspase-3.

Apoptotic pathways induced by extracellular stimuli very rapidly lead to the activation of caspase-3, either through the adapter caspase-8 or by direct activation. The mitochondrial pathway of apoptosis is induced by crosstalk with the extrinsic and/or granzyme b pathways or by diverse intracellular stimuli like cell stress, DNA damage or virus infection. The signals typically activate one or more pro-apoptotic BH3-only (B-cell lymphoma 2 [Bcl-2]-homology domain 3 only) molecules which themselves activate the mitochondrial effector molecules bax and bak. Activation of these molecules leads to the permeabilization of the outer mitochondrial membrane and the subsequent release of pro-apoptotic mediators like cytochrome c from the mitochondrial intermembrane space, finally leading to activation of caspase-3. Activated caspase-3 leads to many cellular apoptotic phenotypes finally resulting in cell death. All apoptotic pathways are tightly regulated by cellular molecules from the bcl-2 family. This family consists of pro- (BH3-only proteins) and anti-apoptotic (e.g. bcl-2, bcl-x_L) family members, which are responsible for the integration of pro- and anti-apoptotic signals.

2.4.2 Vaccinia virus anti-apoptotic protein F1

The vaccinia virus F1L gene encodes a ~26 kDa protein that is expressed during early phases of the viral life cycle and functions to inhibit the intrinsic mitochondrial pathway of apoptosis (Wasilenko et al., 2003). The protein possesses a C-terminal transmembrane domain and a signal sequence which targets the molecule to the outer mitochondrial membrane (Figure 2.6). F1 exerts its anti-apoptotic function by subverting the activation of the mitochondrial effector BH3-only proteins bak and bax (Wasilenko et al., 2005; Taylor et al., 2006), therefore inhibiting the release of pro-apoptotic factors like cytochrome c from the mitochondrial intermembrane space. For this purpose, the protein possesses an N-terminal BH3-like structure which is responsible for the binding to pro-apoptotic BH3-only molecules, like Bim and Bak, thereby inhibiting their function (Fischer et al., 2006; Postigo et al., 2006; Taylor et al., 2006).

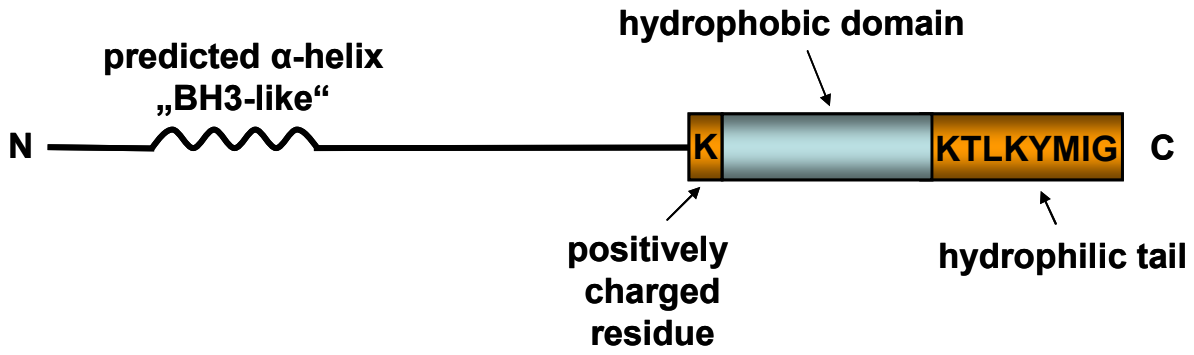

Figure 2.6: The vaccinia virus anti-apoptotic protein F1. Schematic view of the F1 protein encoded by the vaccinia virus ORF F1L. The hydrophobic transmembrane domain is flanked by charged lysine residues and a short C-terminal hydrophilic tail.

The F1L open reading frame is highly conserved between the genomes of MVA and the vaccinia virus strain Western Reserve (WR) and encodes a functional protein. Deletion of F1L from the MVA genome leads to an active viral induction of apoptosis after infection of human HeLa cells (Fischer et al., 2006). To elucidate the influence of F1 *in vivo*, different aspects of the MVA-induced adaptive immune response in the presence and absence of F1L gene function were analyzed in this work.

2.4.3 The structural bcl-2 homologue N1

The vaccinia virus N1L open reading frame encodes a ~14 kDa protein expressed early during the vaccinia virus replication cycle which severely contributes to virulence in several mouse models (Kotwal et al., 1989; Bartlett et al., 2002). Several hypothesis about the molecular function of N1 were supposed until the protein structure was resolved, revealing a bcl-2-like fold (Cooray et al., 2007). Since bcl-2 is an important cellular anti-apoptotic molecule (see chapter 2.4.1), a related function for N1 as a viral inhibitor of apoptosis was assumed.

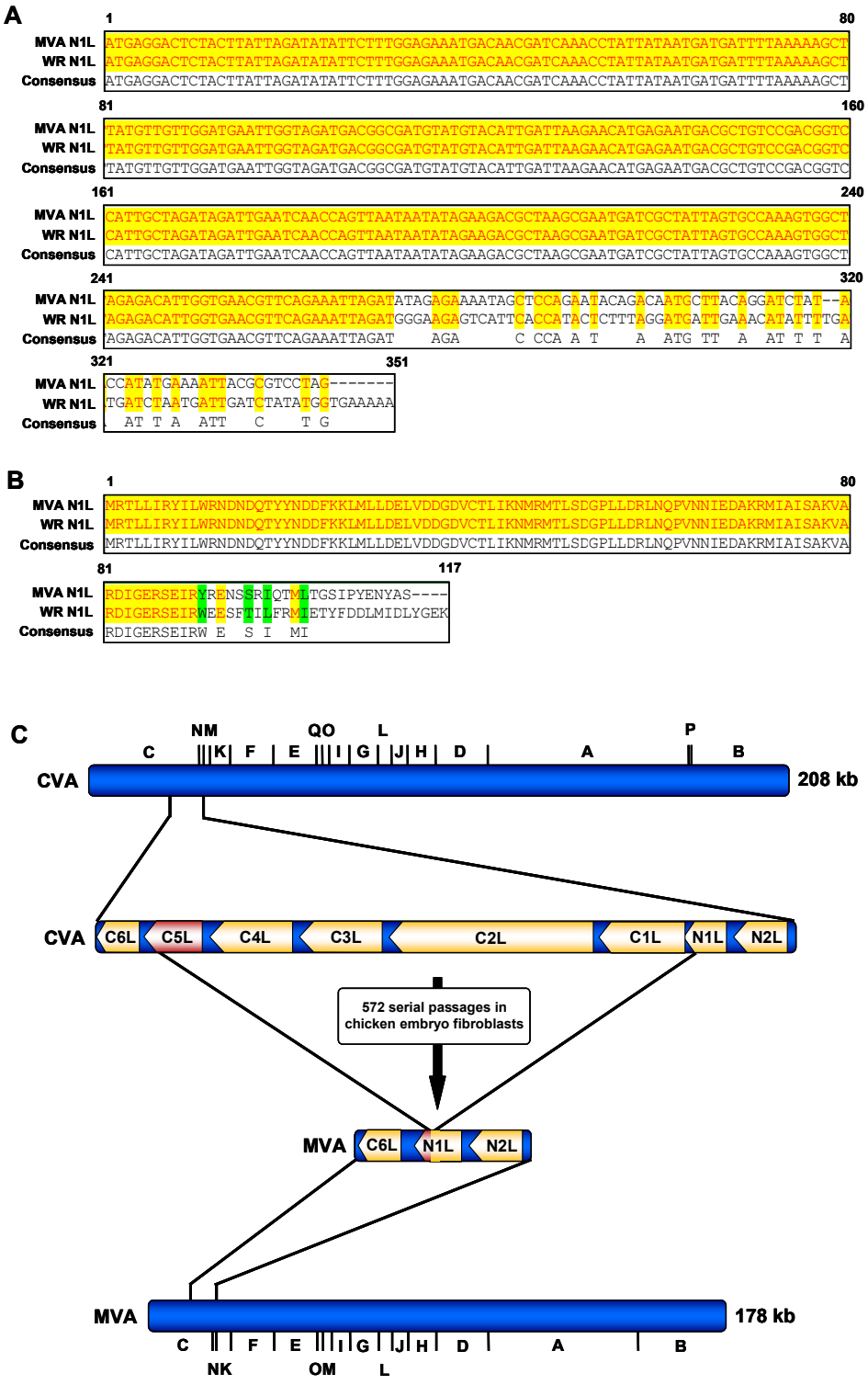

Figure 2.7: Fragmentation of the N1L open reading frame in MVA. A Sequence-alignment of the N1L ORFs from vaccinia virus strain MVA (upper) and Western Reserve (middle). Identical nucleotides are shown in yellow. **B** Protein sequence alignment of N1 encoded by MVA (upper) and WR (middle). Identical and similar amino acids are shown in yellow and green, respectively. **C** Schematic view of the CVA (above) and MVA (below) genomes. During the 572 passages in chicken embryo fibroblast cells a large in-frame deletion from the 5´ part of the C5L ORF to the 5´ part of the N1L ORF, leading to deletion V, occurred, generating a different N1L ORF consisting of parts derived from both N1L and C5L.

Indeed, after vaccinia virus infection of HeLa cells, N1 was able to inhibit the induction of apoptosis mediated by the addition of the potent apoptosis inducer staurosporine. Furthermore, N1 is able to bind to several cellular pro-apoptotic BH3-only molecules, thereby inhibiting their activation and the subsequent induction of apoptosis (Cooray et al., 2007). However, an apoptosis-inducing phenotype caused by the sole absence of N1 during a vaccinia virus infection, as in the case of the viral anti-apoptotic protein F1, was not discovered so far. In MVA, the N1L open reading frame is fragmented due to deletion of a large genomic fragment during the attenuation process (deletion V) ranging from the 5´ end of the N1L ORF to the 5´ end of the C5L ORF (Figure 2.7). This deletion was in-frame, generating a shortened but complete open reading frame encoding for a protein altered in its C-terminus.

2.5 MVA-encoded immunoregulatory gene functions

MVA, like vaccinia virus, has been demonstrated to be a potent inducer of cellular antiviral immune responses. However, some genes with immunomodulatory functions are still conserved between the genomes of MVA and its ancestor CVA (Antoine et al., 1998; Meisinger-Henschel et al., 2007), like the interferon-resistance gene E3L.

2.5.1 The interferon-resistance gene E3L as immune regulator

The vaccinia virus early protein E3, expressed by the conserved open reading frame E3L, possesses a C-terminal double-stranded RNA (dsRNA)-binding motif, which evolved to inhibit dsRNA-induced cellular antiviral responses by sequestering dsRNA molecules (Chang et al., 1992;Chang and Jacobs, 1993). DsRNA produced mainly during the late stages of a vaccinia virus infection initiates a program of drastic cellular responses which attempt to eliminate virus-infected cells. As the first response to dsRNA, the cell produces the antiviral effector molecules interferon-α and –β. This leads inter alia to the induction and activation of protein kinase R (PKR) and RNAseL, ultimately resulting in the inhibition of protein synthesis and apoptosis (Kibler et al., 1997). E3 was found to be responsible for inhibition of apoptosis, as deletion of the ORF from the genome of MVA results in the induction of

programmed cell death after infection of HeLa cells (Fischer et al., 2006). Even under permissive conditions, deletion of E3L from the genome of the replication competent vaccinia virus strain WR results in the induction of apoptosis after infection of HeLa cells (Lee and Esteban, 1994). Furthermore, the absence of E3L during an MVA infection leads to an incomplete replication cycle in normally permissive chicken embryo fibroblasts (CEF) and shows clear alterations in the viral life cycle in HeLa cells (Hornemann et al., 2003; Ludwig et al., 2005).

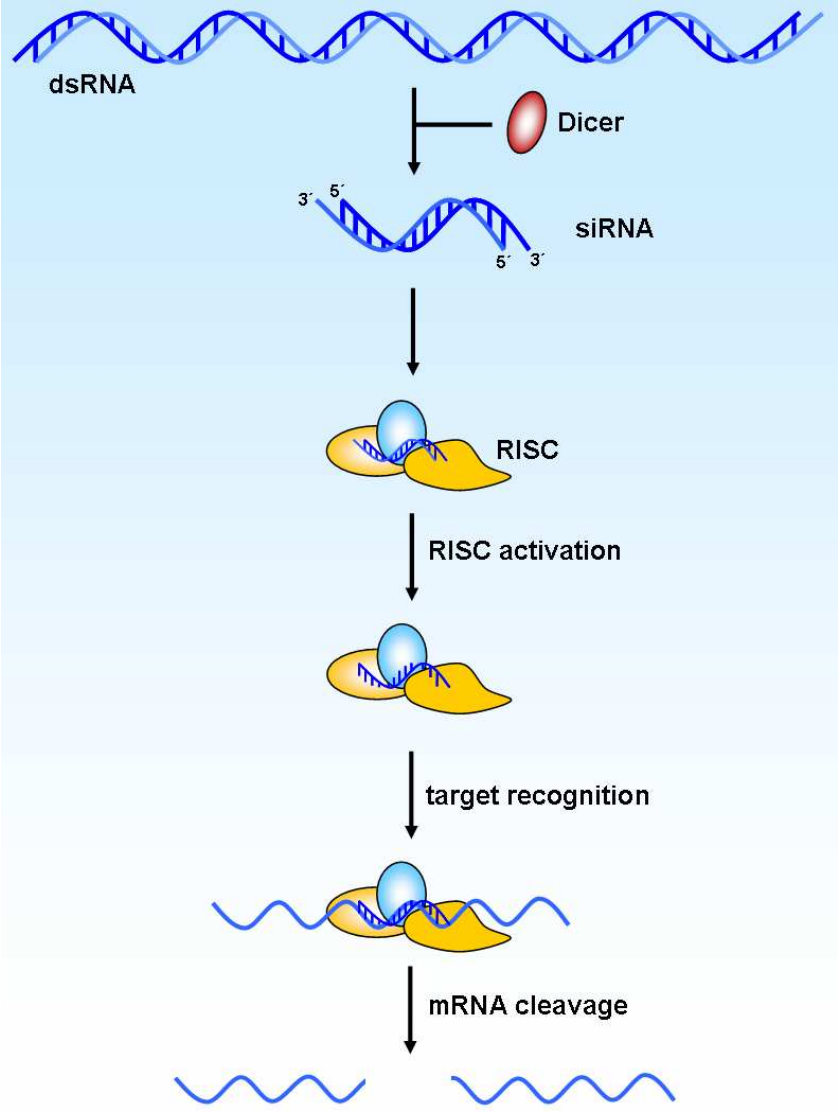

Figure 2.8: The cellular RNA-interference pathway. Long double-stranded (ds)RNA is cleaved by the RNase Dicer into 19-23 nucleotides long short interfering RNAs (siRNAs). These siRNAs, either generated by Dicer or directly transfected into cells are incorporated into the RNA-induced silencing complex (RISC). After unwinding of the siRNA duplex molecule, the single-stranded antisense RNA strand guides the enzyme complex to messenger RNAs with complementary sequence, resulting in cleavage of the target mRNA.

Due to the dsRNA-binding activity of E3 it was hypothesized that the protein also inhibits the RNA-interference (RNAi) pathway (Figure 2.8 , see also Dykxhoorn and Lieberman 2005 or Fire, 2007 for extensive reviews). Interaction of E3 with RNAi was shown after transient expression of the viral protein in insect cells (Li et al., 2004). However, this impediment was neither studied in mammalian cells nor in the context of a vaccinia virus infection where E3 has to bind the viral dsRNA in order to prevent the induction of cellular antiviral effector mechanisms. For this reason the inhibiting capacity of E3 on the RNA interference pathway was analyzed in this work.

2.6 Aim of the thesis

MVA is a good and safe candidate vaccine due to its potent immune stimulating capacity. However, the expression of remaining immunomodulatory and anti-apoptotic gene functions might still hamper an improved immune activation. During this work a possible impact of the anti-apoptotic genes F1L and N1L as well as the interferon-resistance gene E3L on MVA-induced immune activation should be analyzed. Furthermore, the molecular function of these proteins inside MVA-infected cells should be clarified.

The F1L gene encodes an early anti-apoptotic protein responsible for inhibition of the mitochondrial pathway of apoptosis. Since cross-presentation of viral antigens play an important role in the priming of an MVA-induced immune response (see chapter 2.3), and cross-presentation might be influenced by the induction of apoptosis in infected cells, deletion of F1L from the genome of MVA may alter the viral immune stimulating capacity. Therefore, the contribution of F1L to the *in vivo* immunogenicity of MVA should be analyzed in this work by comparing the induction of an adaptive immune response after immunization of mice with MVA-variants with an intact or deleted F1L ORF. Finally, the protective capacity of MVA immunization against a lethal orthopoxvirus challenge in an *in vivo* mouse model should be tested regarding the presence or absence of F1.

The gene N1L, encoding for the anti-apoptotic virulence factor N1, was found to be fragmented in the genome of MVA. Previous experiments showed that the MVA-related N1L ORF is transcribed after MVA infection (unpublished observation). In this work the expression and functionality of the MVA-N1L open reading frame should be further characterized and compared to the original “unmutated” vaccinia virus ORF, derived from the WR strain.

The vaccinia virus protein E3 possesses a dsRNA-binding activity, therefore potentially being able to inhibit cellular signal transduction pathways induced by dsRNA, like the RNA-interference (RNAi) pathway. By using siRNA directed against the mRNA of an MVA-encoded marker gene in the presence or absence of E3, the influence of the dsRNA-binding protein was elucidated in the background of viral infection of mammalian cells.

3. Materials

3.1 Chemicals

Product	Manufacturer
2-propanol	Merck (Darmstadt, Germany)
Acetone	Merck (Darmstadt, Germany)
Acrylamide/Bisacrylamide (30%)	Roth (Karlsruhe, Germany)
Ammonium persulfate	Sigma (Munich, Germany)
Bromochlorophenol blue	Merck (Darmstadt, Germany)
Butan/Propan gas	Camping Gaz (Hungen-Inheiden, Germany)
Chloroform	Merck (Darmstadt, Germany)
Di-sodium hydrogen phosphate	Merck (Darmstadt, Germany)
DMSO	Sigma (Munich, Germany)
Ethanol	Merck (Darmstadt, Germany)
Formaldehyde	Sigma (Munich, Germany)
Glycerol	Sigma (Munich, Germany)
Glycine	Sigma (Munich, Germany)
Hydrogen peroxide	Roth (Karlsruhe, Germany)
Isoamylalcohol	Merck (Darmstadt, Germany)
Lactacystin	Calbiochem (Darmstadt, Germany)
Lithium chloride	Sigma (Munich, Germany)
Low melt agarose	Peqlab (Erlangen, Germany)
Methanol	Merck (Darmstadt, Germany)
N-lauroylsarcosin	Sigma (Munich, Germany)
NP-40	Fluka (Neu-Ulm, Germany)
O-dianisidine	Sigma (Munich, Germany)
Phenol:chloroform:isoamyl alcohol	Sigma (Munich, Germany)
Potassium chloride	Merck (Darmstadt, Germany)
Potassium dihydrogen phosphate	Merck (Darmstadt, Germany)
Skim milk powder	Fluka (Neu-Ulm, Germany)
Sodium azide	Merck (Darmstadt, Germany)
Sodium carbonate	Merck (Darmstadt, Germany)

Sodium chloride	Merck (Darmstadt, Germany)
Sodium dodecyl sulfate	Fluka (Neu-Ulm, Germany)
Sodium hydrogen phosphate	Merck (Darmstadt, Germany)
Sodium hydroxide	Merck (Darmstadt, Germany)
Sucrose	Invitrogen (Karlsruhe, Germany)
TEMED	Sigma (Munich, Germany)
Tris	Merck (Darmstadt, Germany)
Triton X-100	Sigma (Munich, Germany)
Tween-20	Sigma (Munich, Germany)
Universal agarose	Peqlab (Erlangen, Germany)
Xylene cyanol	Merck (Darmstadt, Germany)

3.2 Biochemicals

Product	Manufacturer
Ampicillin	Sigma (Munich, Germany)
CDP Star	Roche (Mannheim, Germany)
Complete protease inhibitor cocktail	Roche (Mannheim, Germany)
DIG-Blocking solution	Roche (Mannheim, Germany)
DMEM medium	Biochrom (Berlin, Germany)
DNA ladders	NEB (Schwalbach, Germany)
FBS Superior	Biochrom (Berlin, Germany)
Fugene HD transfection reagent	Roche (Mannheim, Germany)
Isotone II diluent	Beckman Coulter (Krefeld, Germany)
L-glutamine	Biochrom (Berlin, Germany)
Lipofectamine 2000 transfection reagent	Invitrogen (Karlsruhe, Germany)
MEM (2x) medium	Gibco (Paisley, UK)
MEM-Earl medium	Biochrom (Berlin, Germany)
MESA buffer (powder)	Sigma (Munich, Germany)
PCR Mastermix	Roche (Mannheim, Germany)
Penicillin/Streptomycin	Lonza (Verviers, Belgium)
pNpp ready-to-use	Sigma (Munich, Germany)
Protein assay	BioRad (Munich, Germany)

Red blood cell lysing buffer	Sigma (Munich, Germany)
RPMI 1640 medium	Biochrom (Berlin, Germany)
SeeBlue Plus 2 prestained protein marker	Invitrogen (Karlsruhe, Germany)
Trizol	Invitrogen (Karlsruhe, Germany)
Trypsin	Lonza (Verviers, Belgium)
Western Blot blocking solution	Li-Cor (Bad Homburg, Germany)

3.3 Anesthesia

Product	Manufacturer
Isoflouran	Baxter (Unterschleißheim, Germany)
Ketamin/Xylazin	Bayer Vital (Leverkusen, Germany)

3.4 Buffers and solutions

Buffer	Composition
3M sodium acetate	3M sodium acetate
DEPC-H_2O	0,2% DEPC in H_2O
Dianisidine staining solution	450 µl saturated o-dianisidine in ethanol 15 ml PBS 15 µl H_2O_2 (shortly before usage)
EDTA	Diverse concentrations of EDTA
ELISA blocking buffer	PBS 10% FCS 0,05% Tween-20
ELISA coating buffer	70 mM $NaHCO_3$ 30 mM Na_2Co_3 pH 9,6

ELISA washing buffer	44,5 mM NaCl 0,3 mM KH_2PO_4 1,6 mM Na_2HPO_4 0,3 mM KCl 0,05% Tween-20
LB_{amp} Agar	1,5% Agar in LB-medium 100 ng/ml ampicillin
PBS	0,14 M NaCl 2,7 mM KCl 3,2 mM Na_2HPO_4 1,5 mM KH_2PO_4
PBS/T	PBS 0,1% Tween-20
RNA denaturing solution	50 mM NaOH 10 mM NaCl
RNA loading buffer	6,5 ml Formamide 1,2 ml Formaldehyde 2 ml MESA-buffer (10x) 400 µl DEPC-H_2O 200 ml saccharose 20 mg bromophenol blue 20 mg xylene cyanol
RNA neutralizing solution	100 mM Tris-HCl
RNA pre-hybridization solution	100 ml Formamide 30 ml SSC (20x) 40 ml DIG-blocking solution (10%) 2 ml N-lauroylsarcosin (10%) 0,2 ml SDS (20%)

SDS-lysis buffer	2,1 ml Tris (1,5 M; pH 6,8) 1 g SDS 5 ml glycerol 1,6 ml β-mercaptoethanol 20 mg bromophenol blue add 50 ml H_2O Complete protease inhibitor cocktail
SDS-PAGE running buffer (10x)	19,2 M glycine 5 M Tris (pH 8,9) 10 % SDS (w/v)
SSC (20x)	3 M NaCl 0,3 M sodium citrate
SSC-washing solution (0,1x)	0,1 x SSC 0,1 % SDS
SSC-washing solution (2x)	2 x SSC 0,1 % SDS
TAE (20x)	0,32 M Tris 22,84 ml acetic acid (100%) 40 ml EDTA (0,5 M; pH 8)
TEN buffer (10x)	100 mM Tris; pH 7,5 10 mM EDTA 1 M NaCl
TBS	50 mM Tris 150 mM NaCl
TBS/T	TBS 0,1% Tween-20
Tris	10 mM – 1,5 M Tris
WB blocking buffer	TBS 0,1% Tween-20 5% skim milk powder
WB transfer buffer (10x)	30,4 g Tris 144,3 glycin

WB transfer buffer (1x)	700 ml H_2O 200 ml methanol 100 ml WB transfer buffer (10x)

3.5 Kits

Product	Manufacturer
Cytofix/Cytoperm Fixation/Permeabilization Solution Kit with GolgiPlug	BD Pharmingen (Hamburg, Germany)
DIG RNA labelling system	Roche (Mannheim, Germany)
DIG wash and block buffer set	Roche (Mannheim, Germany)
ECL plus western blot detection system	Amersham (Freiburg, Germany)
PCR Master	Roche (Mannheim, Germany)
Plasmid Maxi Kit	Qiagen (Hilden, Germany)
QIAprep spin miniprep kit	Qiagen (Hilden, Germany)
QIAquick gel extraction kit	Qiagen (Hilden, Germany)
QIAquick PCR purification kit	Qiagen (Hilden, Germany)
QIAshredder	Qiagen (Hilden, Germany)
β-Galactosidase enzyme assay system with reporter lysis buffer	Promega (Mannheim, Germany)

3.6 Enzymes

Product	Manufacturer
Proteinase K	Sigma (Munich, Germany)
Restriction enzymes	NEB (Schwalbach, Germany)
T4 DNA ligase	NEB (Schwalbach, Germany)

All enzymes were used in combination with the buffers recommended and provided by the manufacturer.

3.7 Synthetic oligonucleotides (Primers)

Primer[1]	Sequence (5´ → 3´)	Description
DOM8	ATTCTTTGGAGAAATGACAAC	N1L forward
DOM9	CATATGGTATAGATCCTGTAA	N1L reverse
DOM10	GAACCCGGTATGACACTTT	N1L flank forward
DOM11	ACCGCGTCTATCTTAAACG	N1L flank reverse
DOM18	AAAA**CTCGAG**ATGAGGACTCTACTTATTAGA	N1 forward with *Xho*I site
DOM19	AAAA**TTCGAA**GGACGCGTAATTTTCATATG	MVA-N1 reverse with *BstB*I site
DOM20	AAAA**TTCGAA**TTTTTCACCATATAGATCAAT C	WR-N1 with *BstB*I site
DOM25	GAGACGTGATGATGTAGATA	C7L flank forward
DOM26	GTATATCTTAACGAAAGAAGTT	C7L flank reverse
DOM32	ATCG**GGATCC**GACTACGTGGAAACTAAGTA	MVA-N1L flank forward with *Bam*HI site
DOM33	ATCG**CTGCAG**GTTTTTCGTTGTTTAAGTTGG	MVA-N1L flank reverse with *Pst*I site
DOM34	ATCG**GGATCC**GATGCATTAATTTTTTGTATT GA	WR-N1L flank forward with *Bam*HI site
DOM35	ATCG**CTGCAG**AGGGTCAGTACTCATTATCA	WR-N1L flank reverse with *Pst*I site
DOM47	CTAATACGACTCACTATAGGGAGAGACTGAA CGTTCACCAATGTCTC	N1L reverse for RNA probe
DOM48	AAAA**TTCGAA**TCTAATTTCTGAACGTTCAC	$N1_{90}$ reverse with *BstB*I site
DOM49	AAAA**TTCGAA**TTCAATCATCCTAAAGAGTAT G	$N1_{103}$ reverse with *BstB*I site
HLGSF17	AAA**GGGCCC**TCACCAGTTAGATTTGTTAAG	F1L flank forward
HLGSF23	AAG**ACGCGT**TAAAATATGTAGTCGCGACTC	F1L flank reverse

HLPEI66	TGACGAGCTTCCGAGTTCC	Deletion III forward
HLPEI67	GTACCGGCATCTCTAGCAGT	Deletion III reverse
HLPEI90	GGAGGTTCGAAGACGATCAG	18S rRNA gene forward for RNA probe
HLPEI91	CTAATACGACTCACTATAGGGAGACGCTGAG CCAGTCAGTGTAG	18S rRNA gene reverse for RNA probe
HLPEI170	TCTAAGATCTATATTGACGAGC	E3L forward for RNA probe
HLPEI171	CTAATACGACTCACTATAGGGAGATTATCTA CTGCCAATTTAGCTG	E3L reverse for RNA probe
K1Lint1neu	TTGATGACAAGGGAAACACCGCATTG	K1L forward
K1Lint2neu	GAGTCTGAGTTCCTTGTTTTTG	K1L reverse

Underlined sequences represent T7 polymerase promotor recognition sites, bold nucleotides represent restriction sites.
[1] All primers were obtained from MWG Biotech, Ebersberg, Germany.

3.8 Synthetic oligonucleotides (siRNA)

SiRNA[1]	**Sequence (5´ → 3´)**
E3L-si1	GUGUACAGCUCCGACGAUA (Dave et al., 2006)
E3L-si2	AGAAGCGAGAAGUUAAUAA
GFP	GGCUACGUCCAGGAGCGCACCTT
lacZ	CUCGGCGUUUCAUCUGUGGTT

1 All siRNAs were obtained from MWG Biotech, Ebersberg, Germany.

3.9 Plasmids

The plasmids described here were not constructed in this work and were already present in the laboratory. All plasmids encode for an ampicillin resistance.

Plasmid	Description	Source
pC-mychis	Expression plasmid containing a multiple cloning site between the CMV promotor and a myc-6xhis tag	Invitrogen (Karlsruhe, Germany)
pIII-lacZ2	MVA-specific recombination plasmid for insertion of recombinant genes into the deletion III. K1L selection cassette with lacZ2 flanks	Karin Sperling (PEI, Germany)
pΔK1LΔN1L	MVA-specific recombination plasmid for the deletion of N1L	Joachim Zwilling (PEI, Germany)

3.10 Synthetic peptides

All peptides were purchased from Thermo Electron Corporation (Ulm, Germany). Peptides were dissolved in H_2O to a final concentration of 2 mg/ml and stored at -20°C.

Peptide	MHC restriction	Amino acid sequence	Origin	Reference
$B8_{20}$	H2-K^b	TSYKFESV	Vaccinia B8 protein	(Tscharke et al., 2005)
$K3_6$	H2-K^b	YSLPNAGDVI	Vaccinia K3 protein	(Tscharke et al., 2005)
$lacZ_{876}$	H2-K^b	TPHPARIGL	β-galactosidase	(Gavin et al., 1993)

3.11 Antibodies

Specificity	Conjugate	Purpose	Source	Working dilution
Anti-6x His tag	IRDye700DX	Primary antibody for western blot	Rockland (Gilberstville, USA)	1:5000

Anti-active caspase-3	PE	Antibody for FACS	BD Pharmingen (Hamburg, Germany)	20 µl
Anti-Digoxigenin	Alkaline phosphatase	Secondary antibody for northern blot	Roche (Mannheim, Germany)	1:20000
Anti-E3	-	Primary antibody for western blot	Bertram Jacobs (Arizona State University, USA)	1:2000
Anti-F1	-	Primary antibody for western blot	Eurogentech (Seraing, Belgium)	1:1000
Anti-mouse	Alkaline phosphatase	Secondary antibody for ELISA	Dianova (Hamburg, Germany)	1:5000
Anti-mouse	Peroxidase	Secondary antibody for western blot	Dianova (Hamburg, Germany)	1:2500
Anti-mouse	IRDye800	Secondary antibody for western blot	Li-Cor (Bad Homburg, Germany)	1:15000
Anti-mouse CD16/CD32	-	ICS staining	BD Pharmingen (Heidelberg, Germany)	2,5 µg/ml
Anti-mouse CD4	Pacific Blue	ICS staining	BD Pharmingen (Heidelberg, Germany)	1:100
Anti-mouse CD62L	APC	ICS staining	BD Pharmingen (Heidelberg, Germany)	1:100
Anti-mouse CD8a	Pacific Blue	ICS staining	BD Pharmingen (Heidelberg, Germany)	1:100
Anti-mouse IFN-γ	FITC	ICS staining	BD Pharmingen (Heidelberg, Germany)	1:100
Anti-N1	-	Primary antibody for western blot	Eurogentech (Seraing, Belgium)	1:1000
Anti-Parp	-	Primary antibody for western blot	Cell Signalling (Beverly, USA)	1:1000

Anti-rabbit	Peroxidase	Secondary antibody for western blot	Dianova (Hamburg, Germany)	1:2000
Anti-rabbit	IRDye680	Secondary antibody for western blot	Li-Cor (Bad Homburg, Germany)	1:15000
Anti-vaccinia virus	-	Immunostaining	Acris (Hiddenhausen, Germany)	1:2000
Anti-β-actin	-	Primary antibody for western blot	Acris (Hiddenhausen, Germany)	1:10000

3.12 Flourescent dyes

Dye	Manufacturer
Ethidium bromide solution	Fluka (Neu-Ulm, Germany)

3.13 Viruses

The viruses described here were not constructed in this work and were already present in the laboratory.

Virus	Description	Reference
Ectromelia	Ectromelia wildtype virus (strain Moscow); kindly provided by Marc Buller (St. Louis University School of Medicine, St. Louis, USA)	
MVA-F1L$_{rev}$	Recombinant MVAΔF1L with reinserted F1L open reading frame (deletion III)	-
MVAII$_{new}$	Wildtype virus	(Staib et al., 2003)
MVA-lacZ$_{early}$	Recombinant MVA expressing β-galactosidase under control of the early K1L promotor. The lacZ open reading frame was inserted into the deletion III	-
MVA-lacZ$_{late}$	Recombinant MVA expressing β-galactosidase under control of the late P11 promotor. The lacZ open reading frame was inserted into the deletion III	(Sutter and Moss, 1992)

MVAΔE3L-$lacZ_{early}$	Recombinant MVAΔE3L (Hornemann et al., 2003), expressing β-galactosidase under control of the early K1L promotor. The lacZ open reading frame was inserted into the deletion III	-
MVAΔF1L	Recombinant MVA with deleted F1L open reading frame	(Fischer et al., 2006)

3.14 Cell lines

Cell line	Description	ATCC number	Cell culture medium
BHK21	Baby hamster kidney	CCL-10	RPMI
CEF	Primary chicken embryo fibroblasts	-	EMEM
HEK 293T	Human embryonic kidney	45504	DMEM
HeLa	Human epithelioid carcinoma	CCL-2	RPMI
MEF	Mouse embryo fibroblasts	SCRC-1008	DMEM
Murine splenocytes	Primary murine splenocytes	-	RPMI
NIH-3T3	Murine fibroblasts	CRL-1658	DMEM

3.15 Bacteria

Bacterium	Strain	Source
Escherichia coli	Top10	Invitrogen (Karlsruhe, Germany)

3.16 Animals

	Source of supply
C57BL/6N mice	Charles River (Sulzfeld, Germany)
SPF chicken eggs	Lohmann Tierzucht (Cuxhaven, Germany)

3.17 Media

Medium	Composition
LB-media	1% casein extract (w/v) 0,5% yeast extract (w/v) 0,5% NaCl (w/v) 0,1% glucose (w/v)
DMEM cell culture medium	DMEM 10% heat-inactivated FBS 4 mM L-glutamine 100 U/ml penicillin 100 U/ml streptomycin
EMEM cell culture medium	EMEM 10% heat-inactivated FBS 4 mM L-glutamine 100 U/ml penicillin 100 U/ml streptomycin
RPMI cell culture medium	RPMI 1640 10% heat-inactivated FBS 4 mM L-glutamine 100 U/ml penicillin 100 U/ml streptomycin

Media used for infections were supplemented with only 2% FCS; RPMI cell culture medium for primary murine splenocytes was additionally supplemented with 1 mM sodium pyruvate and 55 µM β-mercaptoethanol

3.18 Consumables

Product	Manufacturer
Blood sample tubes	BD Pharmingen (Hamburg, Germany)
Cell culture flasks	Greiner Bio-One (Frickenhausen, Germany)
Cell culture plates (6-, 12-, 24-, 48-, 96well)	Sarstedt (Newton, USA) Corning (Kaiserslautern, Germany) Nunc (Wiesbaden, Germany)

Centrifuge tubes	Beckman (Munich, Germany)
Cryo tubes	Greiner Bio-One (Frickenhausen, Germany)
Diverse lab consumables (racks, timers etc.)	Roth (Karlsruhe, Germany)
	VWR (Darmstadt, Germany)
ELISA plates (96well)	Nunc (Wiesbaden, Germany)
Expendable cuvettes	Roth (Karlsruhe, Germany)
FACS tubes	BD Pharmingen (Hamburg, Germany)
Filcon filters	Consul (Orbassano, Italy)
Filter paper	Whatman (Maidstone, UK)
Hybridization tubes	Biometra (Göttingen, Germany)
Latex gloves	Braun (Melsungen, Germany)
Nitrile gloves	Ansell (Brussels, Belgium)
Nitrocellulose membrane	BioRad (Munich, Germany)
Nylon membrane	Roche (Mannheim, Germany)
Petri dishes	Nunc (Wiesbaden, Germany)
Pipette tips	Molecular Bioproducts (San Diego, USA)
	Eppendorf (Hamburg, Germany)
Pipettes (2-25 ml)	Greiner Bio-One (Frickenhausen, Germany)
Polypropylene tubes	BD Pharmingen (Hamburg, Germany)
	Greiner Bio-One (Frickenhausen, Germany)
PVDF membrane	BioRad (Munich, Germany)
Reaction tubes	Eppendorf (Hamburg, Germany)
Scalpels	Braun (Melsungen, Germany)
Sterile filters	Millipore (Billerica, USA)
Syringe filters	Millipore (Billerica, USA)
Syringe filters (0,22 + 0,45 µM)	Millipore (Billerica, USA)
Syringes	Braun (Melsungen, Germany)
Western Blot staining chambers	Li-Cor (Bad Homburg, Germany)
X-ray films	Amersham (Freiburg, Germany)

3.19 Laboratory equipment

	Model/type	Manufacturer
Bacteria incubator	Innova 44	New Brunswick Scientific (Nürtingen, Germany)
Breeding incubator	Brut-Control BBD 6220	Heka (Rietberg-Varensel, Germany) Heraeus (Hanau, Germany)
Bunsen burner	Labogaz 206	Camping Gaz (Hungen-Inheiden, Germany)
Cell counter	Z1	Beckman Coulter (Krefeld, Germany)
Centrifuge	5415C Minispin Plus Biofuge 15 Fresco 17 Multifuge 1S-R Micro centrifuge	Eppendorf (Hamburg, Germany) Heraeus (Hanau, Germany) Roth (Karlsruhe, Germany)
Cryo storage system	741	Thermo (Marlette, USA)
Freezer (-80°C)	U535	New Brunswick Scientific (Nürtingen, Germany)
Fridge (4°C/-20°C)	KGT3946	Liebherr (Biberach, Germany)
Gel electrophoresis chamber	40-1410	Peqlab (Erlangen, Germany)
Hybridization oven	OV2	Biometra (Göttingen, Germany)
Ice machine	AF100	Scotsman (Vernon Hills, USA)
Infrared Imager	Odyssey	Li-Cor (Bad Homburg, Germany)
Laminar flow	SterilGARD III Advance	The Baker Company (Sanford, USA)
Lumi-Imager	F1	Roche (Mannheim, Germany)
Micropipette	Reference	Eppendorf (Hamburg, Germany)
Microscope	Axiovert 40C	Zeiss (Oberkochen, Germany)
Microwave	8020	Privileg (Fürth, Germany)
Multi-well plate reader	SpectraMAX 340PC	Molecular Devices (Sunnyvale, USA)
Nitrogen tank	LN2	Cryo (Wilnsdorf, Germany)
PCR cycler	T personal	Biometra (Göttingen, Germany)
Photometer	Ultrospec 1100 pro	Amersham (Freiburg, Germany)

Pipettor	Accu-jet	Brand (Wertheim, Germany)
Power supply	P25	Biometra (Göttingen, Germany)
Roller mixer	SRT6	Sigma (Munich, Germany)
SDS-Page chamber	Mini-Protean 3	BioRad (Munich, Germany)
Shaker	WT16	Biometra (Göttingen, Germany)
	3013	GFL (South Yorkshire, UK)
	Polymax 1040	Heidolph (Schwabach, Germany)
	Promax 1020	
Sonicator	Sonopuls HD 2200	Bandelin (Berlin, Germany)
Thermoblock	TB1	Biometra (Göttingen, Germany)
Thermomixer	RCT basic	IKA (Staufen, Germany)
	Thermomixer compact	Eppendorf (Hamburg, Germany)
Ultracentrifuge rotors	SW 32 Ti	Beckman Coulter (Krefeld, Germany)
	Typ 19	
Ultracentrifuges	Optima L-80 XP	Beckman Coulter (Krefeld, Germany)
UV Crosslinker	BLX-E254	Vilber Lourmat (Eberhardzell, Germany)
UV detection system	Shuttle X	Intas (Göttingen, Germany)
Vacuum aspirator	Vacusafe comfort	IBS (Chur, Switzerland)
Vacuum blot equipment	VacuGene Pump	Amersham (Freiburg, Germany)
	VacuGene XL	
Vacuum gel dryer	583	BioRad (Munich, Germany)
Vortexer	MS1 Minishaker	IKA (Staufen, Germany)
	Vortex Genie 2	Scientific Industries (Bohemia, USA)
Waterbath	WB 22	Memmert (Schwalbach, Germany)
Weighing machines	Adventurer Pro	Ohaus (Pine Brook, USA)
	XP 160 M	Precisa (Dietikon, Switzerland)
X-Ray cassettes	IEC 60406	X-Ray (Augsburg, Germany)
β+γ x-ray monitor	LB145	EG&G Berthold (Bundoora, Australia)

4 Methods

4.1 Cloning procedures using *Escherichia coli*

4.1.1 Transformation of plasmid-DNA into competent *E. coli*

Transformation of plasmid-DNA was performed using competent Top10 *Escherichia coli* bacteria. 500 ng plasmid-DNA or complete ligation probes (see chapter 4.4.6) were added to Top10 *E. coli* bacteria and incubated for 30 minutes on ice. Afterwards the probes were incubated for exact 30 seconds at 42°C in a water bath and subsequently chilled on ice. 200 µl LB-medium was added and probes were shaken at 300 rpm at 37°C for 1 hour. 25 – 100 µl of the bacteria were plated on LB_{amp} plates and incubated over night at 37°C in a bacteria incubator.

4.1.2 Plasmid purification from *E. coli* for analytical purpose (Mini-prep)

For isolation of plasmid DNA from transformed *E. coli* bacteria, single colonies from LB_{amp} plates were picked, transferred to 5 ml liquid LB_{amp} medium and cultured over night in a shaker at 225 rpm and 37°C. The next day, bacteria were pelleted by centrifugation at 13 000 rpm for 30 seconds and plasmids were isolated using the QIAprep spin miniprep kit according to the manufacturer´s instructions. Plasmid-DNA was eluted in 50 µl H_2O and stored at -20°C.

4.1.3 High yield plasmid purification from *E. coli* (Maxi-prep)

For the generation of plasmid-DNA stocks, 20 µl of transformed *E.coli* bacteria grown over night in liquid LB_{amp} medium, were transferred to 200 ml LB_{amp} medium and amplified by cultivation in a shaker at 225 rpm and 37°C over night. The next day, bacteria were pelleted by centrifugation at 4 500 rpm and 4°C for 30 minutes. Plasmid isolation was then performed using the Qiagen plasmid maxi kit according to the manufacturer´s instruction. Plasmid-DNA was dissolved in 500 µl H_2O and stored at -20°C.

4.2 Cell culture

4.2.1 Cell culture conditions and cell split

All eukaryotic cell lines described in this work were maintained in a humidified air-5% CO_2 atmosphere at 37°C.
Cell split was performed when cells achieved confluency. Cell culture medium was removed, cells were washed twice with PBS and subsequently incubated with 3 ml trypsin until detachment from the flask. 7 ml cell culture medium was added and cells were resuspended thoroughly. Cell culture medium was added until the desired split ratio was achieved and the cells were transferred into new cell culture flasks or –plates.

4.2.2 Transient transfection of small interfering RNAs and plasmid DNA

For gene expression analysis, small interfering RNAs (siRNAs) were transiently transfected in HeLa cells using the Lipofectamine 2000 system according to the manufacturer´s instructions. Briefly, 1 µg siRNA in 50 µl RPMI 1640 medium without supplements was mixed with 2 µl Lipofectamine 2000 in 50 µl RPMI 1640 without supplements and incubated for 20 minutes at room temperature. After incubation, the reagent was added to ~80% confluent HeLa cells in 24-well plates. MVA-infections and/or gene expression analysis was performed 24 hours after transfection.
For the transfection of plasmid DNA into cells, two different transfection reagents were used. For expression analysis of plasmid-encoded genes, DNA was transfected using the FugeneHD transfection reagent. For the generation of recombinant MVA, Lipofectamine 2000 transfection reagent was used. All reagents were applied according to the manufacturer´s instructions. Briefly, plasmid DNA and transfection reagent were mixed with cell culture medium without supplements, respectively. After 5 minutes of incubation at room temperature, the probes were mixed and incubated again for 20 minutes at room temperature. Cells were washed with medium without antibiotics and the transfection mixture was dropped onto the cells. Afterwards the cells were incubated at 37°C until further analysis.

4.3 Virological methods

4.3.1 *In vitro* virus infections

Virus stocks were sonicated three times for 1 minute and afterwards diluted in cell culture medium until the desired multiplicity of infection was achieved. Medium was removed from cells and replaced with infectious medium. After 1 hour of virus adsorption at 4°C, cells were washed with fresh cell culture medium and afterwards incubated at 37°C until further analysis. In experiments in which apoptosis was analyzed, virus adsorption was performed at 37°C.

4.3.2 Generation of recombinant MVA

For the generation of recombinant MVA, the transient host range selection method was applied (Staib et al., 2000). Due to the transient introduction of the K1L selection marker into the genome, recombinant virus clones are able to replicate on normally non-permissive RK13 cells. After selection, recombinant virus clones were passaged on CEF cells, in which the K1L selection marker is not essential for replication and therefore sliced out by chance due to identical repetitive sequences flanking the K1L selection marker.

4.3.2.1 Infection and transfection of CEF cells

To generate a recombinant MVA variant, CEF cells were infected with the respective ancestor MVA strain at an moi of 0,05 and incubated for 90 minutes at 37°C. Afterwards 4 µg of the desired recombination plasmid was transfected using Lipofectamine 2000 transfection reagent (see chapter 4.2.4). Cells were harvested together with the supernatant after 2 days at 37°C, freeze-thawed three times and stored at -20°C.

4.3.2.2 Transient host-range selection of recombinant virus clones on RK13 cells

The virus-suspension derived from the infection/transfection described above was plaque passaged on RK13 cells in 6-well plates. Briefly, RK13 cells were infected with the freeze-thawed and sonicated virus suspension in serial dilutions. After 3 – 5 days, single virus plaques were identified and harvested.

4.3.2.3 Selection of K1L-free virus clones

After 4 passages on RK13 cells, virus clones were plaque passaged on permissive CEF-cells in 6-well plates. For inhibition of mixture of different virus clones, the infectious medium was removed 90 minutes after infection and replaced by an agar overlay (1% low melt agarose in 2 x MEM cell culture medium). After 3 - 5 days at 37°C, single virus plaques were identified and harvested. After several plaque passages, virus clones were amplified by infection of CEF cells in 6-well plates. DNA prepared from the harvested virus-cell-suspension was then analyzed by PCR reaction (see chapter 4.4.8) concerning recombination and removement of the K1L selection marker.

4.3.2.4 Amplification and purification of virus clones

The amplification of virus clones was performed by serial passaging in CEF cells until a final volume of thirty T175 cell culture flasks. Virus cell suspensions were harvested, freeze-thawed three times and sonicated 3 times for 1 minute before new infections. After amplification to a volume of one T175 cell culture flasks, the virus clone was once again analyzed by PCR reaction (see chapter 4.4.8). After the final amplification, the cell-virus-suspension was centrifuged at 16 000 rpm and 4°C for 90 minutes. The pellet was dissolved in 5 ml Tris (10 mM; pH 9), freeze-thawed three times and sonicated three times for 1 minute. Tris (10 mM; pH 9) was added to a final volume of 30 ml. 10 ml Sucrose (36% dissolved in Tris; 10 mM; pH 9) was overlayed with 10 ml virus suspension and centrifuged for 60 minutes at 13 500 rpm and 4°C. The pellets were dissolved in a small volume (max. 1 ml) of Tris (10 mM; pH 9). Purificated virus stocks were stored at -80°C.

4.3.2.5 Virus titration

For the determination of virus titers in amplificated and purificated virus stocks, confluent CEF-cells in 6-well plates were infected with virus in serial dilutions. 90 minutes after infection, cells were washed with fresh cell culture medium and incubated for 2 days at 37°C. Afterwards, cells were fixed and immunostained (chapter 4.6.2). Virus titers were calculated by the number of plaques multiplied with the dilution factor. Virus titers are denoted in plaque forming units per ml (pfu/ml).

4.4 DNA analysis

4.4.1 DNA sequencing

To check DNA sequences after cloning procedures, 1 µg plasmid DNA was air-dried in eppendorf tubes and sequenced by MWG Biotech (Ebersberg, Germany).

4.4.2 Analytical gel electrophoresis

For the analysis of DNA derived from restriction digests or PCR analysis, gel electrophoresis was performed using 1% TAE-agarose gels. DNA-probes were mixed with DNA-loading buffer and electrophoresis was carried out by 100 V for 30 – 60 minutes. Gels were stained for 5 minutes in an ethidiumbromide-solution (5 µg/ml). After destaining in water, specific DNA bands were detected under UV light.

4.4.3 DNA purification from agarose gels

DNA fragments of interest were sliced out with an ethanol-cleaned scalpel and transferred to an eppendorf-tube. DNA purification was performed using the QIAquick gel extraction kit according to the manufacturer´s instruction. DNA was eluted in 20 µl H_2O.

4.4.4. Restriction enzyme digestion

Restriction digests were performed for 90 minutes. The temperature and addition of BSA depended on the restriction enzyme used. Generally, 2 µg plasmid-DNA or PCR-product was mixed with 2 µl of the appropriate NEB-buffer (depending on the enzyme used) and 2 µl BSA (10 µg/µl), if required. Water was added to a final volume of 19 µl and digestion was started by the addition of 1 µl restriction enzyme.

4.4.5 Determination of DNA concentration

Concentration of plasmid DNA stocks and other DNA probes was determined photometrically. A 1:100 dilution of the probe was generated with H_2O and measured at 260 nm against H_2O as reference in a photometer.

4.4.6 Ligation

Ligation of DNA fragments was performed at a vector to insert ratio of 1:3. Both DNA fragments were mixed with 2 µl T4-DNA ligase buffer and H_2O until a final volume of 19 µl. 1 µl T4-DNA ligase was added and the ligation reaction was carried out over night in thawing ice. Afterwards probes were stored at -20°C.

4.4.7 Preparation of DNA from vaccinia virus infected cells

Isolation of DNA from infected cells was performed with 500 µl virus-cell-solution derived from infected cells. The freeze-thawed virus-solution was incubated with 50 µl TEN, 50 µl SDS (10%) and 50 µl proteinase k for 1 hour at 56°C and gentle shaking. Afterwards 500 µl phenol:chloroform:isoamylalcohol (25:24:1) was added. After vortexing, the probes were centrifuged for 5 minutes at 13 000 rpm and 4°C. The upper aqueous phase was mixed with 500 µl chloroform:isoamylalcohol and once again vortexed and centrifuged. Again, the upper aqueous phase was transferred to a new tube and mixed with 40 µl sodium-acetate (3M; pH 7) and 1 ml ethanol (-20°C). After an incubation of 1 hour at -80°C, DNA was pelleted by centrifugation at 13 000 rpm and 4°C for 30 minutes. The DNA-pellet was washed with 1 ml

ethanol (70%; -20°C) and once again centrifuged. Afterwards DNA was air-dried and dissolved in 20 µl H_2O by incubation at 50°C for 10 minutes and gentle shaking. DNA was stored at -20°C.

4.4.8 Polymerase chain reaction (PCR)

PCR-analysis was done in 25 µl probes of the following composition:

12,5	µl Roche-PCR-Mastermix
9,5	µl H_2O
0,05	µl of each primer (5 pmol)
3	µl template DNA (~100 ng)

Annealing-temperature and elongation duration was adapted to the fusion temperature of the primers and expected size of the amplified DNA-fragments, respectively.

4.5 RNA analysis

Throughout all work with RNA, only RNase free equipment and solutions were used.

4.5.1 RNA-preparation

The RNA-preparation was performed from mock- or vaccinia virus-infected cells derived from 6-well cell culture plates. Medium was removed and cells were lysed with 1 ml TRIZOL-Reagent, incubated for 5 minutes at room temperature and stored at -80°C until further usage.

After thawing, 200 µl chloroform was added. The probes were inverted several times and incubated for 5 minutes at room temperature. Afterwards the probes were centrifuged for 30 minutes at 13 000 rpm and 4°C. 500 µl isopropanol was added to the aqueous phase and after an incubation of 10 minutes at room temperature once again centrifuged as above. The

RNA pellet was washed with ethanol (75%). After a further centrifugation step, the pellet was dried and dissolved in 50 µl H_2O overnight at 4°C and 10 minutes at 65°C. The RNA was stored at -80°C until further usage.

4.5.2 Determination of RNA concentration

To compare different RNA probes in later experiments, the concentration was determined photometrically. A 1:100 dilution was generated with DEPC-H_2O and measured at 260 nm in a photometer. DEPC-H_2O was used as reference.

4.5.3 RNA gel electrophoresis

RNA was electrophoretically separated in 1% denaturing agarose gels. The gels were composed of 1 g agarose in 81,5 ml DEPC-H_2O and 10 ml MESA-buffer (10x). The solution was boiled until complete solution of the agarose and subsequently tempered to 65°C in a water bath. 8,5 ml pre-warmed (65°C) formaldehyde was added. The casted gels were solidified for 1 hour at room temperature. Electrophoresis was done in MESA-buffer. Before loading, a pre-run was performed for 10 minutes at 100 V.
RNA probes (1 µg RNA dissolved in 10 µl DEPC-H_2O + 5 µl RNA-loading buffer) were denatured for 10 minutes at 65°C, shortly incubated on ice and subsequently loaded into the pockets of the agarose gel. RNA was separated at 70 V for 2 – 4 hours.
After separation, gels were stained in an ethidiumbromide solution (2,5 µg/µl in MESA-buffer) for 5 minutes and washed overnight in cold H_2O. After destaining, the gels were photographed under UV-light.

4.5.4 Northern blot

The transfer of RNA was carried out by vacuum blotting. Positively charged nylon membranes were soaked shortly in DEPC-H_2O and subsequently equilibrated in 20 x SSC. Afterwards the gel was loaded on the membrane and RNA was vacuum-blotted at 50 mbar with the following solutions and incubation periods:

1. Denaturing solution	5 minutes
2. Neutralizing solution	5 minutes
3. 20 x SSC	3 ½ hours

After blotting, the membrane was washed shortly in 2 x SSC and the RNA was fixed with UV irradiation. The membrane was dried and stored under dry and clean conditions until further usage.

4.5.5 Construction of DIG-labeled RNA-probes

In vitro-synthesized DIG-labeled RNA-probes were generated using the DIG-RNA-labeling-system. The 5´ region of the gene of interest was amplified by PCR. The reverse primer additionally contained the sequence for the T7-polymerase promoter (see chapter 3.7). After purification, the PCR-product could be used for the *in vitro*-synthesis of the DIG-labeled RNA-probe.

3 µl PCR-product (~500 ng) was mixed with 2 µl DIG RNA-labeling mix, 2 µl transcription buffer, 12 µl DEPC-H_2O, 1 µl RNase-inhibitor and 1 µl T7-polymerase. The mixture was incubated for 2 hours at 37°C and the enzymatic reaction was stopped by addition of 0,8 µl EDTA (0,5 M; pH 8) and 2,5 µl LiCl (4M). After addition of 70 µl ethanol (-20°C) the RNA could be precipitated over night at -20°C. The probes were centrifuged at 13 000 rpm and 4°C for 15 minutes and the RNA-pellet was washed with ethanol (70%) and once again centrifuged for 5 minutes. The RNA was dried and resuspended for 4 hours at 4°C in 100 µl DEPC-H_2O. The concentrated DIG labelled RNA-probes were stored at -80°C.

Prior to the first application, 7,5 µl of the concentrated RNA-probe was diluted in 50 µl DEPC-H_2O, denatured for 10 minutes at 95°C and inoculated in 10 ml pre-warmed pre-hybridization solution. The diluted RNA-probe was stored at -20°C.

4.5.6 Functional control of generated DIG-labeled RNA-probes

The concentrated RNA-probes were dropped on positively charged nylon membranes and subsequently fixed with UV irradiation. A DIG-specific antibody was used for detection. The protocol is identical with the protocol for the detection of RNA/RNA-hybrids described in chapter 4.5.8.

4.5.7 Hybridization of membrane-bound RNA with DIG-labeled RNA probes

The positively charged nylon membrane carrying the UV-fixed RNA was transferred together with 20 ml pre-hybridization solution in hybridization bottles and was incubated for at least 1 hour at 55°C – 68°C, depending on the RNA-probe used. After incubation, the pre-hybridization solution was replaced with the pre-warmed diluted DIG-labelled RNA-probe. Hybridization was done in general over night.
To remove unspecifically bound RNA-probes, the membrane was washed twice with 2 x SSC at room temperature and three times with pre-warmed 0,1 x SSC at 55°C – 68°C. Afterwards, the membrane could be used for the detection of DIG-labeled RNA/RNA-hybrids.

4.5.8 Detection of RNA/RNA-hybrids

The detection of RNA was done subsequently after hybridization. All steps were carried out at room temperature in hybridization bottles. The membrane was washed for 5 minutes in DIG-washing buffer. Afterwards DIG-blocking solution was used for 30 minutes to block unspecific binding spots. The membrane was incubated with an anti-digoxygenin-antibody diluted in DIG-blocking solution for 30 minutes. After binding of the antibody, the membrane was washed twice in DIG-washing buffer for 30 minutes and equilibrated in DIG-detection buffer for 5 minutes. Afterwards the membrane was incubated for 5 min with substrate solution (5 µl CDP-Star in 1 ml DIG-detection buffer) in the dark after which the RNA/RNA-hybrids were detected with a lumi-imager. The described protocol is equivalent to the manufacturer´s instructions with slight modifications (DIG Wash and block buffer set).

4.6 Protein analysis

4.6.1 Generation of vaccinia virus-specific antibodies

4.6.1.1 Anti-F1 antibody

Anti-F1 antibody was produced by Eurogentec (Seraing, Belgium) by immunization of rabbits with peptide corresponding to amino acids 177 – 203 (CFV DYI TDI SPP DNT IPN TST REY LKL; one amino-acid code) of the F1 protein coupled to KLH. The antibody was affinity purified by the manufacturer.

4.6.1.2 Anti-N1 antibody

Anti-N1 antibody was produced by Eurogentec (Seraing, Belgium) by immunization of rabbits with peptide corresponding to amino acids 78 – 90 (CKV ARD IGE RSE IR; one amino-acid code) of the N1 protein coupled to KLH. The antibody was affinity purified by the manufacturer.

4.6.2 Immunostain of vaccinia virus-infected cells

For the determination of virus titers, infected CEF-cells in 6-well plates were fixed 2 days after infection with 1 ml ice-cold acetone:methanol (1:1). After 5 minutes of incubation at room temperature, the acetone:methanol mixture was removed and fixed cells were dried. Unspecific binding sites were blocked by addition of PBS (3% FCS) for 30 minutes at room temperature and gentle shaking. Afterwards, the fixed cells were incubated with a rabbit anti-vaccinia virus antibody for 3 hours at room-temperature and gentle shaking. After washing the cells twice with PBS, the secondary antibody solution (PO-labelled anti-rabbit antibody) was added for 45 minutes at room temperature. The cells were once again washed twice and stained with dianisidine staining solution.

4.6.3 Western blot

4.6.3.1 Preparation of cell lysates

To isolate proteins, cells were harvested together with the supernatant and centrifuged for 5 minutes at 2000 rpm. The cell pellet was then lysed with SDS-lysis buffer and incubated for 5 minutes at room temperature. The lysates were transferred to a QIAshredder column and centrifuged at 13 000 rpm for 2 minutes. The lysates were stored at -80°C until further usage.

4.6.3.2 Sodium dodecyl sulphate polyacrylamide gel electrophoresis (SDS-PAGE)

Cell lysates prepared as described above were denatured at 95°C for 5 minutes and subsequently incubated on ice. Samples were loaded into the pockets of 5% SDS-stacking gels and proteins were separated on 6% - 15% resolving gels by electrophoresis at 100 V in SDS-PAGE-running buffer. The composition of a typical stacking- and resolving gel is given in table 4.1.

Table 4.1: Composition of SDS-gels

Composition of 10 ml of a 5% SDS-stacking gel:	**Composition of 15ml of a 15% SDS-resolving gel:**
8,6 ml H_2O 1,7 ml acryl-bisacrylamide mix (30%) 1,25 ml Tris (1,5 M; pH 6,8) 100 µl SDS (10%) 100 µl ammonium persulfate (10%) 10 µl TEMED	3,4 ml H_2O 7,5 ml acryl-bisacrylamide mix (30%) 3,8 ml Tris (1,5M; pH 8,8) 150 µl SDS (10%) 150 µl ammonium persulfate (10%) 6 µl TEMED

4.6.3.3 Wet-transfer of proteins

Proteins were blotted on PVDF- or nitrocellulose membranes using a wet-blot apparature. PVDF membranes were equilibrated in methanol and transfer buffer, nitrocellulose

membranes in transfer buffer. SDS-resolving gels were also equilibrated in transfer buffer before blotting. Proteins were transferred at 100 V for 1 hour on ice. The composition of the blotting chamber is given in Figure 4.1.

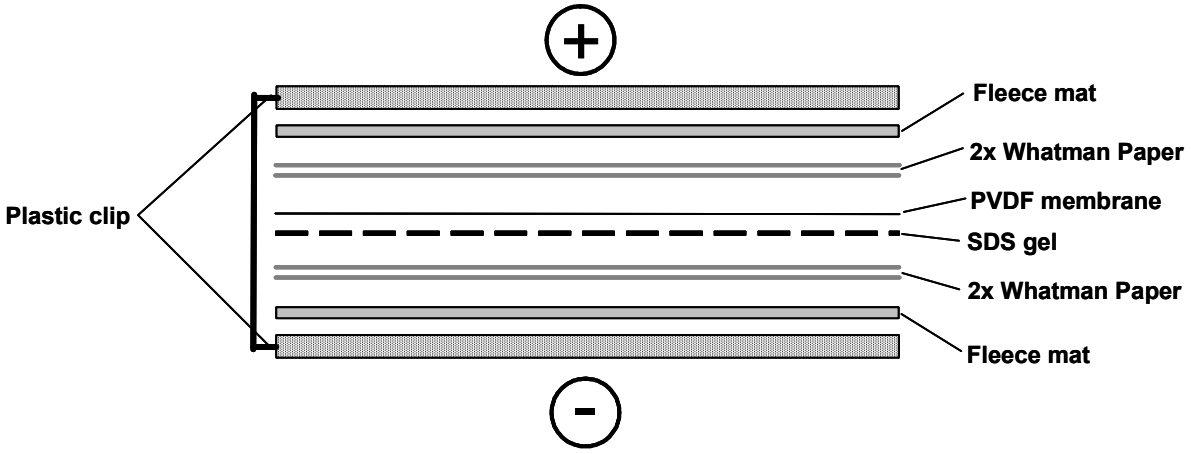

Figure 4.1: Schematic view of the composition of the blotting chamber used for transfer of proteins from SDS-gels to membranes.

4.6.3.4 Immunodetection of proteins on PVDF membranes

After blotting, the membrane was blocked with WB-blocking solution for 1 hour at room temperature. Incubation with primary antibodies (see chapter 3.11) diluted in WB-blocking solution was performed over night at 4°C. After washing three times with TBS/T, the membrane was incubated for 1 hour at room temperature with the appropriate secondary antibodies diluted in WB-blocking solution. After three further washing steps, the membrane was covered with ECL substrate solution and incubated for 5 minutes in the dark. After incubation, specific bands were detected with a lumi-imager.

4.6.3.5 Immunodetection of proteins on nitrocellulose membranes using the Li-Cor detection system

After blotting, the membrane was blocked with Li-Cor Blocking solution for 1 hour at room temperature. Incubation with primary antibodies (see chapter 3.11) diluted in Li-Cor blocking solution supplemented with 0,2 % Tween-20 and 0,02 % SDS was performed overnight at 4°C. After washing three times with PBS/T, the membrane was incubated for 1 hour at room

temperature with the appropriate IRDye-labelled secondary antibodies diluted in Li-Cor blocking solution (supplemented as above). After three further washing steps, the membrane was shortly washed in pure PBS and specific bands were detected with an Odyssey infrared imager.

4.6.3.6 Stripping of PVDF and nitrocellulose membranes

To detect further proteins, membranes were stripped by washing the membrane for 5 minutes in H_2O, NaOH (0,2 N) and H_2O, respectively. After stripping, the membrane was blocked once again with the appropriate blocking solution and immunoprobed as described above (chapter 4.6.3.4 – 4.6.3.5)

4.6.4 [^{35}S]-metabolic labelling of proteins

Confluent monolayers of NIH-3T3 cells in 12-well plates were mock infected or infected with virus at an moi of 20. Following 60 minutes of adsorption at 4°C, virus inocula were replaced by pre-warmed medium and the cells were incubated at 37°C. At desired time points cells were washed once with cysteine- and methionine-free medium and then incubated for 30 minutes at 37°C with 50 µCi of [^{35}S]cysteine-[^{35}S]methionine per well. Afterwards cells were washed once with PBS and lysed directly in SDS-lysis buffer. Samples were separated by 10% SDS-PAGE (see chapter 4.6.3.2), gels were dryed for 2 hours at 80°C in a vacuum gel dryer and analyzed by autoradiography.

4.6.5 FACS analysis of virus-induced apoptosis

Infected cells were harvested. After washing twice with PBS, the cells were analyzed using the Cytofix/Cytoperm Fixation/Permeabilization kit according to the manufacturer´s instructions. Briefly, cells were fixed and permeabilized on ice with 200 µl Fix/Perm for 20 minutes. Cells were washed twice with Perm/Wash and stained with PE-conjugated rabbit anti-active caspase-3 antibody diluted in Perm/Wash. FACS analysis was performed on a LSR II using FACSDiva Software.

4.6.6 β-galactosidase enzyme activity assay

4.6.6.1 Preparation of cell lysates

Cell lysates were prepared with reporter lysis buffer according to the manufacturer´s instructions with slight modifications. Cells in 6-well plates were trypsinized and pelleted by centrifugation at 2000 rpm for 5 minutes. After washing the cells with PBS, the pellet was resuspended in 200 µl reporter lysis buffer and incubated for 15 minutes at room temperature in a shaker at 500 rpm. After vortexing, the probes were centrifuged at 13 000 rpm for 2 minutes and the supernatant was stored at -20°C.

4.6.6.2 Determination of protein yield

Protein concentrations for β-galactosidase enzyme activity assays were measured with the BioRad protein assay. 20 µl of cell lysate was mixed with 780 µl H_2O and 200 µl BioRad protein assay. After an incubation of 5 minutes at room temperature the probes were measured at 595 nm in a photometer. Concentrations were calculated with the help of a calibration curve (Figure 4.2).

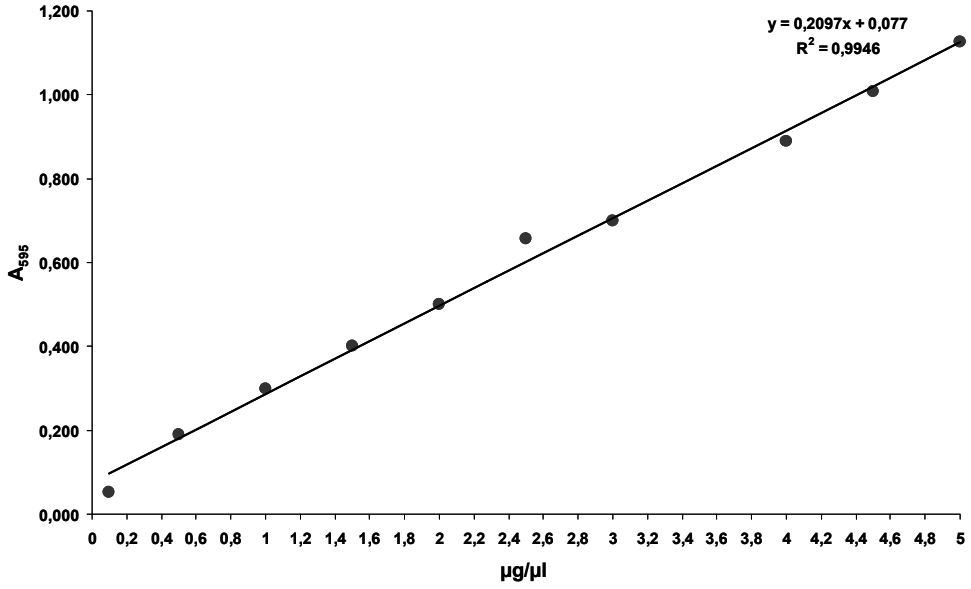

Figure 4.2: Calibration curve for the calculation of protein concentrations. The curve was generated by photometric measurement of defined amounts of BSA protein.

4.6.6.3 β-galactosidase enzyme activity assay

To determine the β-galactosidase enzyme activity in cell lysates prepared as described in chapter 4.6.6.1, the β-galactosidase enzyme assay system with reporter lysis buffer was used. 25 µl of cell lysate was mixed with 25 µl reporter lysis buffer and 50 µl assay buffer in 96-well plates. The mixture was incubated for 30 minutes at 37°C and colorimetric reaction was stopped by the addition of 150 µl sodium carbonate. Afterwards, the probes were photometrically analyzed in a multi-well plate reader at 420 nm against probes containing no cell lysates as reference. Every probe was measured in triplicate.

4.7 *In vivo* and *ex vivo* analysis

4.7.1 Immunization of mice

C57BL6/N mice were immunized with virus by the intramuscular (i.m.) route. Virus was sonicated three times and the desired virus dose was diluted with PBS to a final volume of 100 µl and injected into the left hamstring muscle.

4.7.2 Blood serum withdrawal

Blood samples from immunized C57BL/6N mice were taken from a tail vein scratch. Blood was collected in Microtainer tubes and incubated for 30 minutes at room-temperature. Afterwards, blood samples were centrifuged at 13 000 rpm for 90 seconds and serum was transferred into fresh tubes. Blood sera was stored at -20°C until further usage.

4.7.3 Determination of MVA-specific antibody titers

96-well immunoplates were coated with 2 µg/ml MVA (diluted in coating-buffer) for 3 hours at 37°C and overnight at 4°C. After washing four times with ELISA-washing buffer, unspecific binding sites were blocked with blocking buffer for 1 hour at 37°C. After washing,

the plates were incubated with serial dilutions of mouse blood sera for 1 hour at 37°C. After a further washing step, the plates were incubated with an alkaline-phosphatase conjugated anti-mouse antibody diluted in ELISA-blocking buffer for 30 minutes at 37°C. 75 µl p-nitrophenyl phosphate (pNpp) as substrate was added after washing for exact 20 minutes and the colorimetric enzymatic reaction was stopped by addition of 50 µl NaOH (0,5 M). Probes were then measured photometrically at 405 nm in a multi-well plate reader. The denoted antibody titers correspond to the highest reciprocal dilution factor, in which a colorimetric reaction was observed.

4.7.4 Quantification of vaccinia virus-specific T cell responses

4.7.4.1 Preparation of splenocytes

Splenocytes were prepared from immunized C57BL/6N mice. Mice were anesthetized with isofluran and sacrificed by cervical dislocation. Splenocytes were prepared from dissected spleens and transferred to room-temperatured PBS. After centrifugation at 1 100 rpm for 5 minutes, erythrocytes left in the cellular pellet were lysed with 3 ml red blood cell lysing buffer for 2 minutes. After addition of 7 ml PBS, cells were centrifuged as above and resuspended in 5 ml RPMI-splenocytes medium. After filtration through 70 µm falcon filters, cells were once again centrifuged and resuspended in 1 ml RPMI-splenocytes medium.

4.7.4.2 Determination of splenocyte cell count

Splenocytes were diluted 1:1 000 in isotone II diluent and counted in a Z1 Coulter particle counter.

4.7.4.3 Vaccinia virus-specific stimulation and staining of splenocytes

10^7 splenocytes dissolved in 500 µl cell culture medium were stimulated in 24-well cell culture plates with $lacZ_{876}$, $B8R_{20}$ or $K3L_6$ peptide dissolved in 500 µl cell culture medium (2 µg/ml) for 5 hours. 1 µl GolgiPlug was added for the last 3 hours according to the

manufacturer´s recommendation. Splenocytes were harvested and centrifuged at 1 500 rpm for 5 minutes. Unspecific binding sites were blocked with purified anti-mouse CD16/CD32 Fc-block antibody for 30 minutes at 4°C. After washing with PBS, cell surface markers were stained for 30 minutes with pacific blue-conjugated rat anti-mouse CD8a or pacific blue-conjugated rat anti-mouse CD4 and APC-conjugated anti-mouse CD62L antibodies. Afterwards, cells were fixed and permeabilized by addition of 100 µl fix/perm. Intracellular IFN-γ staining was performed using FITC-labelled anti-mouse IFN-γ antibody diluted in perm/wash. After washing, cells were FACS-analyzed using an LSR II using FACSDiva Software.

For the analysis of total MVA-specific CD8/CD4 T-cell responses freshly prepared splenocytes from vaccinated C57BL/6N mice were stimulated by infection with MVA at an moi of 1 for 19 hours. GolgiPlug was added for the last 12 hours. The staining and analysis was performed as described above. Fix/perm, perm/wash and GolgiPlug were derived from the Cytofix/cytoperm fixation/permeabilization solution kit with GolgiPlug.

4.7.5 Analysis of protective capacity against a lethal ectromelia virus challenge

C57BL/6N mice were infected 21 days after immunization (chapter 4.7.1) with 2000 pfu ectromelia virus (strain Moscow) by the intranasal route. From day -3 pre- to day 21 post-challenge, mice were monitored daily concerning weight loss, signs of illness and survival. Animals that had lost more than 30% weight or showed a signs of illness rate of 4 were sacrificed because of ethical reasons. Signs of illness were characterized as followed:

1 : ruffled fur
2 : 1 and arched back
3 : 2 and respiratory distress with reduced mobility
4 : 2 and respiratory distress with diminished motility

Intranasal infection was performed by administration of the desired virus amount into the nostrils of ketamin/xylazin anesthetized mice. Ketamin/xylazin was used in amounts of 10 µl/g body weight.

4.8 Statistical analysis

All statistical analysis was performed by [redacted] (Paul-Ehrlich-Institut, Langen, Germany). Error bars in diagrams are expressed as mean +/- s.d. or +/- SEM, as denoted in the figure legends.

5. Results

5.1 Impact of the anti-apoptotic vaccinia virus protein F1 on MVA-immunogenicity

The highly attenuated vaccinia virus strain MVA encodes for the apoptosis inhibitor F1 which functions by inhibiting the activation of the mitochondrial effector molecules bax and bak (see chapter 2.4.2). Due to the importance of the cross-presentation pathway for priming of an MVA-specific cellular immune response (see chapter 2.3) and the relevance of F1 during the inhibition of apoptosis, deletion of F1L from the genome of MVA, leading to an enhanced induction of apoptosis in infected cells and therefore presumably to an increased cross-presentation of viral antigens, might have an impact on the immune stimulating capacity of the virus. To analyze this question, an F1L deletion virus (MVAΔF1L (Fischer et al., 2006) and a revertant virus (MVA-F1L$_{rev}$ - unpublished), in which the F1L open reading frame was reinserted into the deletion III of the MVAΔF1L genome, were compared concerning their immune stimulating capacities.

5.1.1 Molecular characterization of MVAΔF1L

To verify the deletion and reinsertion of the F1L open reading frame in MVAΔF1L and MVA-F1L$_{rev}$, respectively (Figure 5.1A), PCR analysis was performed with DNA prepared from CEF cells infected with the recombinant virus clones.
Deletion of the F1L gene sequence at its original position in MVAΔF1L and MVA-F1L$_{rev}$ was confirmed by PCR analysis using primers derived from the flanking regions of the F1L open reading frame (Figure 5.1B). PCR products with sizes of ~1 kb from DNA of MVAΔF1L- and MVA-F1L$_{rev}$-infected cells showed the expected smaller size due to the deletion event, compared to the ~1,5 kb band derived from the MVA control. In a second PCR using primers flanking the deletion III, the successful reinsertion of the F1L ORF was proven for MVA-F1L$_{rev}$ by a shift of the PCR product from ~0,7 kb in MVA- and MVAΔF1L- up to 1,6 kb in MVA-F1L$_{rev}$-derived DNA.

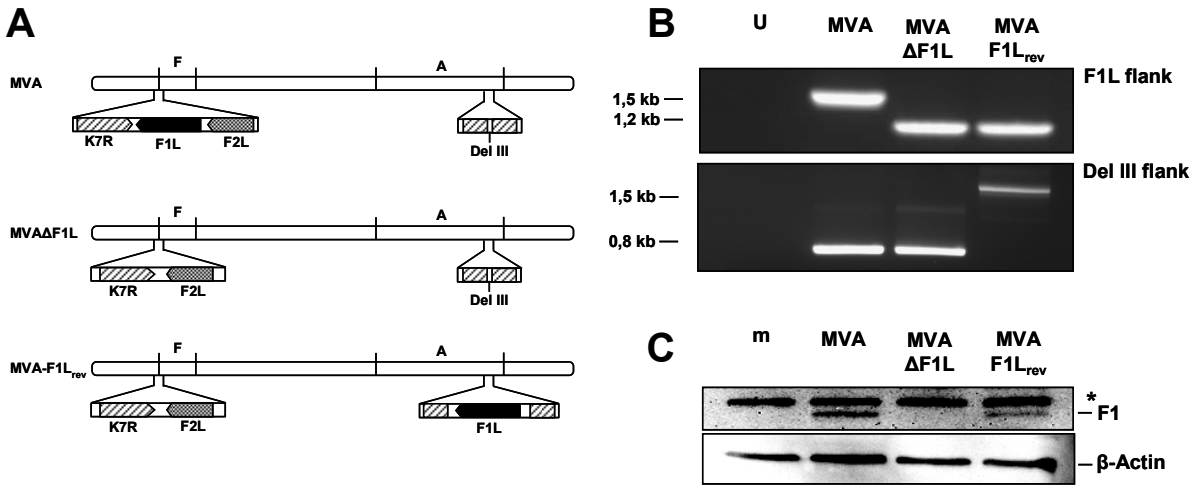

Figure 5.1: Characterization of recombinant MVA with a deleted and/or reinserted F1L open reading frame. (A) Schematic view of the linear dsDNA genomes of MVA, MVAΔF1L and MVA-F1L$_{rev}$. Genomic alterations introduced at the original position of F1L and deletion III in MVAΔF1L and MVA-F1L$_{rev}$ are shown. (B) PCR analysis of viral DNA prepared from CEF cells infected with MVA, MVAΔF1L and MVA-F1L$_{rev}$ using primers HLGSF17 and HLGSF23 derived from flanking regions of the natural F1L ORF (upper panel) or with primers HLPEI66 and HLPEI67 flanking the deletion III (lower panel). Numbers on the left indicate the size of molecular weight standard. U: water control (C) Western-blot analysis of NIH-3T3 cells infected with MVA, MVAΔF1L or MVA-F1L$_{rev}$ at an moi of 10. Cell lysates were prepared 5 hours post infection, separated by SDS-PAGE, transferred to a PVDF membrane and probed with an anti-F1 antibody. Equal loading was confirmed by detection of β-actin. The asterisk indicates an unspecific F1 antibody cross-reactive protein. m: mock-infected control.

To check for the functionality of the F1L open reading frame in MVA-F1L$_{rev}$, expression of the F1 protein in infected NIH-3T3 cells was monitored by western blot analysis. Cells were infected with MVA, MVAΔF1L or MVA-F1L$_{rev}$ at an moi of 10. 5 hours after infection, cell lysates were analyzed by SDS-PAGE and immunoprobed with an F1-specific antibody (chapter 3.11 - Figure 5.1C). In cell lysates derived from MVA- and MVA-F1L$_{rev}$-infected cells, a specific band of the calculated 26 kDa was detected, demonstrating expression of the F1 protein, whereas no F1 protein could be detected in the lysate of MVAΔF1L-infected cells. Therefore, the genomic alterations introduced into the genomes of MVAΔF1L and MVA-F1L$_{rev}$ led to the desired deletion and reconstitution of the F1L encoded gene function in MVAΔF1L and MVA-F1L$_{rev}$, respectively.

To analyze possible unwanted alterations in the genomes of the generated recombinant MVA variants not recognized by the characterization performed above, the total protein expression profile of both recombinant viruses was assessed. For this purpose, MVA-, MVAΔF1L and MVA-F1L$_{rev}$-infected NIH-3T3 were metabolically labelled for 30 minutes with [^{35}S]-methionine/cystein at different time points after infection. As shown in figure 5.2, cell lysates derived from MVAΔF1L and MVA-F1L$_{rev}$-infected cells showed the same typical viral protein expression pattern also recognized in MVA-infected cells, with prominent expression

of viral late proteins. Additionally, all viruses induced the typical shutoff of host cell protein synthesis observed in vaccinia virus-infected cells as early as 3 hours after infection.

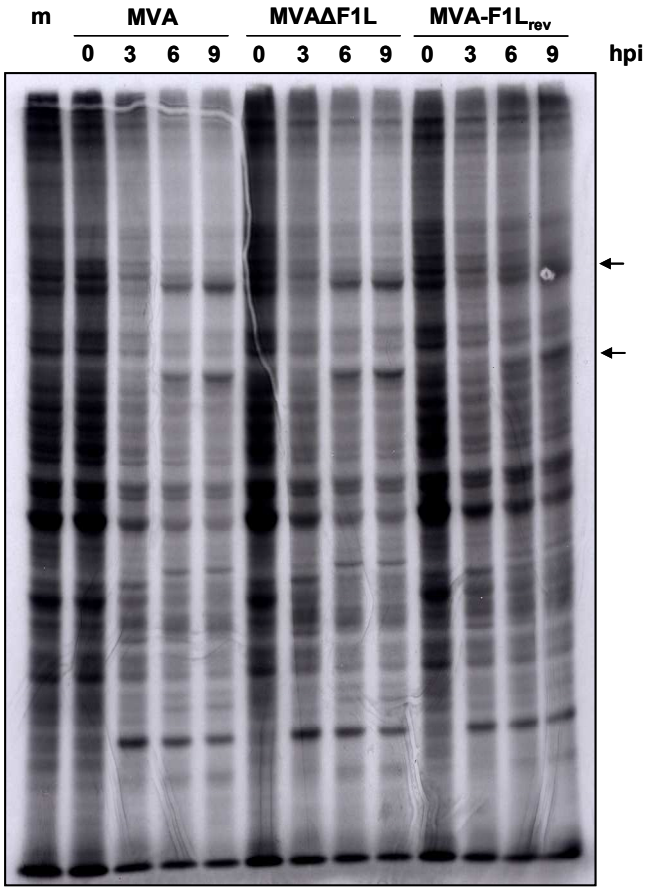

Figure 5.2: Metabolic labelling of virus-infected NIH-3T3 cells. Cells were infected with MVA, MVAΔF1L or MVA-F1L$_{rev}$ at an moi of 20 and labelled with [^{35}S]methionine/cysteine for 30 minutes at the indicated time points post-infection. Proteins from complete cell lysates were separated by SDS-PAGE and analyzed by autoradiography. Typical viral late proteins are indicated by arrows. m: mock-infected control.

The data obtained from these experiments suggest that the recombinant MVA clones MVAΔF1L and MVA-F1L$_{rev}$ are identical but differ in the expression of the F1 protein.

5.1.2 MVAΔF1L induces apoptosis in murine cells

The vaccinia virus F1 protein was shown to effectively inhibit apoptosis induced by a variety of external stimuli (Fischer et al., 2006; Wasilenko et al., 2005; Taylor et al., 2006). Furthermore, infection of HeLa cells with MVAΔF1L leads to an active viral induction of apoptosis, suggesting a role of the protein in the inhibition of virus-induced apoptosis (Fischer et al., 2006). However, this inhibiting function has not been confirmed so far in murine cells.

Thus, the apoptosis-inducing capacity of MVAΔF1L should be analyzed first in murine NIH-3T3 cells. Activation of caspase-3, the main apoptotic effector caspase, was measured by FACS analysis after infection of NIH-3T3 cells with MVA or MVAΔF1L. Cells infected with the F1L deletion mutant showed a statistically significant higher amount of active caspase-3-positive cells compared to MVA infection (Figure 5.3A), confirming the reported capacity for apoptosis induction also in murine cells.

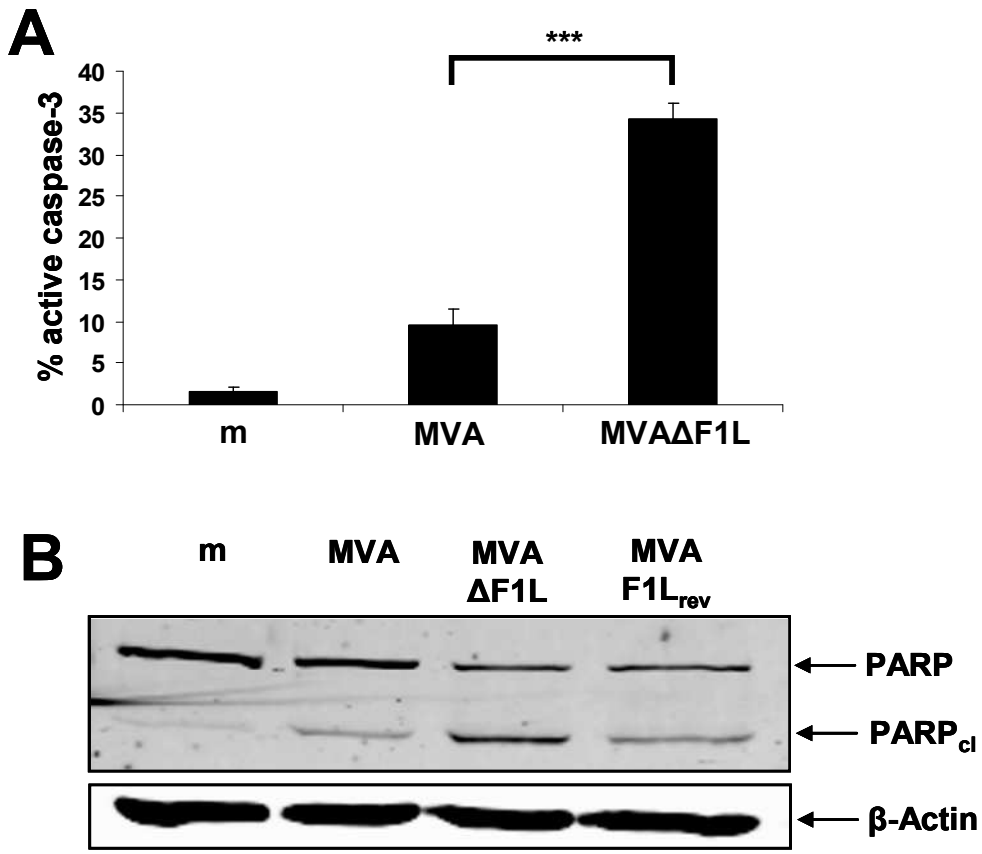

Figure 5.3: Analysis of MVAΔF1L-induced apoptosis. NIH-3T3 cells were mock infected or infected with MVA or MVAΔF1L at an moi of 10. (A) Cells were harvested 15 hours post-infection, stained with an PE-conjugated anti-active caspase-3 antibody and analyzed by FACS (***: $P < 0{,}0001$; t test, p-values Bonferroni adjusted for multiple comparisons). (B) Cell lysates were prepared 15 hours post infection, separated by SDS-PAGE and immunoblotted against PARP/cleaved PARP ($PARP_{cl}$). Detection of β-actin served as loading control. m: mock-infected control

The result of the experiment was confirmed by western blot analysis, detecting cleaved poly-ADP ribose polymerase (PARP), which is a substrate of caspase-3. As shown in figure 5.3B, infection of NIH-3T3 cells with MVAΔF1L leads to a higher amount of cleaved PARP ($PARP_{cl}$) compared to the MVA-, MVA-$F1L_{rev}$- or mock-infected cells 15 hours post infection.

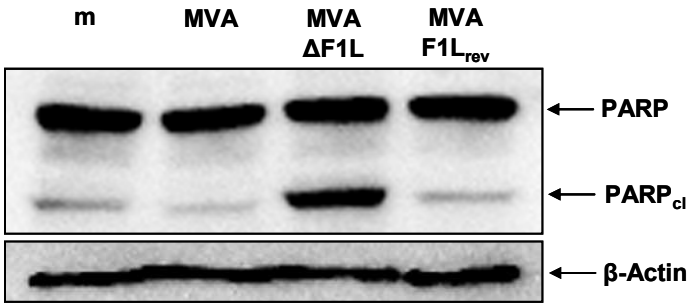

Figure 5.4: Analysis of MVAΔF1L-induced apoptosis in murine embryonic fibroblasts (MEF). MEF cells were infected with MVA, MVAΔF1L or MVA-F1L$_{rev}$ at an moi of 10 and cell lysates were prepared 8 hours post infection. Proteins were separated by SDS-PAGE and immunblotted against PARP/cleaved PARP (PARP$_{cl}$). Detection of β-actin confirmed equal loading. m: mock-infected control

To reflect the more natural situation in mice, the apoptosis-inducing capacity of MVAΔF1L was assessed in murine embryonic fibroblasts (MEF), derived from prenatal C57BL/6 mice. After infection with the F1L deletion mutant, cells showed a strong induction of PARP cleavage (PARP$_{cl}$) already 8 hours after infection, which was absent in lysates derived from wild-type or revertant virus-infected cells (Figure 5.4). Interestingly, induction of PARP cleavage was even more predominant in the embryonic fibroblasts than in the established murine cell line. In summary, the data obtained demonstrate that infection with MVAΔF1L strongly induces apoptosis not only in human (Fischer et al., 2006) but also in murine cells and the inhibition of apoptosis could be reversed by reconstitution of F1L gene function.

5.1.3 Induction of humoral immune responses by MVAΔF1L

MVA infection of mice leads to the induction of long-lived virus-specific antibody titers (Cosma et al., 2004). To assess whether deletion of the F1L ORF has an impact on serum antibody titers, C57BL/6 mice were immunized with 10^7 plaque forming units (pfu) MVA, MVAΔF1L or MVA-F1L$_{rev}$ by the intramuscular route (i.m.). Antibodies specific for MVA virus particles were measured by ELISA (chapter 4.7.3) from sera collected at day -3 (pre-immune) and day 18 after immunization (Figure 5.5). No measurable antibody titers were detected in pre-immune sera and in sera from mice immunized with PBS (diluted 1:400). In contrast, virus-specific antibodies were found in all sera from immunized mice at day 18 in serum-dilutions ranging from 1:1600 to 1:6400.

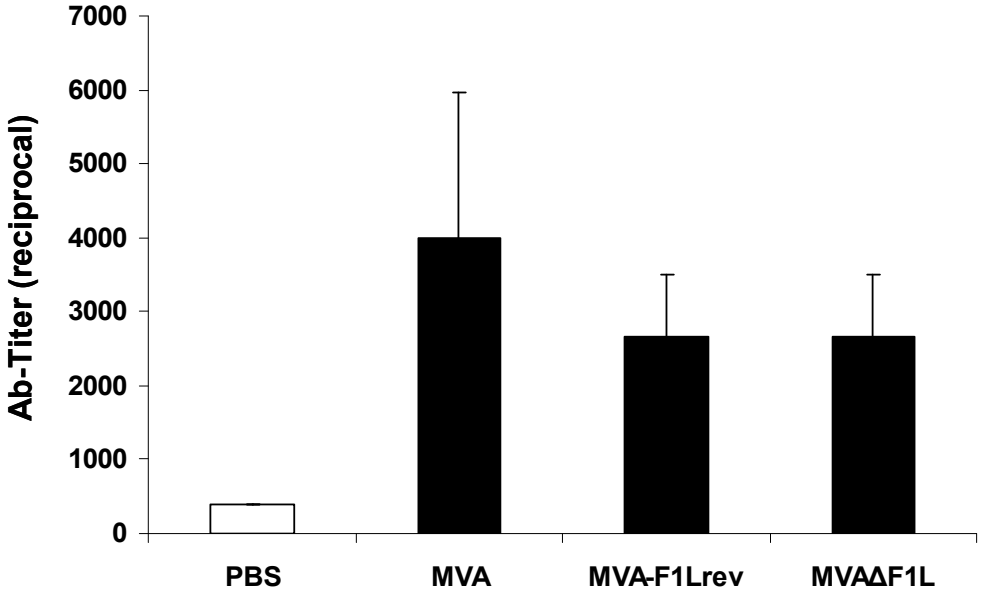

Figure 5.5: MVA-specific antibody titers in sera from immunized mice. Groups of 6 C57BL/6 mice were immunized with 10^7 pfu of MVA, MVAΔF1L, MVA-F1L$_{rev}$ or PBS as control by the i.m. route. At day 18 post-infection, blood sera were collected from a tail vein scratch and ELISA was performed on immunoplates coated with 2 µg/ml MVA virus particles to measure MVA-specific antibody titers. Bars represent reciprocal antibody titers as mean +/- s.d.

Interestingly, no significant difference between any of the groups of immunized mice were detected concerning the amount of induced antibodies, suggesting that the deletion of F1L seems to have no effect regarding the induction of MVA-specific antibody titers.

5.1.4 MVAΔF1L immunization effectively primes VACV-specific T-cell responses

Virus-induced apoptosis in infected cells may have an impact on the induction of an adaptive cellular immune response against viral antigens due to an increased and/or accelerated uptake of infected apoptotic cells by professional antigen presenting cells (pAPC), leading to enhanced presentation of viral antigens through the cross-presentation pathway (Gasteiger et al., 2007; Albert 2004). Therefore, the induction of total MVA-specific $CD8^+$ and $CD4^+$ T cell responses were analyzed after i.m. immunization of C57BL/6 mice with 10^7 pfu MVA, MVAΔF1L, MVA-F1L$_{rev}$ or PBS as control. An intracellular cytokine stain (ICS) was performed at day 7 after immunization using freshly prepared splenocytes. For stimulation of MVA-specific T cell responses, splenocytes were infected with MVA at an moi of 1 directly after preparation to generate autologous antigen-presenting cells directly inside each

splenocyte culture (chapter 4.7.4). As control, splenocyte cultures were left uninfected in parallel settings.

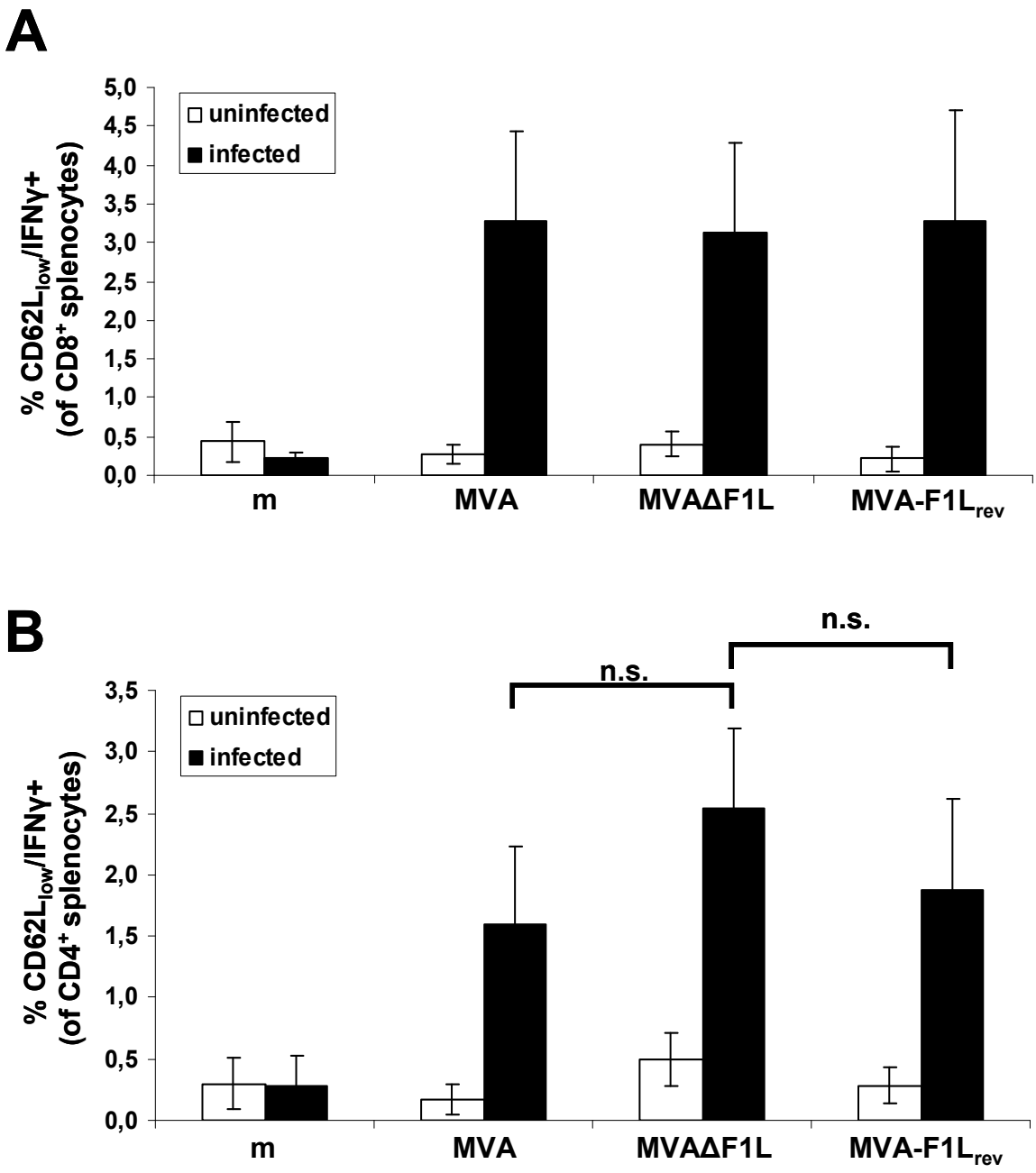

Figure 5.6: Intracellular cytokine stain of splenocytes derived from immunized mice. Groups of 6 C57BL/6 mice were immunized i.m. with 10^7 pfu MVA, MVAΔF1L, MVA-F1L$_{rev}$ or PBS as control. 7 days post infection mice were sacrificed. Splenocytes were prepared and subsequently infected for stimulation with MVA at an moi of 1 (black bars) or mock-infected (white bars). 7 hours after infection, GolgiPlug was added and 19 hours after infection cells were stained for FACS analysis with antibodies recognizing CD8 or CD4, CD62L and IFN-γ. Cells were gated on CD8$^+$ (A) or CD4$^+$ (B). Bars represent the mean of the group +/- s.d. m: PBS-immunized mice; n.s.: not significant ($p > 0,05$; f-test, p-values Bonferroni adjusted for multiple comparisons).

Only background levels of $CD8^+$ or $CD4^+$ T cell activity were measured in splenocytes that were either uninfected or derived from PBS-immunized control mice. In contrast, all groups of virus-immunized mice showed about 3% of IFN-γ-producing activated ($CD62L_{low}$) $CD8^+$ T cells (Figure 5.6A) and ~1,6 to 2,5% of respective $CD4^+$ T cells (Figure 5.6B). Although the induction of the $CD4^+$ T cell response seems to be slightly enhanced in MVAΔF1L-immunized mice, no statistical significance could be calculated.

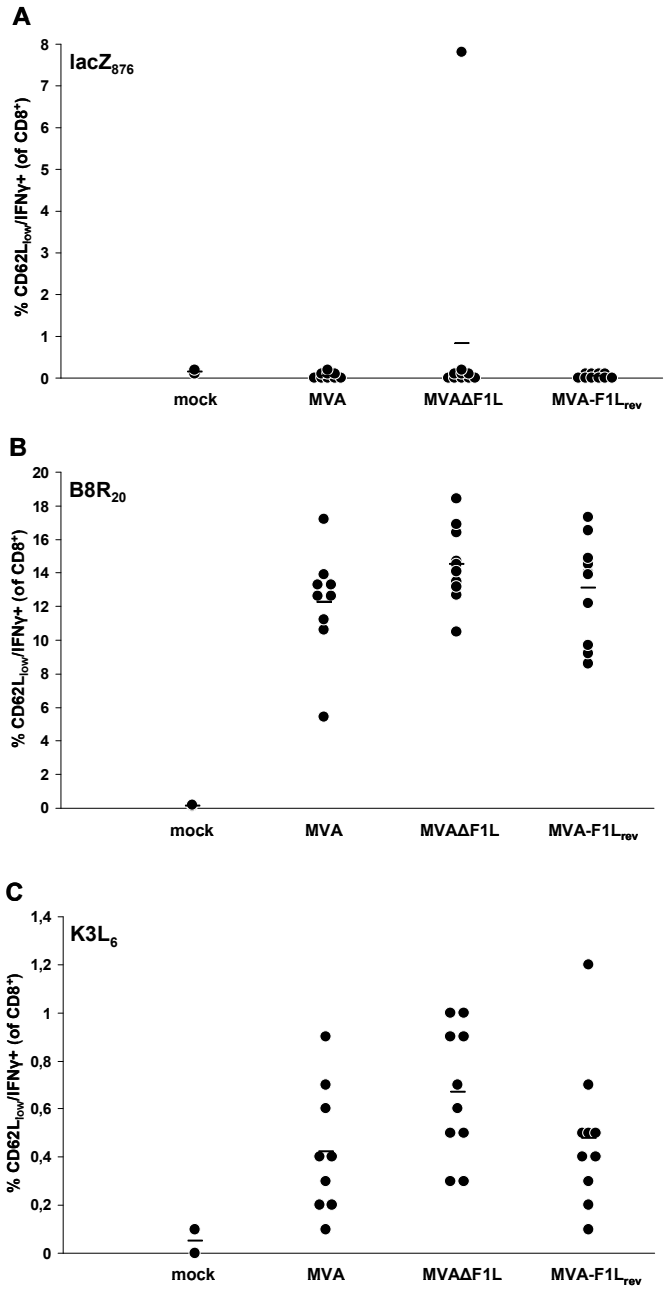

Figure 5.7: Intracellular cytokine stain of peptide-stimulated splenocytes derived from immunized mice. Mice were immunized i.m. with 10^7 pfu MVA, MVAΔF1L, MVA-F1L_{rev} or PBS as control. 7 days after immunization, mice were sacrificed, splenocytes were prepared and subsequently stimulated with $lacZ_{876}$ (A), $B8R_{20}$ (B) or $K3L_6$ (C) peptide for 5 hours. After 2 hours, GolgiPlug was added. Intracellular cytokine stain was performed against $CD8^+$, $CD62L_{low}$, IFN-γ-producing cells. Circles represent single mice, lines the mean of the analyzed group.

In order to detect possible epitope-specific differences in the repertoire of activated $CD8^+$ T cells, which could not be seen in the total T cell response induced by stimulation with MVA infection, splenocytes derived from immunized mice were specifically stimulated with the immunodominant vaccinia virus MHC class I-restricted peptide $B8R_{20}$ and the subdominant $K3L_6$ peptide, respectively (Moutaftsi et al., 2006). As in the experiment above (Figure 5.6) splenocytes were isolated at day 7 after immunization of C57BL/6 mice with MVA, MVAΔF1L, MVA-$F1L_{rev}$ or PBS and subsequently stimulated with peptide. FACS analysis revealed comparable amounts of IFN-γ-producing activated antigen-specific $CD8^+$ T cells with responses ranging from ~6 - 18% and ~0,1 - 1,3% in the $B8R_{20}$ and $K3L_6$ stimulated splenocytes, respectively, again with slightly enhanced responses measured in splenocytes derived from MVAΔF1L-immunized mice (Figure 5.7). No induction of $B8R_{20}$- or $K3L_6$-specific IFN-γ-producing T cells were measured in PBS immunized mice or $lacZ_{878}$-peptide-stimulated controls.

These data suggest that MVAΔF1L induces a potent adaptive immune response on the cellular level. Nevertheless, the strong apoptotic stimulus delivered by MVAΔF1L seems not to influence the strength of T cell activation early (day 7) after a single immunization pattern.

5.1.5 Protective capacity of MVAΔF1L against lethal poxvirus infections

The immunogenicity of MVA is a prerequisite for protection against a challenge orthopoxvirus infection. To further analyze the impact of F1L on the immunogenicity of MVA, the protective capacity of MVAΔF1L was studied in an ectromelia virus (ECTV) mouse challenge model, a model system closely resembling the human smallpox infection (Coulibaly et al., 2005; Paran et al., 2009). C57BL/6 mice were immunized intramuscularly with 10^5 – 10^7 pfu MVA, MVAΔF1L or MVA-$F1L_{rev}$ and challenged 21 days later with 2000 pfu ECTV (representing ~ 25 x LD_{50}) by the intranasal route (i.n.). Despite this highly lethal dose, monitoring the protective efficacy by immunization with MVA long before challenge should be possible. As control, mice were immunized with PBS or 10^7 - 10^8 pfu MVA. The animals were monitored daily for weight-loss (Figure 5.8, left panels), survival (Figure 5.8, right panels) and signs of illness (Figure 5.9) from day -3 pre- to day 21 post-challenge (chapter 4.7.5). Mice which had lost more than 30% of weight were sacrificed due to ethical regulations.

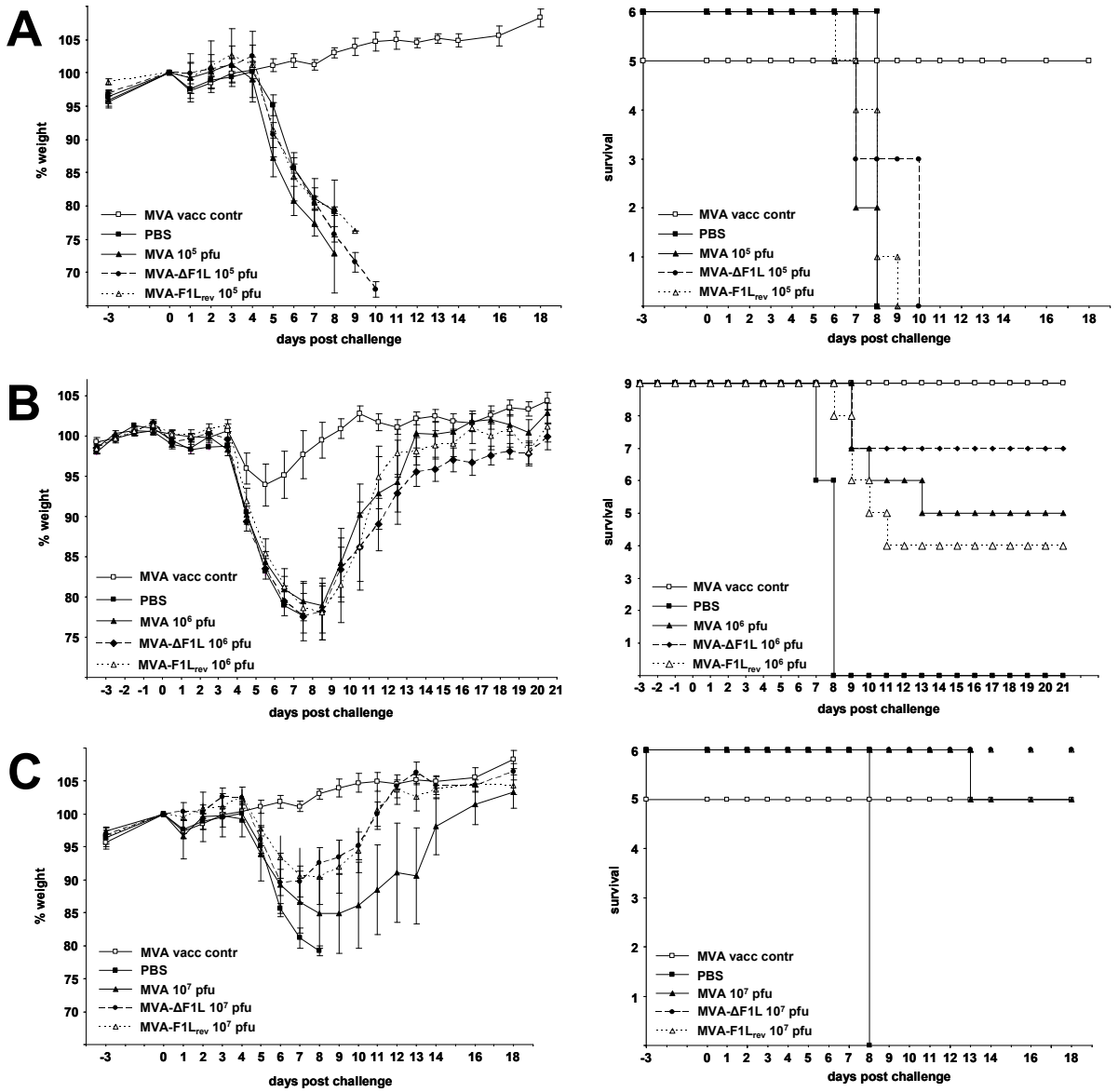

Figure 5.8: Protection assay against lethal ECTV infection. Groups of 6 mice (5 in the MVA control group in A and C) were immunized i.m. with 10^5 (A), 10^6 (B) or 10^7 (C) pfu MVA, MVAΔF1L or MVA-F1L$_{rev}$. Control groups received 10^7 (A and C) or 10^8 (B) pfu MVA or PBS. At day 21 after immunization mice were infected with 2000 pfu ECTV i.n. and were monitored from day -3 pre-challenge to day 21 post-challenge concerning weight loss (left panels) and survival (right panels). MVA-immunized control mice in A and C were challenged with PBS. Curves represent the mean values +/- SEM. Vacc contr: vaccination control

All PBS-immunized but challenged mice rapidly showed loss of weight (Figure 5.8) and progressive signs of illness (Figure 5.9) from day 5 on and died on day 7 and 8, confirming the highly lethal conditions of infection. In contrast, immunization with 10^8 pfu MVA 21 days before infection with ectromelia virus protected the mice completely from death (Figure 5.8B, right panel – MVA vacc contr), attributed with a very mild weight loss (Figure 5.8B, left panel) and no detectable signs of illness (Figure 5.9B). The lower immunization dose of 10^6 pfu was not able to completely protect mice resulting in severe weight loss, signs of illness and almost 50% mortality (Figure 5.8B and 5.9B). No significant differences

concerning weight loss and signs of illness were observed between the groups of mice immunized with MVA, MVA-ΔF1L or MVA-F1L$_{rev}$. Interestingly, less mice had to be sacrificed within the group immunized with MVAΔF1L than within the MVA and MVA-F1L$_{rev}$-immunized groups, respectively. This result, however, might provide some benefit in the protective capacity against a lethal orthopoxvirus challenge with MVA deleted for the anti-apoptotic F1L gene.

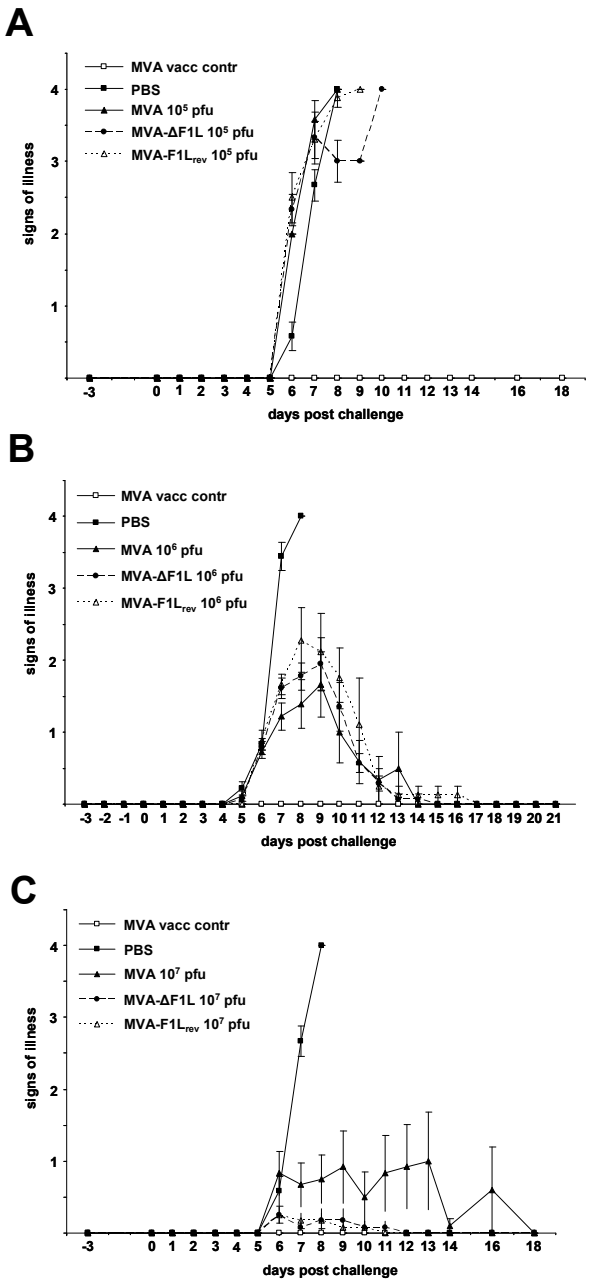

Figure 5.9: Protection assay against lethal ECTV infection. Groups of 6 mice (5 in the MVA control group in A and C) were immunized i.m. with 10^5 (A), 10^6 (B) or 10^7 (C) pfu MVA, MVAΔF1L or MVA-F1L$_{rev}$. Control groups received 10^7 (A and C) or 10^8 (B) pfu MVA or PBS. At day 21 after immunization mice were infected with 2000 pfu ECTV i.n. and were monitored from day -3 pre-challenge to day 21 post-challenge concerning signs of illness. MVA-immunized control mice in A and C were challenged with PBS. Curves represent the mean values +/- SEM.

To prove possible differences attributed to the immunization dose, we immunized mice with 10^5 or 10^7 pfu prior to challenge with ectromelia virus. However, these doses demonstrated either a complete failure of or a generalized protection without major disease symptoms, respectively, whether F1L was encoded by the immunizing MVA variant or not (Figure 5.8/5.9 A and C). Together our data indicate, that immunization with MVA deficient for the important apoptosis-inhibitor F1L, still has the capacity to induce an effective immune response, which protects against a highly lethal orthopoxvirus infection.

5.2 Functional characterization of the N1L open reading frame encoded by MVA

The N1L open reading frame encoded by MVA is a natural fusion of the two ORFs N1L and C5L, encoding a protein whose functionality is questionable (chapter 2.4.3). In order to clarify this query, the expression and functionality of the N1L ORF derived from MVA was compared to the authentic and functional N1L ORF encoded by the vaccinia virus strain Western Reserve (WR). For this purpose, several recombinant MVA variants with a deleted and/or reinserted N1L ORF, either derived from MVA itself (MVA-$N1L_{rev}$) or from vaccinia virus WR (MVA-$WRN1L_{rev}$), as well as four expression plasmids encoding different N1L constructs were generated and molecularly analyzed.

5.2.1 Generation and characterization of MVA variants encoding for different N1 proteins

To analyze expression and functionality of the N1L ORF encoded by MVA, several recombinant MVA variants were constructed in which the ORF was either deleted or reinserted with the MVA-related sequence or the sequence derived from the vaccinia virus strain WR. The transient host range selection method was used for the generation of recombinant MVA, using the vaccinia virus K1L gene as selection marker (Staib et al., 2000). According to this method, insertion of the K1L ORF into the genome of MVA enables the virus to replicate on RK13 cells, which are non-permissive for a natural MVA infection. After successful recombination, repetitive sequences flanking the K1L ORF allow the deletion of the selection marker by homologous recombination on permissive CEF cells, in which the K1L selection marker is dispensable for productive replication.

5.2.1.1 Plasmids used for the generation of recombinant MVA with modified N1L ORF

For the deletion of the N1L ORF from the genome of MVA, the plasmid pΔK1LΔN1L was used. This plasmid was already present in the laboratory and contains the K1L selection cassette (Staib et al., 2000) flanked by two homologous sequences derived from the flanking regions of the N1L ORF (Figure 5.10).

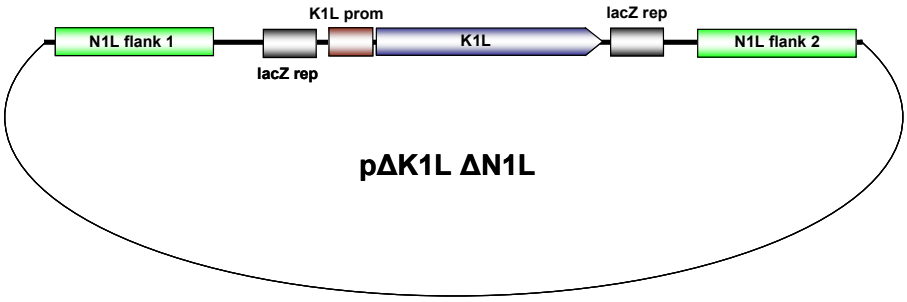

Figure 5.10: Schematic view of the N1L-deletion plasmid pΔK1LΔN1L.

For the generation of N1L-specific revertant MVA variants, two recombination plasmids were constructed, containing the MVA-related N1L ORF (pIII-N1L-lacZ2) or the WR-related N1L ORF (pIII-WRN1L-lacz2). The K1L selection cassette present in the constructed vector plasmids is flanked by lacZ2-repeats, which are different from the lacZ-repeats in the N1L-deletion plasmid pΔK1LΔN1L. Due to the remaining of one lacZ repeat in the virus genome (see chapter 5.2.2.1), double-recombinant viruses have to be generated with different lacZ-repeat-sequences because of possible unwanted recombination events between sequences in the plasmid and virus genome.

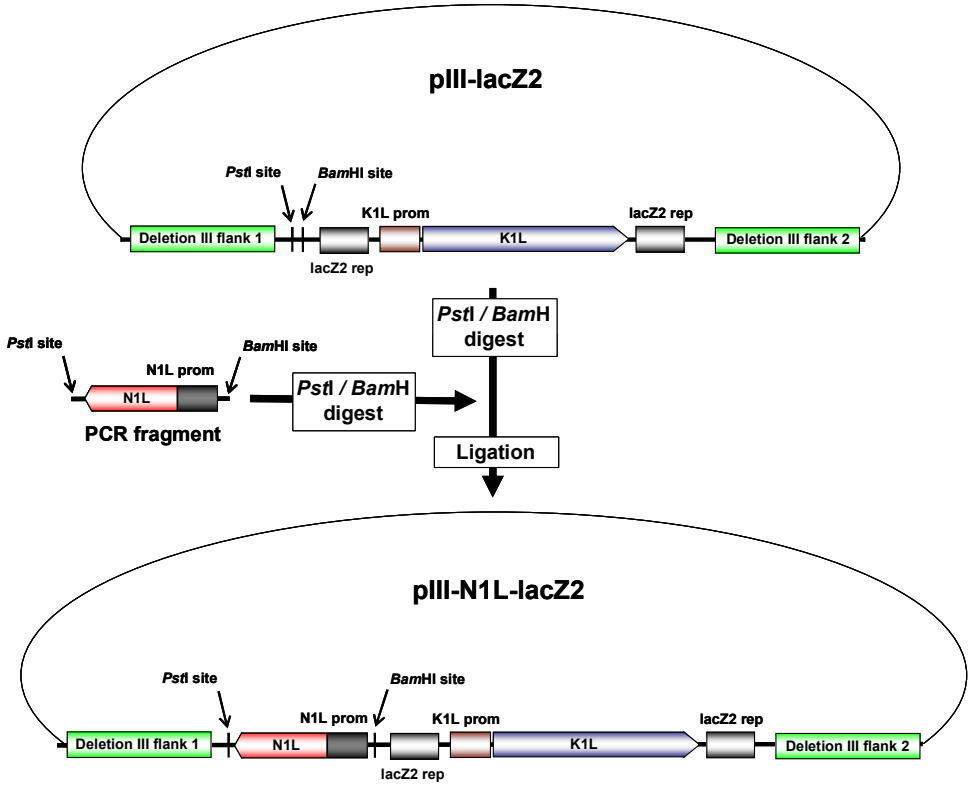

Figure 5.11: Construction of N1L ORF-containing insertion plasmids. Both the vector plasmid pIII-lacZ2 and the PCR-amplificated N1L fragment were digested with *Pst*I and *Bam*HI and afterwards ligated to generate pIII-N1L-lacZ2. An equal strategy was performed to construct the plasmid pIII-WRN1L-lacZ2.

For construction of the insertion plasmids pIII-N1L-lacZ2 and pIII-WRN1L-lacZ2 both the MVA- and WR-related N1L ORFs including a ~150 bp upstream genomic region, containing the gene promotor, were amplified by PCR using the primers DOM32 + DOM33 (MVA-N1L) and DOM34 + DOM35 (WR-N1L). The forward primers possess a *Bam*HI restriction site and the reverse primers a *Pst*I restriction site, each at their 5´ end. The amplified PCR fragments were digested with *Bam*HI and *Pst*I and ligated into the likewise digested vector plasmid pIII-lacZ2 (Figure 5.11). Correct insertion of the PCR products was verified by endonuclease restriction analysis and sequencing.

5.2.1.2 Generation of MVAΔN1L

To generate an N1L deletion mutant of MVA, CEF cells were infected with MVA and transfected with the deletion plasmid pΔK1LΔN1L 90 minutes post infection. The plasmid contains the K1L selection cassette between two homologous regions derived from flanking regions of the N1L ORF, allowing the exchange of the MVA-N1L gene with the K1L selection cassette by homologous recombination (Figure 5.12 and chapter 4.3.2).
After the infection/transfection, recombinant virus clones were isolated by four plaque passages on RK13 cells. Only recombinant virus clones encoding the K1L selection marker are able to replicate on this normally non-permissive cell line. Deletion of N1L was verified by PCR analysis using the primers DOM10 and DOM11, derived from flanking regions of the N1L ORF. Positive virus clones were then plaque-passaged on permissive CEF cells, in which the K1L selection marker is not essential for replication. Two homologous lacZ-repeats flanking the K1L ORF recombine and the selection marker is sliced out of the MVA genome leaving one lacZ-repeat. All successful recombination events were verified by PCR analysis after amplification of the final virus clone (Figure 5.13).
The deletion of the N1L ORF from the genome of MVA in MVAΔN1L was demonstrated by the inability to amplify a PCR fragment with primers derived from internal regions of the N1L ORF (Figure 5.13A). In contrast, N1L was detected by the same PCR with DNA derived from MVA-infected cells. Some instability on the left end side of the MVA genome was often recognized during the generation process of recombinant MVA variants (own observation). PCR analysis of the C7L ORF located within this region is therefore routinely performed during the generation of recombinant MVA. The presence of C7L in both, the recombinant

genome of MVAΔN1L and the wild type MVA genome demonstrates the integrity of the recombinant MVAΔN1L virus clone (Figure 5.13B).

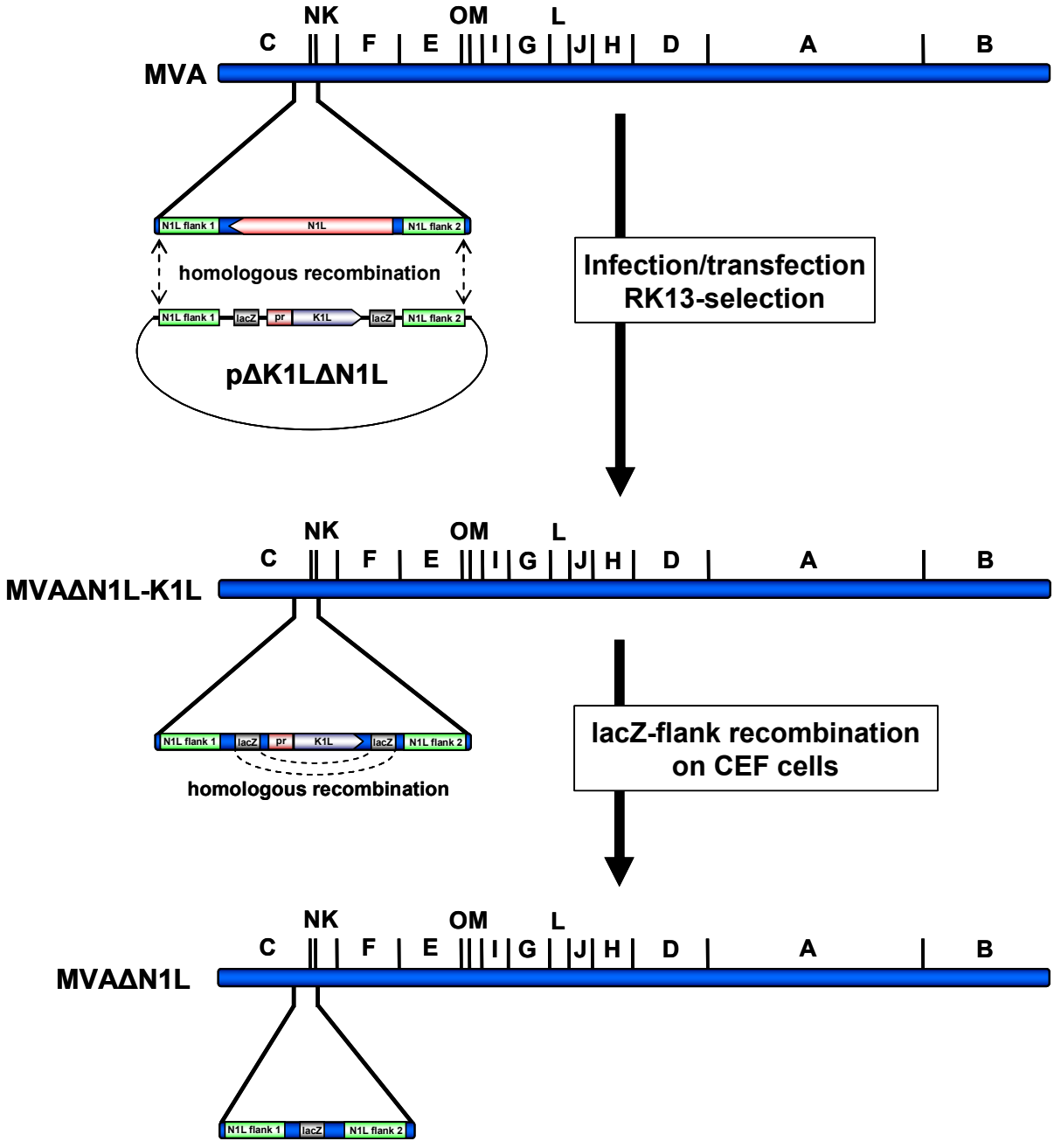

Figure 5.12: Generation of MVAΔN1L. Schematic presentation (not in scale) of the generation of recombinant MVA with a deleted N1L ORF. Further descriptions are given in the text.

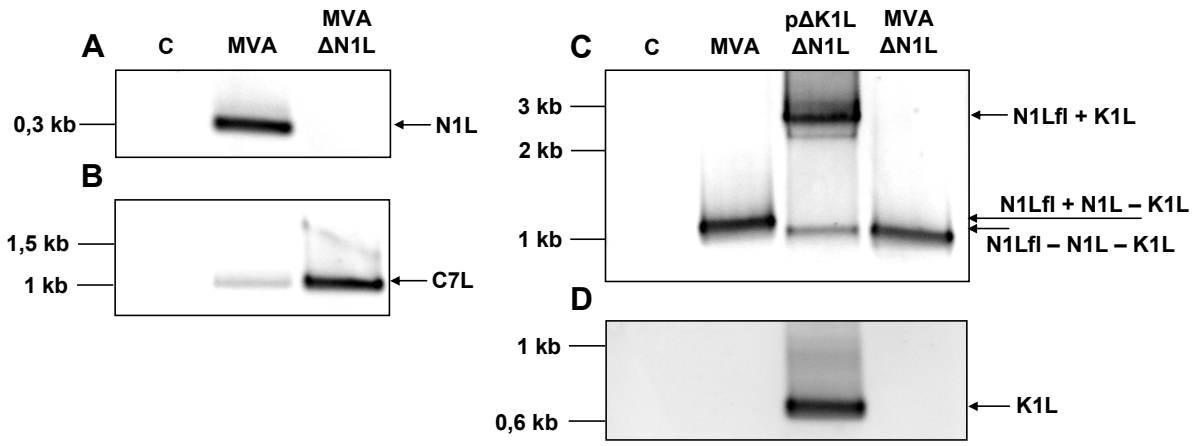

Figure 5.13: PCR analysis of MVAΔN1L. Viral DNA derived from infected CEF cells was analyzed by PCR with primers DOM8 and DOM9 derived from the N1L ORF (A), DOM25 and DOM26 derived from C7L ORF flanking regions (B), DOM10 and DOM11 derived from N1L ORF flanking regions (C) or K1Lint1neu and K1Lint2neu derived from the K1L ORF (D). Molecular sizes are given on the left, description of the bands on the right side. C: Water control.

To monitor the deletion of the K1L selection marker after plaque passaging on CEF cells, a PCR analysis was performed using primers derived from the N1L flanking regions and from internal regions of the K1L ORF. As shown in figure 5.13C and D, no fragment containing K1L was amplified in both PCR reactions using template DNA derived from MVAΔN1L-infected CEF cells. As expected, K1L containing bands were visible when the plasmid DNA derived from pΔK1LΔN1L was used as template. The PCR with primers derived from the flanking regions of the N1L ORF shows a very small shift of ~100 bp in MVA compared to MVAΔN1L (Figure 5.13C, lower bands). This fact is due to the deletion of the small N1L ORF (342 bp) and the remaining of one lacZ repeat sequence (~200 bp). The prominent band of ~2,5 kb detected in the PCR using plasmid DNA as template (Figure 5.13C, upper band) represents the whole recombination cassette including the K1L selection marker. Together, the PCR analyses of MVAΔN1L showed that all desired recombination events were successfully introduced into virus genome. The virus was then amplified and sucrose-purified as described in the Methods (chapter 4.3.2).

5.2.1.3 Generation of revertant viruses MVA-N1L$_{rev}$ and MVA-WRN1L$_{rev}$

The generation of an MVA variant with a reinserted N1L open reading frame was done by infection of CEF cells with MVAΔN1L and transfection with the recombination plasmid pIII-N1L-lacZ2 90 minutes post infection (Figure 5.14). Recombinant virus clones were selected by serial plaque passaging on RK13 cells and during the following passages on CEF cells the

K1L selection marker was sliced out of the genome of the MVA-N1L$_{rev}$ virus. The identification of recombinant virus clones is analog to the construction of MVAΔN1L (see chapter 5.2.2.1) with the difference of the used parental virus and insertion plasmid used for recombination. After PCR analysis of the selected virus clone, MVA-N1L$_{rev}$ was amplified and sucrose purified.

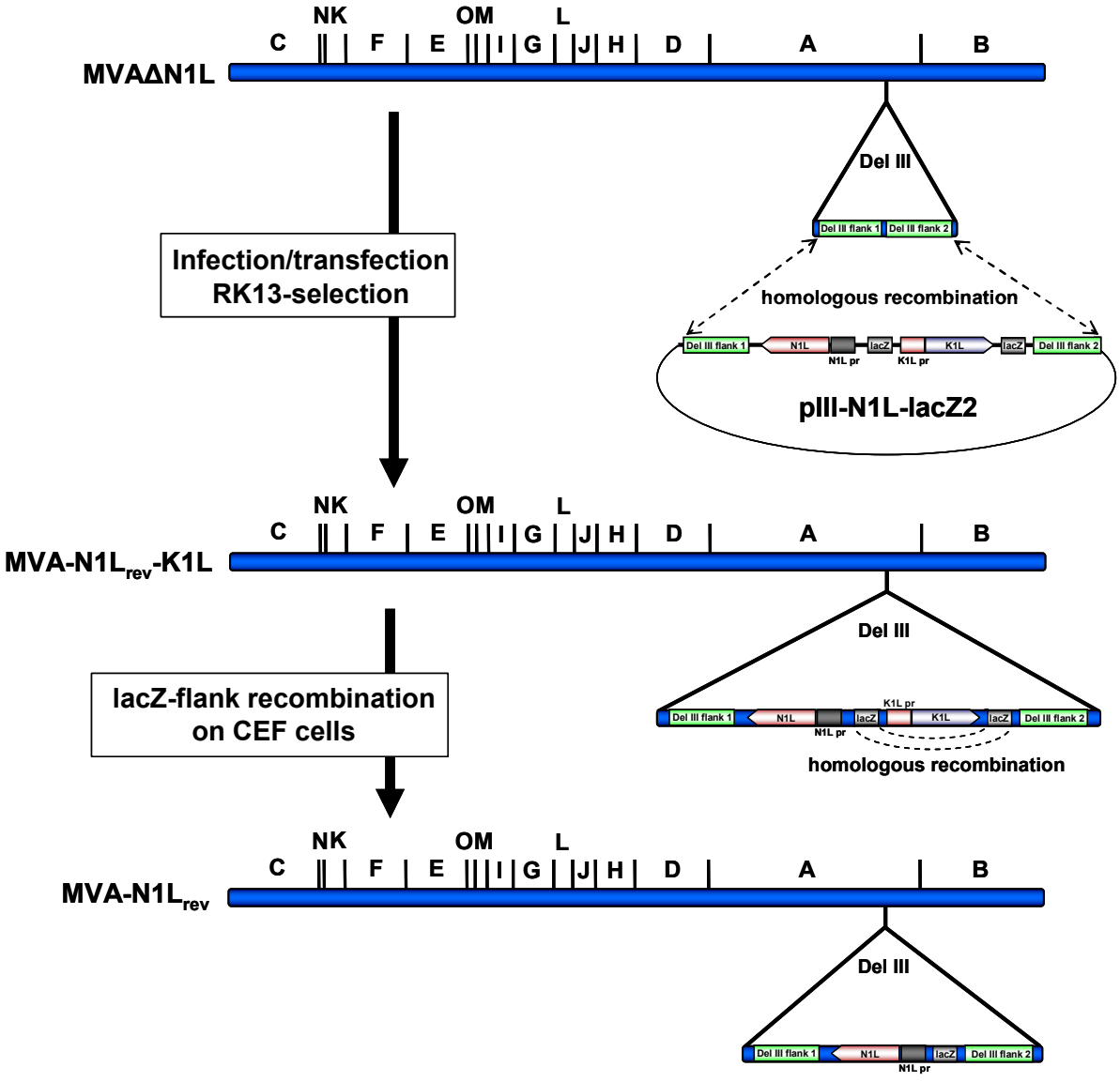

Fig. 5.14: Generation of MVA-N1L$_{rev}$. Schematic presentation (not in scale) of the generation of recombinant MVAΔN1L with a reinserted N1L ORF. Further descriptions are given in the text.

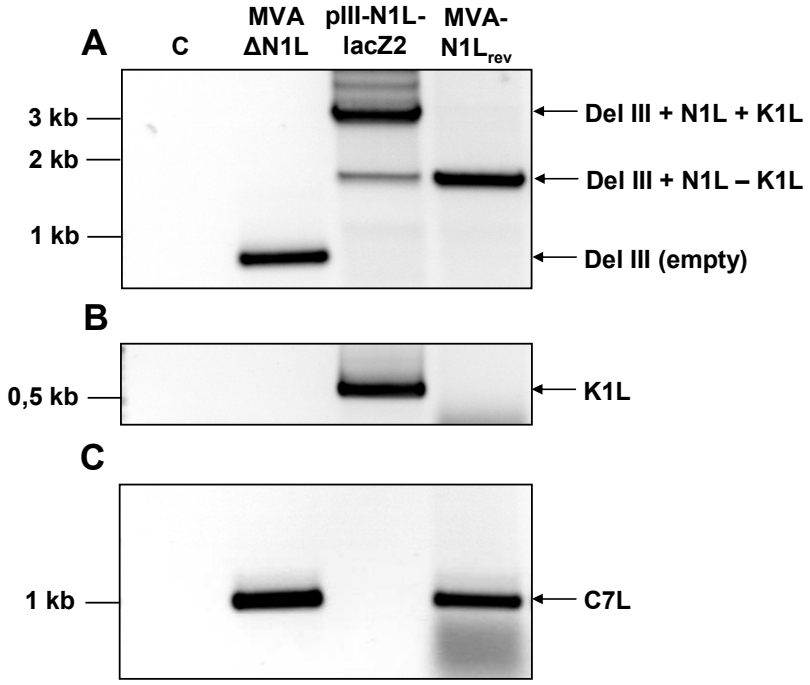

Figure 5.15: PCR analysis of MVA-N1L$_{rev}$. Viral DNA derived from infected CEF cells was analyzed by PCR with primers HLPEI66 and HLPEI67 derived from flanking regions of the deletion III (A), K1Lint1neu and K1Lint2neu derived from internal regions of the K1L (B) or DOM25 and DOM26 derived from flanking regions of the C7L (C) ORFs. Molecular sizes in kb are given on the left, description of the bands on the right side. C: water control.

Insertion of the N1L ORF into the deletion III of the MVAΔN1L genome was proved by PCR analysis using primers derived from flanking regions of the deletion III. A band of ~3 kb represents the recombination cassette in the plasmid pIII-N1L-lacZ2. This band shifted to ~1,8 kb when the K1L selection marker is removed from the genome (Figure 5.15A). An additional PCR with primers derived from the K1L ORF confirmed the deletion of K1L sequence from the genome of MVA-N1L$_{rev}$ virus (Figure 5.15B). The stability of the left side of the genome was analyzed by PCR with primers derived from flanking regions of the C7L ORF. A band of ~1 kb showed the presence of C7L in both viruses analyzed (Figure 5.15C).
The generation of a further revertant MVA with an inserted N1L ORF derived from vaccinia virus WR was identical to the generation of MVA-N1L$_{rev}$ (Figure 5.14) with the difference of using the plasmid pIII-WRN1L-lacZ2 for recombination. The PCR analysis of the selected final virus clone is shown in Figure 5.16.

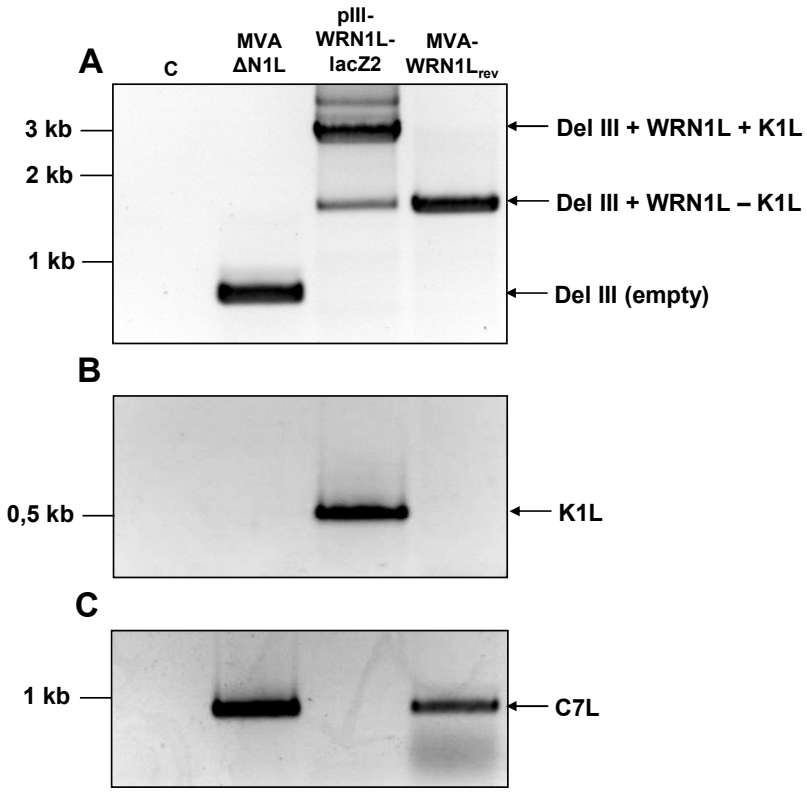

Figure 5.16: PCR analysis of MVA-WRN1L$_{rev}$. Viral DNA derived from infected CEF cells was analyzed by PCR with primers HLPEI66 and HLPEI67 derived from flanking regions of the deletion III (A), K1Lint1neu and K1Lint2neu derived from internal regions of the K1L (B) or DOM25 and DOM26 derived from flanking regions of the C7L (C) ORFs. Molecular sizes in kb are given on the left, description of the bands on the right side. C: water control.

As in the PCR analysis for MVA-N1L$_{rev}$ (Figure 5.15), the insertion of the WR-derived N1L ORF (WRN1L) including the K1L selection marker was monitored by an ~3 kb PCR fragment. This band shifted to ~1,8 kb after deletion of the K1L selection cassette in the MVA-WRN1L$_{rev}$ virus (Figure 5.16A). Deletion of the selection marker was confirmed by a K1L ORF-specific PCR (Figure 5.16B) and stability of the left-side of the genome was proved by detection of a C7L-specific PCR fragment (Figure 5.17C). Afterwards, the virus was amplified on CEF cells and sucrose purified.

5.2.1.4 Growth analysis of recombinant MVA

To characterize the newly generated recombinant MVA variants MVAΔN1L, MVA-N1L$_{rev}$ and MVA-WRN1L$_{rev}$, the growth capacity of the viruses was analyzed under conditions which were permissive (Figure 5.17) and non-permissive (Figure 5.18) for MVA replication.

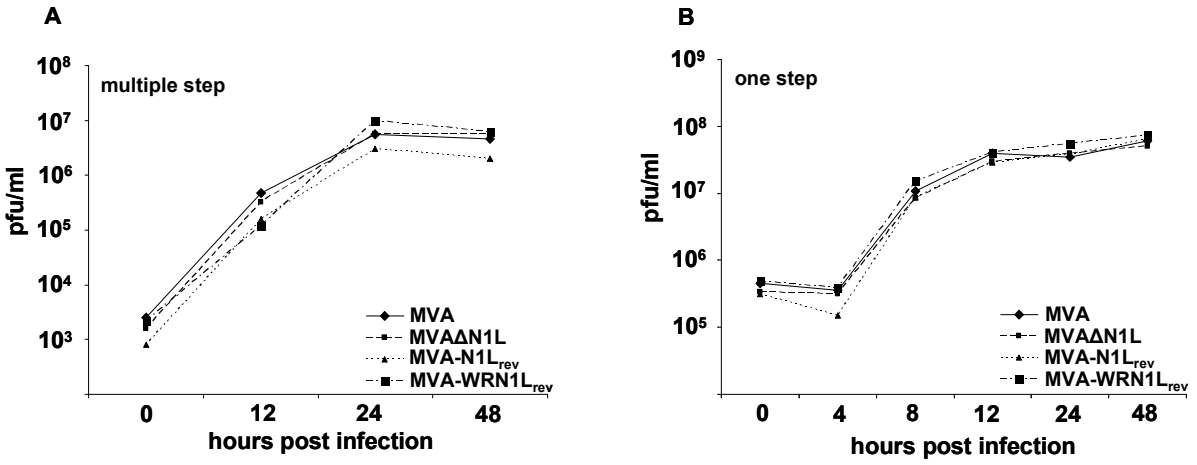

Figure 5.17: Growth analysis of recombinant MVA under permissive conditions. CEF cells were infected with MVA, MVAΔN1L, MVA-N1L$_{rev}$ or MVA-WRN1L$_{rev}$ at an moi of 0,05 (A) or 10 (B). After the delineated time points, cell-virus suspensions were harvested and back-titrated on CEF cells.

All recombinant N1L-specific MVA variants replicated to high titers in infected permissive CEF cells with equal kinetics to MVA (Figure 5.17). No differences in replication under multiple step, where cells were infected with an moi of 0,05 to ensure multiple replication cycles, as well as under one step conditions, where only one replication cycle is performed due to the high moi of 10, were detectable. Therefore, deletion of N1L from the genome of MVA has no influence on replication of the virus in permissive chicken embryo fibroblasts. Moreover, an MVA variant with a reconstituted N1L open reading frame derived from the replication competent vaccinia virus WR shows no alteration in replicative ability in these cells.

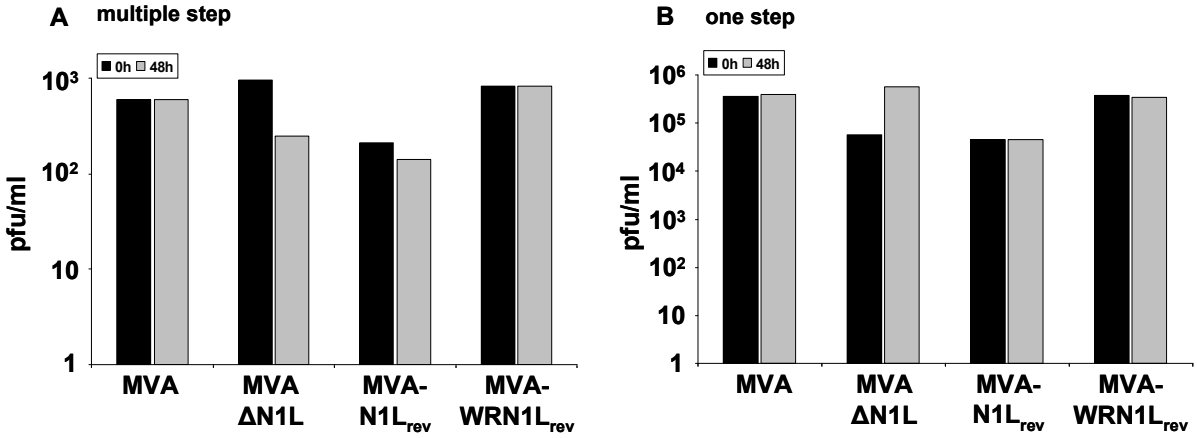

Figure 5.18: Growth analysis of recombinant MVA under non-permissive conditions. NIH-3T3 cells were infected with MVA, MVAΔN1L, MVA-N1L$_{rev}$ or MVA-WRN1L$_{rev}$ at an moi of 0,05 (A) or 10 (B). After 0 and 48 hours, cell-virus suspensions were harvested and back-titrated on CEF cells.

Under non-permissive conditions, in the murine NIH-3T3 cell line, all analyzed viruses were unable to replicate (Figure 5.18). After 48 hours of infection, a time-point at which several replication cycles were performed in permissive cells, no increase in viral infectivity could be measured. Therefore, the reconstitution of a functional N1L open reading frame in MVA has no influence on replicative ability in murine NIH-3T3 cells, suggesting that functional N1 expression did not broaden the MVA tropism to murine cells.

5.2.1.5 Anti-apoptotic function of N1

The N1 protein encoded by WR structurally resembles the cellular anti-apoptotic molecule bcl-2 and was shown to have the capability to inhibit staurosporine-induced apoptosis after infection with vaccinia virus (Cooray et al., 2007). To confirm the apoptosis-inhibiting capacity of the WR-derived N1 protein encoded by MVA and to compare its activity with the natural MVA-derived N1 protein, NIH-3T3 cells were infected with the generated MVA variants. 11 hours post infection, apoptosis was induced by the addition of staurosporine, whereas in a parallel control experiment, the infected cells were left untreated. After 4 hours of staurosporine treatment cells were harvested and analyzed by FACS with an antibody directed against activated caspase-3, the main cellular apoptotic effector caspase.

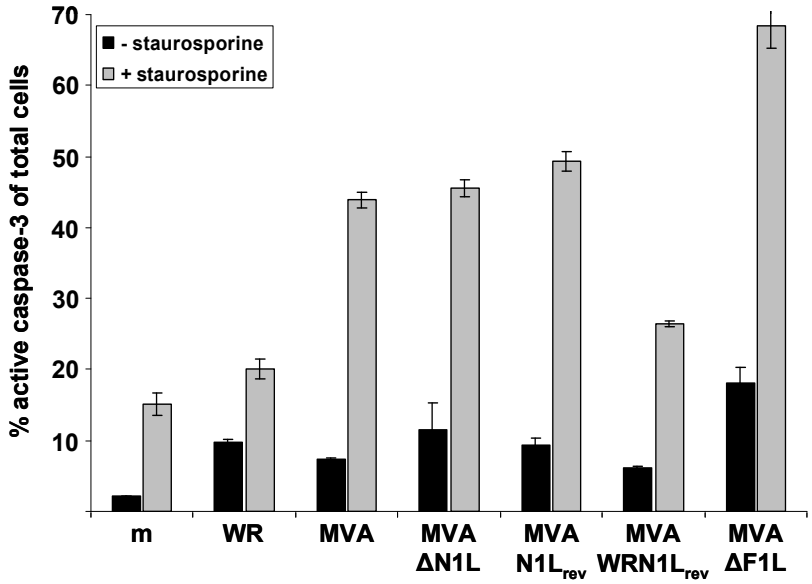

Figure 5.19: Inhibition of staurosporine-induced apoptosis by vaccinia viruses encoding N1. NIH-3T3 cells were mock-infected or infected with WR, MVA, MVAΔN1L, MVA-N1Lrev, MVA-WRN1Lrev or MVAΔF1L at an moi of 10. 11 hours post infection cells were treated with 1 µM staurosporine for 4 hours. Cells were then harvested and analyzed by FACS with an antibody detecting active caspase-3. Results represent mean +/- s.d. of three independent experiments. m: mock-infected control

As shown in Figure 5.19, the addition of staurosporine led to a strong induction of apoptosis in MVA-infected cells as ~45% of all NIH-3T3 cells showed activation of caspase-3. However, when the cells were infected with WR or with the MVA variant encoding the WR-related N1L ORF (MVA-WRN1L$_{rev}$), only ~25% of cells showed activation of caspase-3, confirming the apoptosis-inhibiting capacity of the WR-derived N1 protein, also when expressed by MVA. In contrast, MVA-derived N1 encoded by MVA and MVA-N1Lrev, respectively, did not result in inhibition of staurosporine-induced apoptosis, indicating that the apoptosis-inhibiting function of N1 is lost in MVA. Deletion of the N1L ORF from the genome of MVA did also not alter the number of active caspase-3-positive cells compared to MVA infection, supporting the hypothesis of a non-functional N1L ORF encoded by MVA. Deletion of the F1L ORF, encoding a known inhibitor of apoptosis, from the genome of MVA leads to a strong induction of apoptosis after infection and an absolute inability to inhibit staurosporine-induced apoptosis (Figure 5.19, last lane and Fischer et al., 2006). The addition of staurosporine alone, in the absence of infection, led only to a minor number of active caspase-3 positive cells, reflecting the relative resistance of NIH-3T3 cells against staurosporine treatment under the experimental conditions applied. However, MVA infection presumably leads to a sensitization of the cells, as treatment with staurosporine after MVA-infection leads to the high amount of apoptosis described above.

5.2.1.6 N1L expression after viral infection

To prove if the loss of functionality of the MVA-derived N1L is possibly due to different expression levels compared to the WR-derived N1L, expression of the gene was analyzed after infection of human HeLa and murine NIH-3T3 cells. N1L-expression is driven by an vaccinia virus early promotor (Bartlett et al., 2002), therefore, northern blot analysis was performed already two hours after infection of HeLa cells to prove the functional transcription of the N1L ORF (Figure 5.20).

In cells infected with WR, MVA, MVA-N1L$_{rev}$ and MVA-WRN1L$_{rev}$, transcripts hybridizing with an N1L-specific RNA probe were detected. Interestingly, N1L transcripts derived from the N1L gene located on its natural position near the left side of the genome appeared as two different transcripts, presumably because of two different transcription start sites. The different size between WR and MVA-encoded mRNAs is likely due to different transcription termination sites as the natural transcription termination signal in WR is deleted in MVA.

When reinserted into the deletion III of the MVA genome, both the MVA- and WR-derived N1L ORFs encode for only one transcript of comparable size. In MVAΔN1L-infected HeLa cells no N1L specific mRNA was detected, confirming the deletion of the ORF from the genome of MVA.

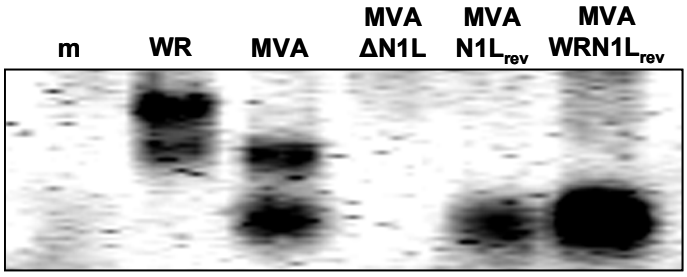

Figure 5.20: N1L transcript-specific northern blot analysis of infected HeLa cells. Cells were mock-infected or infected with WR, MVA, MVAΔN1L, MVA-N1L$_{rev}$ or MVA-WRN1L$_{rev}$ at an moi of 10. 2 hours post infection total RNA was harvested, blotted on positively charged nylon membranes and analyzed with an N1L-specific RNA-probe. M: mock-infected control.

To analyze the production of a functional N1 protein expressed by the different N1L-specific MVA variants as well as WR, western blot analysis was performed with cell lysates from infected NIH-3T3 cells. Interestingly, only the WR-derived N1L ORFs encoded by vaccinia virus WR and MVA-WRN1L$_{rev}$ were translated into a stable protein (Figure 5.21). In contrast, detection of N1 expressed from the MVA-derived N1L ORFs encoded by MVA and MVA-N1L$_{rev}$ was not possible, despite the presence of N1L-specific transcripts (Figure 5.20). When analyzed in the presence of lactacystin, an irreversible inhibitor of the proteasome, a faint band was detected in these probes, indicating that the MVA-derived N1 protein is expressed but rapidly degraded, possibly due to the mutated C-terminus, derived from the fused C5L ORF.

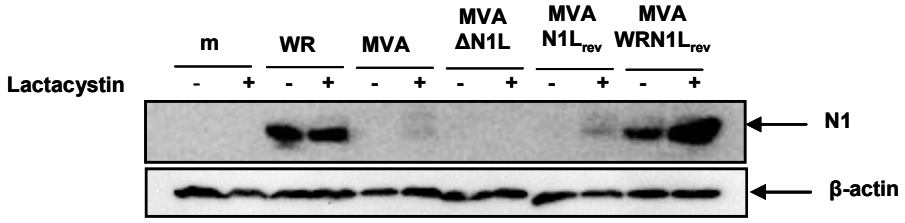

Figure 5.21: N1 protein-specific western-blot analysis of cell lysates derived from infected NIH-3T3 cells. Cells were mock-infected or infected with WR, MVA, MVAΔN1L, MA-N1L$_{rev}$ at an moi of 10 and cell lysates were prepared 24 hours after infection. Western-blot analysis was performed using an N1-specific primary and a PO-labelled rabbit-specific secondary antibody (upper panel). Equal loading was confirmed by detection of β-actin. m: mock-infected control.

5.2.2 Expression of N1 variants after transfection

5.2.2.1 Construction of plasmids expressing N1 variants

To analyze if the modified N1L ORF encoded by MVA, meaning the C-terminal fusion towards the part of C5, is the reason for the rapid degradation of the protein, four different variants of the ORF were cloned into the expression plasmid pC-mychis (Figure 5.22). The full length N1L ORFs derived from WR and MVA, respectively, were chosen (WRN1 and MVAN1) as well as one shortened version representing the first 270 nucleotides of N1L, which are identical in MVA and WR, encoding a protein of 90 amino acids ($N1_{90}$), and a longer construct with 39 additional nucleotides, derived from the WR-derived N1L sequence encoding a further α-helix in the protein (Cooray et al., 2007), which may be important for protein stability and functionality ($N1_{103}$).

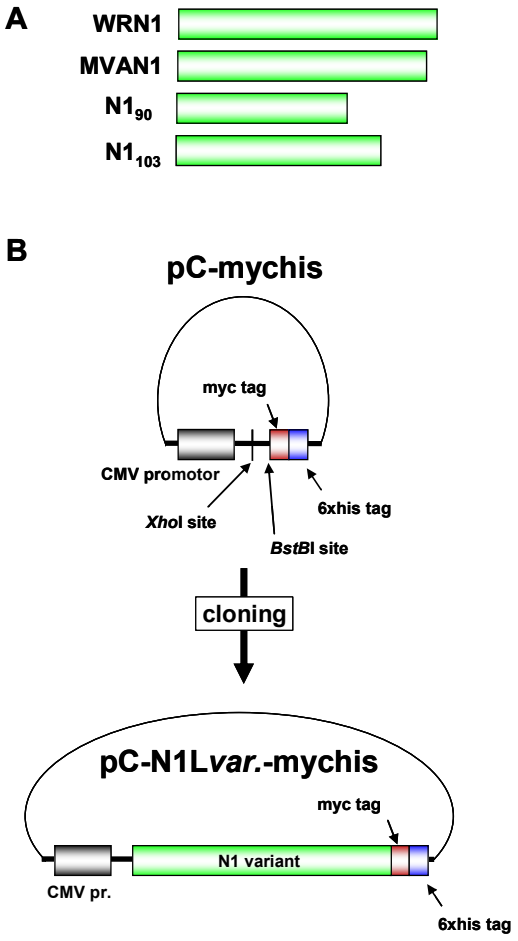

Figure 5.22: Cloning of N1L-specific expression plasmids. A Schematic presentation of different N1L variants. Numbers describe the amino acid length of the encoded proteins. **B** Schematic presentation of the cloning procedure.

The different N1L sequences were amplified by PCR using primer DOM18 with DOM20 (WRN1), DOM19 (MVAN1), DOM48 ($N1_{90}$) or DOM49 ($N1_{103}$). The forward (DOM18) and reverse primers possess an *Xho*I and *BstB*I restriction site, respectively (chapter 3.7). The terminal stop codon of the full length variants MVAN1 and WRN1 were not amplified by the PCR reaction because of a desired fusion of a mychis-tag derived from the expression plasmid. The PCR fragments and the pC-mychis expression plasmid were digested with *Xho*I and *BstB*I and the N1 variants were ligated in frame into the plasmid to obtain pC-N1*var*.-mychis. All plasmids were controlled by sequencing after the cloning procedures. In all plasmids, N1 expression is driven by a CMV promotor to guarantee continuous, highlevel and vaccinia virus independent expression. Additionally, all variants possess a c-terminal mychis-tag for detection.

5.2.2.2 Expression of N1 variants

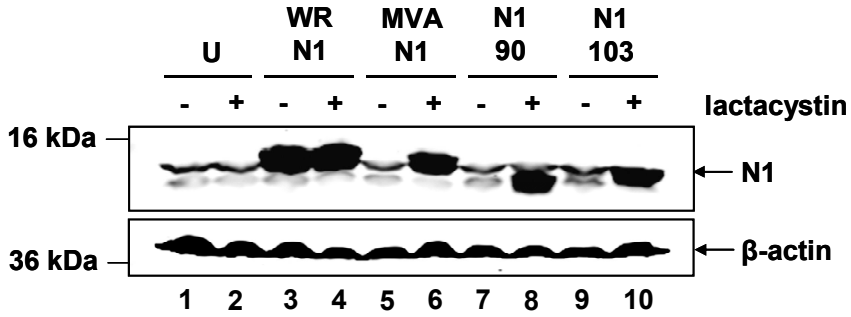

Figure 5.23: Plasmid-derived expression of N1 variants. 293T cells were transfected with expression plasmids encoding N1 variants in the absence or presence of 2 µM lactacystin. 48 hours after transfection, cell lysates were analyzed for N1 expression by western blot analysis with a his-specific antibody. Equal loading was confirmed by detection of β-actin. U: untransfected control.

For expression analysis, 293T cells were transfected with the different N1-specific plasmids. 48 hours after transfection, cell lysates were prepared and western blot analysis was performed with a his-specific antibody. As shown in Figure 5.23 (lane 3) only the WR-derived N1L open reading frame was expressed into a stable protein. In contrast, the MVA-related N1 protein could not be detected (Figure 5.23, lane 5) confirming the expression analysis in the background of viral infection (chapter 5.2.1.6). Both shortened N1 variants were also not detected in the transient expression analysis (Figure 5.24, lane 7 and 9). However, the expression of all undetectable variants was rescued when the proteasome-inhibitor lactacystin was added to the culture (Figure 5.23, lanes 6, 8 and 10), which indicates

the need for a functional C-terminus to stabilize the N1 protein and inhibit the rapid proteasome-mediated degradation of the molecule after translation. In summary, the MVA encoded N1L ORF is expressed after infection but the protein is rapidly degraded due to the non-authentic C-terminus and therefore presumably not able to exert its anti-apoptotic function.

5.3 Influence of the double-stranded RNA-binding protein E3 on the cellular RNA interference pathway

Sequence-specific gene silencing (RNA interference - RNAi) has developed into a useful tool for analyzing gene functions (Dykxhoorn et al., 2003). It is mediated by transfection of short interfering RNAs (siRNA), 19-23 nt long dsRNA molecules which perfectly match the target messenger RNA sequence (Tuschl 2002). The vaccinia virus E3 protein, encoded by the open reading frame E3L is known to bind and sequester dsRNA and thereby inhibits host cellular antiviral responses (Chang et al., 1992). E3 could potentially also sequester siRNA duplexes after vaccinia virus infection of the cell and therefore prevent gene silencing. To address this possibility, recombinant MVA encoding the *Escherichia coli lacZ* gene as a quantification marker for gene silencing using *lacZ*-specific siRNA was used.

5.3.1 SiRNA-mediated downregulation of a vaccinia virus-encoded marker gene

5.3.1.1 Downregulation of lacZ-expression early after MVA-infection

In the initial experiments, the MVA-encoded *lacZ* gene is encoded under the transcriptional control of the vaccinia virus K1L promotor, allowing β-galactosidase expression only during the early phase of the MVA life cycle. Two variants of MVA were used, MVA-lacZ$_{early}$ and an E3L gene deletion mutant of the MVA-lacZ virus (MVAΔE3L-lacZ$_{early}$).
HeLa cells were transfected with 1 µg *lacZ*-specific siRNA and were infected 24 hours later with either MVA-lacZ$_{early}$ or MVAΔE3L-lacZ$_{early}$ at an moi of 0,5. MVA-infected HeLa cells transfected with a siRNA directed against the green fluorescent protein (GFP) were used as a negative control. At different time points after infection, cell lysates were prepared and analyzed for β-galactosidase activity. As shown in figure 5.24A, β-galactosidase acitivity of MVA-lacZ$_{early}$-infected and lacZ-siRNA-treated cells was significantly reduced from 3 hours post infection, compared to GFP-siRNA-transfected cells. There was still a high level of β-galactosidase activity 10 hours post-infection in GFP-siRNA-treated cells, even though β-galactosidase was produced under the control of an early promoter. This is most likely due to an accumulation of the β-galactosidase protein which can be ascribed to its high stability. In MVAΔE3L-lacZ$_{early}$ infected HeLa cells, the same rate of β-galactosidase activity reduction

by treatment with lacZ-specific siRNA was found (Figure 5.25B), indicating that the E3 protein dos not interfere with RNAi.

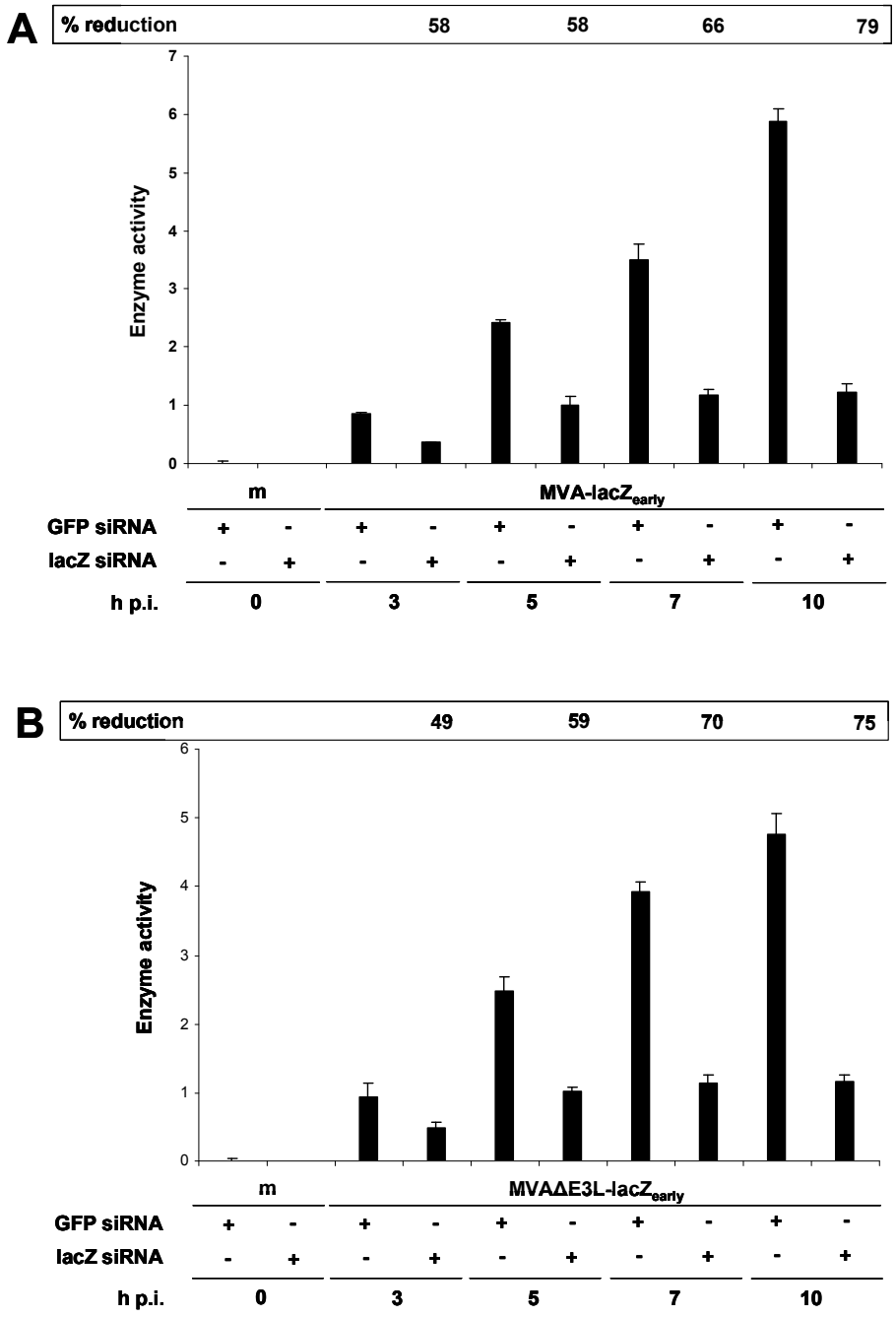

Figure 5.24: MVA-encoded E3 protein does not influence lacZ-specific RNAi analyzed by β-galactosidase activity. HeLa cells were transfected with 1 µg lacZ- or GFP-siRNA. After 24 hours, cells were infected with MVA-lacZ$_{early}$ (A) or MVAΔE3L-lacZ$_{early}$ (B) at an moi of 0,5. β-galactosidase activity of cell lysates equalized to the protein amount used is given for the indicated time points post-infection. The relative reduction mediated by the lacZ-siRNA was calculated with the use of the appropriate GFP-siRNA-transfected control. Results represent means and s.d. of three independent experiments. m: mock-infected control

The downregulation of lacZ-specific mRNA encoded by MVA was further analyzed by Northern blot analysis, which shows the target site of RNAi more directly, using the same

experimental setting as described above. Comparison of lacZ-siRNA-treated with GFP-siRNA-treated cells showed a clear reduction in the amount of *lacZ* transcripts at 3 and 5 hours after infection (Figure 5.25). No differences in the downregulation of lacZ-specific mRNA could be detected in the presence (MVA-lacZ$_{early}$, Figure 5.25A) or absence (MVAΔE3L-lacZ$_{early}$, Figure 5.25B) of the E3 protein. The higher lacZ-specific mRNA levels observed 3 hours after infection with MVAΔE3L-lacZ$_{early}$ only reflect the overall higher early mRNA levels as illustrated by the GFP-siRNA-treated sample 3 hours after infection (Figure 5.25B, third left lane). However, a full reduction in mRNA levels or enzyme activity could not be observed, which is most probably due to the efficiency of the siRNA used, which is not able to completely downregulate the lacZ transcript levels (Reynolds et al., 2004). The results indicate that MVA-encoded early genes can be downregulated by the cellular RNA interference machinery following transfection of sequence-specific siRNAs prior to infection. Moreover, the presence of the dsRNA-binding protein E3 did not affect RNAi at early time points after infection.

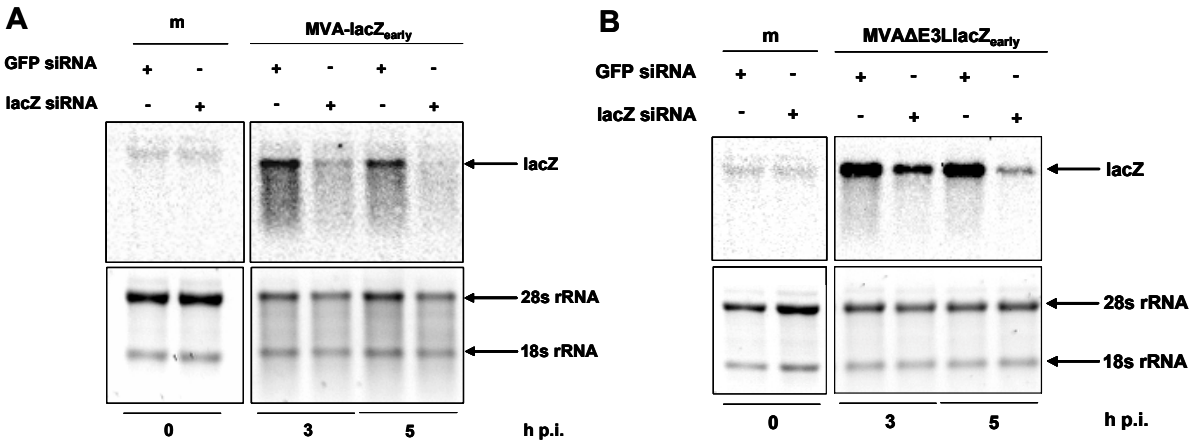

Figure 5.25: MVA-encoded E3 protein does not influence MVA-encoded lacZ-specific RNAi analyzed by Northern blot. HeLa cells were transfected with 1 µg lacZ- or GFP-siRNA. After 24 hours, cells were infected with MVA-lacZ$_{early}$ (A) or MVAΔE3L-lacZ$_{early}$ (B) at an moi of 0,5. Total RNA was isolated at the delineated time points post infection and Northern blot analysis was performed with a probe specific for the lacZ transcript. Ethidium bromide staining of rRNA was used as a loading control. The results are representative of at least three independent experiments. m: mock-infected control

5.3.1.2 Downregulation of lacZ-expression during late stages after infection

The E3L gene is expressed early during the viral infection cycle (Chang et al., 1992). However, after infection of HeLa cells with MVA, the E3 protein could be detected by Western blot analysis even 24 hours after infection (Figure 5.26A). The amount of E3 mRNA

however, declined as illustrated by Northern blot analysis in Figure 5.26B and was barely detectable after 24 hours, indicating a high protein stability of E3. It has been described that deletion of E3L from the MVA genome results in a block of intermediate gene expression and a lack of late gene products (Hornemann et al., 2003; Ludwig et al., 2005), impeding the analysis of RNAi of late gene products devoid of the presence of E3. Therefore, analysis of the impact of E3 on RNAi of late gene products was done solely in the presence of E3.

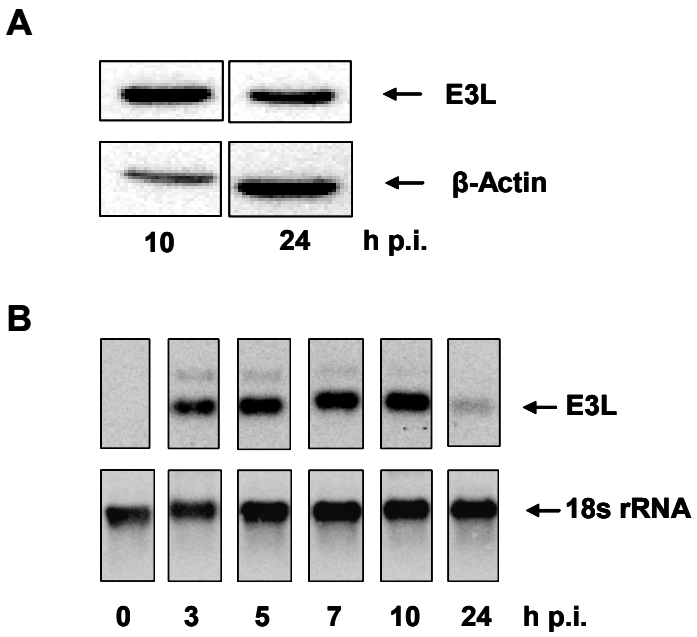

Figure 5.26: Analysis of the E3L expression kinetics. (A) HeLa cells were infected with MVA at an moi of 0,5 and after 10 and 24 hours cell lysates were prepared and analyzed by Western blot using an E3 specific antibody. Equal loading was confirmed by detection of β-actin. (B) HeLa cells were infected with MVA at an moi of 0,5. Total RNA was isolated at the delineated time points post infection and Northern blot analysis was performed with a probe specific for the E3L transcript. The amount of 18S rRNA detected after hybridization was used as a loading control.

To assess RNAi of late gene products, a recombinant MVA expressing the *lacZ* gene under the control of the vaccinia virus late promoter P11 (Sutter and Moss, 1992) was used, which enables *lacZ* transcription only at late time points during the infection cycle (MVA-lacZ$_{late}$). HeLa cells were again transfected with lacZ-specific or GFP-specific siRNA 24 hours prior to infection with MVA-lacZ$_{late}$. Cell lysates were prepared at different time points after infection and β-galactosidase activity was measured. As shown in Figure 5.27, β-galactosidase activity was strongly impaired by transfection of lacZ-specific siRNA compared to GFP-specific siRNA. The relative reduction was as high as that observed with lacZ expressed during early time points of infection using MVA-lacZ$_{early}$ or MVAΔE3L-lacZ$_{early}$ (Figure 5.24A).

However, the absolute values obtained after RNAi with MVA-lacZ$_{late}$ were higher due to a naturally higher expression rate mediated by the strong late promoter P11.

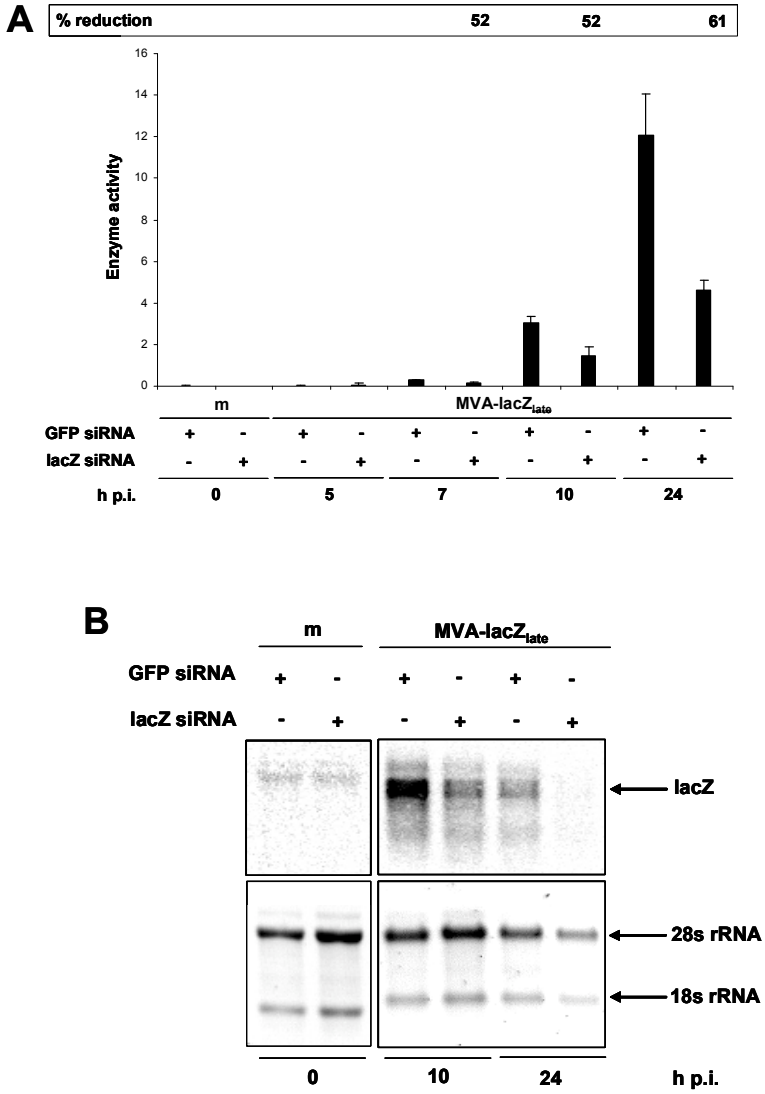

Figure 5.27: LacZ silencing in MVA-lacZ$_{late}$ infected HeLa cells. (A) HeLa cells were transfected with 1 µg lacZ- or GFP-siRNA. After 24 hours, cells were infected with MVA-lacZ$_{late}$ at an moi of 0,5. β-galactosidase activity equalized to the protein amount used is given for the indicated time points post infection. The relative reduction mediated by the lacZ-siRNA was calculated with the use of the appropriate GFP-siRNA-transfected control. Results represent means and s.d. of three independent experiments. (B) HeLa cells were treated as mentioned above. Total RNA was isolated at the delineated time points post infection and Northern blot analysis was performed with a probe specific for the lacZ transcript. Ethidium bromide staining of rRNA was used as loading control. The results are representative of at least three independent experiments. m= mock-infected control.

Again, the downregulation of the *lacZ* transcripts was analyzed by Northern blot analysis and showed a significant decrease in *lacZ* mRNA in lacZ-siRNA-transfected cells (Figure 5.27B). This indicates that it is possible to target early and late viral gene products with sequence-specific siRNA during vaccinia virus infections and E3 does not interfere with RNAi.

5.3.2 SiRNA-mediated gene knock-out of the E3L gene product induces phenotypic alterations in the MVA life cycle

Since it is possible to downregulate vaccinia virus gene products using siRNA, it would be interesting if MVA gene function could be analyzed with the help of RNAi. The E3L gene product was chosen for downregulation, as the MVA-E3L-deletion mutant shows a defined phenotype in HeLa cells, consisting of a block in the viral life cycle at the level of intermediate gene expression and, therefore, a lack of late gene products (Hornemann et al., 2003; Ludwig et al., 2005; Ludwig et al.,2006). HeLa cells were transfected with two different siRNAs specific for the E3L transcript 24 hours prior to MVA infection. Northern blot analysis of mRNA prepared at different time points after infection revealed a downregulation of E3L-specific transcripts (Figure 5.28). The levels of reduction produced by the different siRNAs were unequal, which demonstrates a frequently observed ability for different siRNAs (Sliva and Schnierle, 2006).

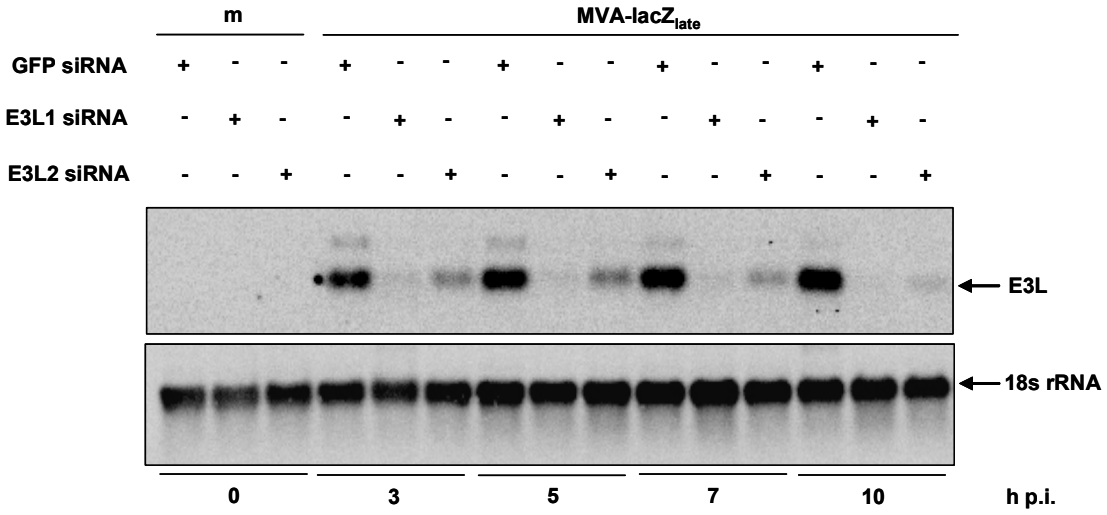

Figure 5.28: SiRNA-mediated downregulation of vaccinia virus E3L transcripts. HeLa cells were transfected with 1 µg E3L-si1-, E3L-si2- or GFP-siRNA. After 24 hours, cells were infected with MVA-lacZ$_{late}$ at an moi of 0,5. Total RNA was isolated at the delineated time points post infection and Northern blot analysis was performed with a probe specific for the E3L transcript. The amount of 18S rRNA detected after hybridization was used as a loading control. m: mock-infected control

To determine whether the siRNA-mediated phenotype represents an E3L knock-out mutant of MVA, we analyzed late lacZ-expression in MVA-lacZ$_{late}$-infected cells. The change in phenotype was investigated with siRNA E3L-si1 (Dave et al., 2006), which proved to be more potent in inhibiting E3L gene expression (Figure 5.28). HeLa cells were transfected with E3L-si1 or GFP siRNA 24 hours prior to infection. Cell lysates were prepared 10 and 24 hours

after infection and analyzed for β-galactosidase activity (Figure 5.29). E3L-si1 treatment severly decreased the amount of β-galactosidase in MVA-lacZ$_{late}$-infected cells compared to treatment with the GFP-specific siRNA, and thus mimicked the absence of late gene products upon infection with an E3L deletion mutant (Ludwig et al., 2006).

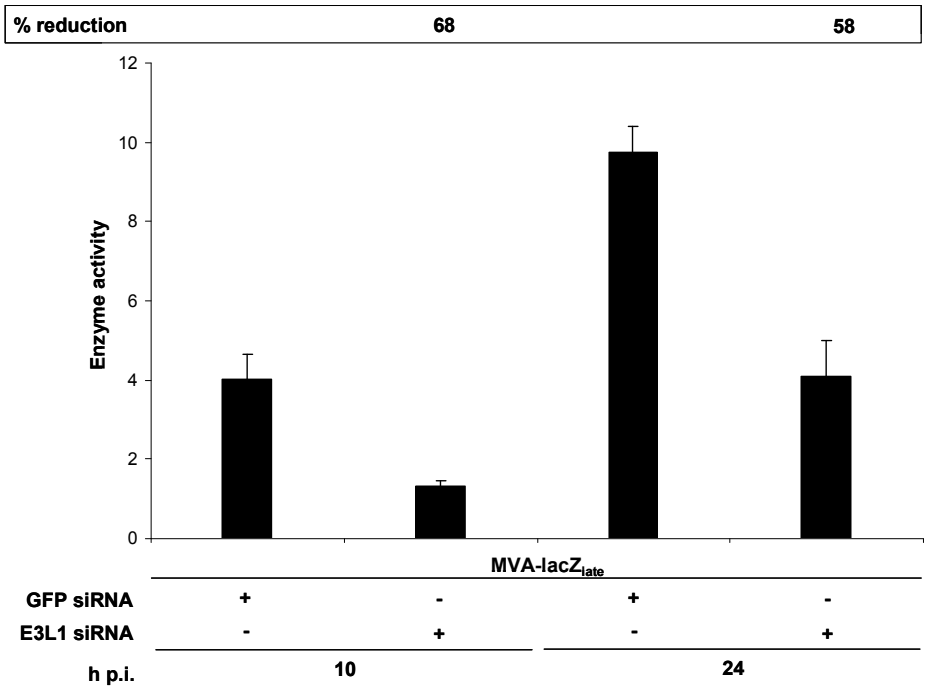

Figure 5.29: Simulation of MVA deletion mutants by RNAi. HeLa cells were transfected with 1 µg E3L-si1- or GFP-siRNA. After 24 hours, cells were infected with MVA-lacZ$_{late}$ at an moi of 0,5. Cell lysates were prepared 10 and 24 hours after infection and analyzed for β-galactosidase activity. Results represent data of three independent experiments.

Dave et al. showed recently that inhibition of E3L gene expression by siRNA can be used to block vaccinia virus replication in human cells which resembles the phenotype of an E3L knock-out vaccinia virus and confirms our results (Dave et al., 2006). These data indicate that siRNA can be used to analyze vaccinia virus gene function and might be applied as a screening procedure to identify genes generating a specific phenotype.

6 Discussion

The Modified vaccinia virus Ankara is being developed as a third generation smallpox vaccine as well as recombinant vector vaccine against infectious diseases and cancer. Its potent immunogenicity and the very good safety profile make the virus well suited for its application as novel vaccine in humans. During the attenuation process on chicken embryo fibroblast cells, the virus lost many immunomodulatory gene functions, present in the genome of the parental chorioallantois vaccinia virus Ankara (CVA), normally responsible for the counteraction of host/cellular antiviral responses. However, some immunomodulatory genes are still conserved in the genome of MVA. The cellular induction of apoptosis is one of the important antiviral mechanisms, the virus has to prevent after infection to fully enable virus replication. Thus, it is not astonishing that several anti-apoptotic gene functions are still encoded by MVA, including F1L, N1L and E3L. The potent inhibitor of apoptosis F1L was shown to interfere with the mitochondrial apoptotic signal transduction pathway by inhibiting the activation of the mitochondrial effector molecules Bax and Bak (Fischer et al.,2006; Wasilenko et al., 2005; Taylor et al., 2006). The N1L open reading frame encodes a protein with structural bcl-2 homology, which seems to bind several cellular pro-apoptotic BH3-only proteins and thereby also inhibit the mitochondrial pathway of apoptosis (Cooray et al., 2007). The vaccinia virus early E3 protein functions by binding to dsRNA molecules and therefore inhibiting the antiviral RNaseL and PKR pathways, the activation of which also results in the induction of apoptosis (Chang et al., 1992; Rivas et al.,1998; Garcia et al., 2002). In order to better understand the individual function and influence of these genes, also in the context of MVA as a vaccine, they were analyzed in this work.

6.1 MVAΔF1L efficiently provides protective immunity against lethal orthopoxvirus challenge

The MVA ORF 031 encodes for the well-characterized vaccinia virus F1L homologue which had been clearly demonstrated *in vitro* to prevent apoptosis. Deletion of F1L from the genome of vaccinia virus or MVA resulted in the induction of apoptosis in human cell lines (Wasilenko et al., 2005; Fischer et al., 2006), a phenotype which could be confirmed in this work for MVAΔF1L infection of the murine cell line NIH-3T3. Interestingly, apoptosis

induction was even more profound in primary mouse embryonic cells infected with MVAΔF1L suggesting a potent apoptosis induction in primary cells and presumably also *in vivo*.

DNA viruses of different families exploit the induction of apoptosis for efficient virus spreading (Roulston et al., 1999). Very recently it was found that apoptotic mimicry by vaccinia virus is a potent mechanism also for cell entry and spreading (Mercer and Helenius, 2008). This could imply that F1L counteracts with virus entry and spreading, however, deletion of F1L in vaccinia virus did not result in any appreciable effect concerning viral assembly or overall life cycle (Postigo et al., 2006; Wasilenko et al., 2005). This fact was also confirmed for MVA in this work by the analysis of the viral gene expression profile in infected murine NIH-3T3 cells, in which no alterations in the viral life cycle could be detected in the absence of F1, suggesting F1L to be rather necessary for other virus functions like a possible role in immune evasion.

T cell priming by vaccinia virus occurs through different pathways, either by direct presentation of antigens via MHC class I molecules in infected professional antigen presenting cells (pAPC) or by cross-presentation through phagocytosis of vaccinia virus-infected cells by pAPCs (Liu et al., 2008; Gasteiger et al., 2007). Interestingly, cross-priming of T cells was shown to represent an essential mechanism by which MVA-encoded antigens are presented to the immune system (Gasteiger et al., 2007). Preventing apoptosis could therefore likely decrease cross-presentation of viral antigens due to the reduction of virus-infected apoptotic cells which are uptaken and processed by professional antigen presenting cells, and therefore could be a logic immune evasion strategy of the virus. Due to the importance of the indirect antigen presentation pathway after MVA infection and the expression of several anti-apoptotic proteins by MVA, deletion of F1L from the genome of MVA could lead potentially to an enhancement of the viral immune stimulating capacity. Alternatively, apoptosis might interfere with antigen synthesis and have a negative impact on vaccine induced immune responses (Kim et al., 2003). This latter assumption seemed to be relevant, because *in vitro* infections with another MVA mutant inactivated in the E3L gene are characterized by an abrupt onset of apoptosis associated with the collapse of late viral antigen synthesis (Ludwig et al., 2006). In contrast, MVAΔF1L can efficiently induce apoptosis in murine NIH-3T3 cells with an apparent retained viral late gene expression and antigen production. This data is in line with the previous observation that deletion of F1L in vaccinia virus strain Copenhagen did not disturb the overall virus life cycle (Wasilenko et al., 2005). The early induction of apoptosis at already 8 hours after infection as it was observed in

primary mouse embryo fibroblast cells could argue for a premature stop of the overall viral protein synthesis *in vivo*. However, late vaccinia virus transcripts normally peak at already 5 to 6 hours after infection which could still allow for late antigen synthesis within these cells (Moss, 2007). Additionally, synthesis of late viral antigens might not be that critical for T cell priming and might thus not determine protective immunity after a single vaccination (Kastenmuller et al., 2007). The overall amount and composition of antigens produced by MVAΔF1L *in vivo* was efficient enough to mount a cellular and humoral immune response as strong as the parental MVA and was similarly potent to protect against a lethal orthopoxvirus challenge. The effect of an enhanced apoptosis induction on memory phases of an immune response and its impact in a prime/boost regimen, however, still remains to be analyzed.

Besides inhibiting cell autonomous apoptosis, viruses have evolved a variety of strategies to oppose the killing activity of cytotoxic T and NK cells against infected target cells. This strategy, however, does not have an impact on the stimulation of immune cells but rather on different downstream processes of immune recognition. With this regard, F1L could also be responsible for the protection of infected cells from cytolysis during the course of vaccinia virus disease progression. The ability of F1 to prevent bax activation after stimulation of infected cells with TNF-α (Taylor et al., 2006), a pathway attracted by cytotoxic T cells resulting in the killing of target cells, is going in line with this hypothesis. This might be a possible explanation why no significant differences in the induction of T and B cell responses and consequently also no differences in the protection of mice from a lethal orthopoxvirus challenge were measured.

Some poxvirus-encoded anti-apoptotic proteins are implicated in virulence. Deletion of the structural bcl-2 homologues M11L or N1L from the genome of myxoma virus (genus leporipoxviruses) or vaccinia virus, respectively, strongly reduces the virulence of the virus strains *in vivo* (Opgenorth et al., 1992; Bartlett et al., 2002). This led room to speculate if F1 might also represent an orthopoxvirus virulence factor necessary for virus replication and spreading inside the host, a hypothesis not analyzed so far. Future studies using for example ECTV deleted for the F1L homologue could be used to analyse this putative *in vivo* function of F1L.

The obtained data clearly demonstrate that deletion of the strong anti-apoptotic protein F1 alone is not sufficient to alter MVA immunogenicity. On the other hand, for an MVA vaccine, deletion of F1L is possible without loosing its immunogenic potential. Together, these results might even further demonstrate that clearly more detailed informations including *in vivo* analyses are needed to understand the final function of F1L for the virus life cycle,

pathogenesis and virulence. Additionally, careful analysis of other regulatory genes conserved in MVA would likely be required for the design of a most safe, immunogenic and efficient MVA vaccine.

6.2 The vaccinia virus N1 protein is presumably non-functional in MVA

The vaccinia virus N1L ORF encodes a 14 kDa early protein with structural and functional homology to members of the cellular anti-apoptotic bcl-2 family (Cooray et al., 2007; Aoyagi et al., 2007). Additional to its anti-apoptotic action, the N1 protein was implicated to be a potent virulence factor *in vivo* (Bartlett et al., 2002; Billings et al., 2004), since deletion of N1L from the genome of vaccinia virus leads to robust cellular and humoral immune responses and a significant attenuation of the virus in different mouse infection models (Mathew et al., 2008). The N1L ORF is conserved between vaccinia virus and MVA, however, during sequence analysis it was found that the MVA-encoded N1L ORF is composed of the main part of the original N1L and a short 3´ sequence derived from the C5L ORF, which fused in-frame due to deletion of the interjacent sequence during the MVA attenuation process (deletion V). Because of the "unnatural" C-terminus derived from the C5L ORF, functionality of the MVA-encoded N1 was questionable. To prove this possibility, several recombinant MVA variants with deleted (MVAΔN1L) or reinserted (MVA-N1L$_{rev}$ and MVA-WRN1L$_{rev}$) N1L ORFs, derived either from MVA or vaccinia virus WR, respectively, were generated and characterized in this work. No differences concerning growth capacities of the different viruses in permissive and non-permissive cell lines were detected, indicating no alterations in host range due to deletion of N1L or, more importantly, due to reinsertion of the functional WR-related N1L ORF into the genome of MVA.

It was shown that the WR-related N1 protein is able to inhibit induction of apoptosis by the addition of staurosporine in the background of viral infection presumably by binding to several cellular pro-apopototic BH3-only molecules, thereby inhibiting their action (Cooray et al., 2007). However, an apoptosis-inducing phenotype of a vaccinia virus strain deleted for N1L gene function, as it is observed after deletion of F1L, was not discovered so far. After infection of murine NIH-3T3 cells with the N1L-specific MVA-variants generated in this work it was found that the MVA-related ORF is unable to inhibit the induction of apoptosis mediated by the addition of staurosporine, whereas the WR-related ORF was indeed able to block the activation of caspase-3 when reinserted into the MVA genome, confirming the

published data. Therefore, the hypothesis that the MVA-related N1L ORF is non-functional is encouraged by the performed experiments.

Mutated and/or misfolded proteins are often degraded shortly after expression. Expression analysis of N1 revealed that all N1L ORFs encoded by the generated recombinant MVA variants are efficiently transcribed at levels comparable to WR-driven N1L expression after infection of HeLa cells. Interestingly, despite the presence of high amounts of N1L-specific messenger RNA, protein was only produced by the WR-related ORF, no matter if it was expressed by WR or MVA. The degradation of misfolded and/or unfunctional proteins is mediated in most cases by the cellular proteasome. The addition of lactacystin, an irreversible inhibitor of the proteasome, resulted in detectable MVA-related N1 protein after infection, at least to very weak levels, confirming the assumption of a rapid degradation of the MVA-related N1 protein after translation.

The degradation could be caused by the fusion of the unnatural C5 protein-derived C-terminus and/or by the absence of the natural C-terminal N1L-encoded sequence, which may be important for protein integrity and stability. To prove both possibilities, the MVA-related N1L as well as two shortened WR-related N1L variants were expressed in 293T cells and compared to expression of the original WR-related ORF. The natural C-terminal sequence of N1, which is replaced in the MVA genome encodes two α-helical structural motifs (Cooray et al., 2007). Therefore, the expression of N1L variants lacking one or both α-helix-encoding sequences was analyzed in addition to the MVA- and WR-related sequences. Neither the MVA-related nor the truncated gene sequences were able to express a detectable protein in the absence of proteasome inhibition, whereas the WR-related ORF was expressed at high levels. Because of these results it was concluded, that the expression of a stable and functional N1 protein requires the original vaccinia virus WR-related C-terminal sequence and that the MVA-encoded N1L gene is unfunctional due to the replacement of this sequence with parts derived from the C5L ORF. This fact leads to the rapid proteasome-mediated degradation of the protein, presumably due to incorrect protein folding, resulting in remaining protein levels too low to efficiently interact with its proposed partners and therefore with an unability to inhibit the induction of apoptosis.

6.3 The vaccinia virus double-stranded RNA-binding protein E3 does not interfere with siRNA-mediated gene silencing in mammalian cells

Sequence-specific RNAi is an important defence mechanism against invading viruses, pathogens and nucleic acids in plants and invertebrates, because they lack important aspects of the immune system found in higher vertebrates (Tijsterman et al., 2002). However, RNA silencing is also a mechanism for evading viral infection in vertebrates. Multiple virus families have therefore developed strategies to counteract RNAi to ensure viral replication (Haasnoot et al., 2007). Poxviruses have developed a multitude of strategies to evade the host immune response and it seems likely that anti-RNAi directed mechanisms are also in the viral repertoire. The vaccinia virus- and MVA-encoded protein E3 is a favourable candidate for RNAi inhibition due to its dsRNA-binding property. In this regard, it has been shown that expression of the vaccinia virus E3 protein in *Drosophila* cells interferes with RNAi (Li et al., 2004). However, its direct effect in vaccinia virus-infected cells, especially of human origin, remained to be elucidated. Therefore, the application of siRNA-mediated viral gene silencing at early and late stages of the vaccinia virus replication cycle and a possible negative regulatory function of the vaccinia virus dsRNA-binding protein E3 was investigated during this work.

Despite the ability of E3 to sequester dsRNA molecules, the downregulation of an MVA-encoded marker gene was possible by transfection of sequence specific siRNA prior to infection, independent of the presence of E3. The inhibition of dsRNA-induced antiviral responses is especially important during late phases of the vaccinia virus replication cycle, because of the production of high amounts of dsRNA due to incomplete termination of viral late gene transcription. Therefore, it remained possible that E3 exerts its activity mainly at late times after infection due to the presence of E3 in infected cells as long as 24 hours, despite its production at early stages. Additionally, the vaccinia virus-induced shut-down of host protein synthesis, which is also recognized in MVA-infected cells (Moss, 1968; Sutter and Moss, 1992) may have a negative impact on siRNA-mediated gene silencing during late time points of infection (e.g. 12 to 24 hours post infection). Interestingly, siRNA-mediated gene silencing could be induced throughout the whole MVA replication cycle, as the amount of siRNA-mediated downregulation was comparable when the targeted marker gene was expressed at early or late phases of the MVA life cycle. However, RNA interference at late times after infection was only analyzed in the presence of E3, since infection of HeLa cells with MVA

devoid of E3 function leads to an early block in the viral replication cycle, resulting in the absence of late gene expression (Ludwig et al., 2005).

The equal amount of downregulation at early and late time points after infection additionally suggests that the RISC complex including the complementary RNA strand is quite stable and functional over a long period after its synthesis. Once loaded onto the RISC complex, one might speculate that the siRNA is covered by cellular RISC-associated proteins and is, therefore, not accessible to the E3 protein, especially when the siRNA is transfected 24 hours prior to virus infection. The rapid virus-induced shutdown of host cell macromolecular synthesis may inhibit RNAi induced by transfection of siRNA after infection, however, this hypothesis has still to be analyzed.

The discrepancy with the published data (Li et al., 2004), in which E3 was shown to inhibit siRNA-mediated RNAi in insect cells, is presumably due to the different cellular systems used. Likewise, the influenza viral protein NS1 has been described in the same publication to have a negative regulatory role in RNA silencing in insect cells (Li et al., 2004), but recent data clearly shows that NS1 does not suppress RNAi in mammalian cells (Kok and Jin, 2006). Moreover, it was recently suggested that in mammalian cells RNA interference as a first-line anti-viral defense system seems to be replaced by the potent interferon system. Interestingly, the vaccinia virus E3 protein is known as interferon-resistance gene due to its inhibitory capacity on interferon-induced antiviral pathways in mammalian cells. Virally encoded suppressors of RNA silencing in insect cells, like the E3 or NS1 protein, may have their specificity for siRNA mainly coincidental (Cullen, 2006).

Our data clearly show the potential of siRNA to study vaccinia virus gene functions at all stages of viral replication. Moreover, we were able to confirm a previously determined phenotype of an MVA-E3L deletion mutant by using a siRNA directed against E3L-specific mRNA. Downregulation of E3 protein function using siRNA leads to a decrease of viral late gene expression in HeLa cells, mimicking the early block during the viral life cycle after infection of HeLa cells with MVAΔE3L. The exploitation of the RNAi machinery may therefore be a tool for the analysis of vaccinia virus gene functions. The interference with essential viral genes might even be used in a therapeutic setting. In with this, Dave and co-workers showed recently that inhibition of E3L gene expression by siRNA can be used to block vaccinia virus replication in human cells (Dave et al., 2006).

The results clearly show that siRNA-mediated downregulation of a MVA-encoded marker gene is possible at both early and late time points of infection and the E3 protein does not suppress RNAi.

6.4 Concluding remarks – Outlook

The retainment of several anti-apoptotic gene functions in the genome of the highly attenuated vaccinia virus strain MVA highlights the importance of inhibition of programmed cell death after viral infection. For a better molecular analysis of these gene functions and for a possible improvement of MVA as a vaccine, single anti-apoptotic genes were deleted from the MVA genome. It is possible that deletion of distinct apoptosis-inhibiting gene functions from the genome of MVA can have different effects on viral replication and immunmodulatory functions. No alterations concerning host range or viral replication was observed when F1L or N1L were deleted from the genome of MVA, whereas deletion of E3L led to clear alterations in the viral life cycle of MVA and vaccinia virus Copenhagen (Ludwig et al., 2006; Hornemann et al., 2003; Beattie et al.,1996).

The structural homology of F1 and N1 to cellular anti-apoptotic bcl-2 family members is representative for their ability to effectively inhibit the induction of apoptosis. As N1 is already described *in vivo* as an important virulence factor (Bartlett et al., 2002; Billings et al., 2004), nothing is known about the *in vivo* function of F1. Thus, the influence of F1 on MVA immunogenicity was analyzed in this work. Immunization of mice with an MVA vaccine devoid of the F1L ORF leads to the induction of an effective immune response comparable to wild type MVA immunization and equal protection against a highly lethal orthopoxvirus challenge. Interestingly, a further anti-apoptotic protein structurally related to F1, encoded by a leporipoxvirus, the myxoma M11L gene, was also implicated in virus virulence *in vivo* (Opgenorth et al., 1992). It therefore remains to be elucidated with replication-competent vaccinia virus, if the F1L encoded gene function has a possible role in virus virulence *in vivo*.

The final molecular mechanisms by which poxvirus-encoded anti-apoptotic proteins influence aspects of a virus-specific immune response obviously need further investigations. Due to the conservation of several anti-apoptotic genes, exerting their functions at different points of the cellular apoptotic machinery, and the action of multiple viral immunomodulatory proteins working together to subvert an antiviral response, the deletion of one gene function presumably can be compensated in most cases. Therefore, to finally prove the influence of apoptosis-inhibition on *in vivo* immunogenicity of poxviruses, multiple strategies, e.g. multiple deletions of anti-apoptotic gene functions from the genome of vaccinia virus strains with subsequent analysis of viral immunogenicity, have to be analyzed in parallel.

7 Literature

Ackerman, A. L. and P. Cresswell. "Cellular mechanisms governing cross-presentation of exogenous antigens." Nat.Immunol. 5.7 (2004): 678-84.

Albert, M. L. "Death-defying immunity: do apoptotic cells influence antigen processing and presentation?" Nat.Rev.Immunol. 4.3 (2004): 223-31.

Antoine, G., et al. "The complete genomic sequence of the modified vaccinia Ankara strain: comparison with other orthopoxviruses." Virology 244.2 (1998): 365-96.

Aoyagi, M., et al. "Vaccinia virus N1L protein resembles a B cell lymphoma-2 (Bcl-2) family protein. Protein Sci. 16(1) (2007): 118-24

Baroudy, B. M., S. Venkatesan, and B. Moss. "Incompletely base-paired flip-flop terminal loops link the two DNA strands of the vaccinia virus genome into one uninterrupted polynucleotide chain." Cell 28.2 (1982): 315-24.

Bartlett, N., et al. "The vaccinia virus N1L protein is an intracellular homodimer that promotes virulence." J.Gen.Virol. 83.Pt 8 (2002): 1965-76.

Beattie, E., et al. "Host-range restriction of vaccinia virus E3L-specific deletion mutants." Virus Genes 12.1 (1996): 89-94.

Billings, B., et al. "Lack of N1L gene expression results in a significant decrease of vaccinia virus replication in mouse brain." Ann.N.Y.Acad.Sci. 1030 (2004): 297-302.

Carroll, M. W. and B. Moss. "Host range and cytopathogenicity of the highly attenuated MVA strain of vaccinia virus: propagation and generation of recombinant viruses in a nonhuman mammalian cell line." Virology 238.2 (1997): 198-211.

Carter, G. C., et al. "Entry of the vaccinia virus intracellular mature virion and its interactions with glycosaminoglycans." J.Gen.Virol. 86.Pt 5 (2005): 1279-90.

Chang, H. W. and B. L. Jacobs. "Identification of a conserved motif that is necessary for binding of the vaccinia virus E3L gene products to double-stranded RNA." Virology 194.2 (1993): 537-47.

Chang, H. W., J. C. Watson, and B. L. Jacobs. "The E3L gene of vaccinia virus encodes an inhibitor of the interferon-induced, double-stranded RNA-dependent protein kinase." Proc.Natl.Acad.Sci.U.S.A 89.11 (1992): 4825-29.

Cooray, S., et al. "Functional and structural studies of the vaccinia virus virulence factor N1 reveal a Bcl-2-like anti-apoptotic protein." J.Gen.Virol. 88.Pt 6 (2007): 1656-66.

Cosma, A., et al. "Neutralization assay using a modified vaccinia virus Ankara vector expressing the green fluorescent protein is a high-throughput method to monitor the humoral immune response against vaccinia virus." Clin Diagn Lab Immunol 11.2 (2004): 406-10.

Coulibaly, S., et al. "The nonreplicating smallpox candidate vaccines defective vaccinia Lister (dVV-L) and modified vaccinia Ankara (MVA) elicit robust long-term protection." Virology 341.1 (2005): 91-101.

Cullen, B. R. "Is RNA interference involved in intrinsic antiviral immunity in mammals?" Nat.Immunol. 7.6 (2006): 563-67.

Damon, I. K. "Poxviruses." Fields Virology. Ed. D. M. Knipe and P. M. Howley. 5th Edition ed. Lippincott Williams & Wilkins, 2007. 2948-75.

Dave, R. S., et al. "siRNA targeting Vaccinia virus double-stranded RNA binding protein [E3L] exerts potent antiviral effects." Virology 348.2 (2006): 489-97.

Drexler, I., C. Staib, and G. Sutter. "Modified vaccinia virus Ankara as antigen delivery system: how can we best use its potential?" Curr.Opin.Biotechnol. 15.6 (2004): 506-12.

Dykxhoorn, D. M. and J. Lieberman. "The silent revolution: RNA interference as basic biology, research tool, and therapeutic." Annu.Rev.Med. 56 (2005): 401-23.

Dykxhoorn, D. M., C. D. Novina, and P. A. Sharp. "Killing the messenger: short RNAs that silence gene expression." Nat.Rev.Mol.Cell Biol. 4.6 (2003): 457-67.

Fire, A. Z. "Gene silencing by double-stranded RNA." Cell Death.Differ. 14.12 (2007): 1998-2012.

Fischer, S. F., et al. "Modified vaccinia virus Ankara protein F1L is a novel BH3-domain-binding protein and acts together with the early viral protein E3L to block virus-associated apoptosis." Cell Death.Differ. 13.1 (2006): 109-18.

Fonteneau, J. F., et al. "Characterization of the MHC class I cross-presentation pathway for cell-associated antigens by human dendritic cells." Blood 102.13 (2003): 4448-55.

Frey, S. E., et al. "Clinical and immunologic responses to multiple doses of IMVAMUNE (Modified Vaccinia Ankara) followed by Dryvax challenge." Vaccine 25.51 (2007): 8562-73.

Garcia, M. A., et al. "Anti-apoptotic and oncogenic properties of the dsRNA-binding protein of vaccinia virus, E3L." Oncogene 21.55 (2002): 8379-87.

Garon, C. F., E. Barbosa, and B. Moss. "Visualization of an inverted terminal repetition in vaccinia virus DNA." Proc.Natl.Acad.Sci.U.S.A 75.10 (1978): 4863-67.

Gasteiger, G., et al. "Cross-priming of cytotoxic T cells dictates antigen requisites for modified vaccinia virus Ankara vector vaccines." J.Virol. 81.21 (2007): 11925-36.

Gavin, M. A., et al. "Alkali hydrolysis of recombinant proteins allows for the rapid identification of class I MHC-restricted CTL epitopes." J.Immunol. 151.8 (1993): 3971-80.

Haasnoot, J., E. M. Westerhout, and B. Berkhout. "RNA interference against viruses: strike and counterstrike." Nat.Biotechnol. 25.12 (2007): 1435-43.

Hawkridge, T., et al. "Safety and immunogenicity of a new tuberculosis vaccine, MVA85A, in healthy adults in South Africa." J.Infect.Dis. 198.4 (2008): 544-52.

Hengartner, M. O. "The biochemistry of apoptosis." Nature 407.6805 (2000): 770-76.

Hornemann, S., et al. "Replication of modified vaccinia virus Ankara in primary chicken embryo fibroblasts requires expression of the interferon resistance gene E3L." J Virol 77.15 (2003): 8394-407.

Kastenmüller, W., et al. "Cross-competition of CD8+ T cells shapes the immunodominance hierarchy during boost vaccination." J.Exp.Med. 204(9) (2007): 2187-98

Kettle, S., et al. "Vaccinia virus serpin B13R (SPI-2) inhibits interleukin-1beta-converting enzyme and protects virus-infected cells from TNF- and Fas-mediated apoptosis, but does not prevent IL-1beta-induced fever." J.Gen.Virol. 78 (Pt 3) (1997): 677-85.

Kibler, K. V., et al. "Double-stranded RNA is a trigger for apoptosis in vaccinia virus-infected cells." J.Virol. 71.3 (1997): 1992-2003.

Kim, T. W., et al. "Enhancing DNA vaccine potency by coadministration of DNA encoding antiapoptotic proteins." J.Clin.Invest 112.1 (2003): 109-17.

Kok, K. H. and D. Y. Jin. "Influenza A virus NS1 protein does not suppress RNA interference in mammalian cells." J.Gen.Virol. 87.Pt 9 (2006): 2639-44.

Kotwal, G. J., A. W. Hugin, and B. Moss. "Mapping and insertional mutagenesis of a vaccinia virus gene encoding a 13,800-Da secreted protein." Virology 171.2 (1989): 579-87.

Lee, S. B. and M. Esteban. "The interferon-induced double-stranded RNA-activated protein kinase induces apoptosis." Virology 199.2 (1994): 491-96.

Li, W. X., et al. "Interferon antagonist proteins of influenza and vaccinia viruses are suppressors of RNA silencing." Proc.Natl.Acad.Sci.U.S.A 101.5 (2004): 1350-55.

Liu, L., R. Chavan, and M. B. Feinberg. "Dendritic cells are preferentially targeted among hematolymphocytes by Modified Vaccinia Virus Ankara and play a key role in the induction of virus-specific T cell responses in vivo." BMC.Immunol. 9 (2008): 15.

Ludwig, H., et al. "Role of viral factor E3L in modified vaccinia virus ankara infection of human HeLa Cells: regulation of the virus life cycle and identification of differentially expressed host genes." J.Virol. 79.4 (2005): 2584-96.

Ludwig, H., et al. "Double-stranded RNA-binding protein E3 controls translation of viral intermediate RNA, marking an essential step in the life cycle of modified vaccinia virus Ankara." J.Gen.Virol. 87.Pt 5 (2006): 1145-55.

Mathew, A., et al. "Robust intrapulmonary CD8 T cell responses and protection with an attenuated N1L deleted vaccinia virus." PLoS.ONE. 3.10 (2008): e3323.

Mayr, A., V. Hochstein-Mintzel, and H. Stickl. "Abstammung, Eigenschaften und Verwendung des attenuierten Vaccinia-Stammes MVA." Infection 3 (1975): 6-14.

Mayr, A., et al. "[The smallpox vaccination strain MVA: marker, genetic structure, experience gained with the parenteral vaccination and behavior in organisms with a debilitated defence mechanism (author's transl)]." Zentralbl.Bakteriol.[B] 167.5-6 (1978): 375-90.

McFadden, G. "Poxvirus tropism." Nat.Rev.Microbiol. 3.3 (2005): 201-13.

Meisinger-Henschel, C., et al. "Genomic sequence of chorioallantois vaccinia virus Ankara, the ancestor of modified vaccinia virus Ankara." J.Gen.Virol. 88.Pt 12 (2007): 3249-59.

Meyer, H., et al. "Mapping of deletions in the genome of the highly attenuated vaccinia virus MVA and their influence on virulence." J.Gen.Virol. 72.Pt 5 (1991): 1031-38

Mercer, J. and A. Helenius. "Vaccinia virus uses macropinocytosis and apoptotic mimicry to enter host cells." Science 320.5875 (2008): 531-35.

Monu, N. and E. S. Trombetta. "Cross-talk between the endocytic pathway and the endoplasmic reticulum in cross-presentation by MHC class I molecules." Curr.Opin.Immunol. 19.1 (2007): 66-72.

Moss, B. "Inhibition of HeLa cell protein synthesis by the vaccinia virion." J.Virol. 2.10 (1968): 1028-37.

Moss, B. "Poxviridae: The Viruses and Their Replication." Fields Virology. Ed. D. M. Knipe and P. M. Howley. 5th Edition ed. Lippincott Williams & Wilkins, 2007. 2906-45.

Moutaftsi, M., et al. "A consensus epitope prediction approach identifies the breadth of murine T(CD8+)-cell responses to vaccinia virus." Nat.Biotechnol. 24.7 (2006): 817-19.

Opgenorth, A., et al. "Deletion analysis of two tandemly arranged virulence genes in myxoma virus, M11L and myxoma growth factor." J.Virol. 66.8 (1992): 4720-31.

Paran, N., et al. "Postexposure Immunization with Modified Vaccinia Virus Ankara or Conventional Lister Vaccine Provides Solid Protection in a Murine Model of Human Smallpox." J.Infect.Dis. (2009).

Perez-Jimenez, E., et al. "MVA-LACK as a safe and efficient vector for vaccination against leishmaniasis." Microbes.Infect. 8.3 (2006): 810-22.

Pogo, B. G. and S. Dales. "Two deoxyribonuclease activities within purified vaccinia virus." Proc.Natl.Acad.Sci.U.S.A 63.3 (1969): 820-27.

Postigo, A., et al. "Interaction of F1L with the BH3 domain of Bak is responsible for inhibiting vaccinia-induced apoptosis." Cell Death.Differ. 13.10 (2006): 1651-62.

Reynolds, A., et al. "Rational siRNA design for RNA interference." Nat.Biotechnol. 22.3 (2004): 326-30.

Rivas, C., et al. "Vaccinia virus E3L protein is an inhibitor of the interferon (i.f.n.)-induced 2-5A synthetase enzyme." Virology 243.2 (1998): 406-14.

Roulston, A., R. C. Marcellus, and P. E. Branton. "Viruses and apoptosis." Annu.Rev.Microbiol. 53 (1999): 577-628.

Samuelsson, C., et al. "Survival of lethal poxvirus infection in mice depends on TLR9, and therapeutic vaccination provides protection." J.Clin.Invest 118.5 (2008): 1776-84.

Sliva, K. and B. S. Schnierle. "Stable integration of a functional shRNA expression cassette into the murine leukemia virus genome." Virology 351.1 (2006): 218-25.

Smith, G. L. "Vaccinia virus immune evasion." Immunol.Lett. 65.1-2 (1999): 55-62.

Staib, C., et al. "Transient host range selection for genetic engineering of modified vaccinia virus Ankara." Biotechniques 28.6 (2000): 1137-42.

Staib, C., et al. "Improved host range selection for recombinant modified vaccinia virus Ankara." Biotechniques 34.4 (2003): 694-6.

Stetson, D. B. and R. Medzhitov. "Type I interferons in host defense." Immunity. 25.3 (2006): 373-81.

Sutter, G. and B. Moss. "Nonreplicating vaccinia vector efficiently expresses recombinant genes." Proc Natl Acad Sci U S A 89.22 (1992): 10847-51.

Sutter, G. and C. Staib. "Vaccinia vectors as candidate vaccines: the development of modified vaccinia virus Ankara for antigen delivery." Curr Drug Targets Infect Disord 3.3 (2003): 263-71.

Taylor, J. M. and M. Barry. "Near death experiences: poxvirus regulation of apoptotic death." Virology 344.1 (2006): 139-50.

Taylor, J. M., et al. "The vaccinia virus protein F1L interacts with Bim and inhibits activation of the pro-apoptotic protein Bax." Journal of Biological Chemistry 281.51 (2006): 39728-39.

Taylor, R. C., S. P. Cullen, and S. J. Martin. "Apoptosis: controlled demolition at the cellular level." Nat.Rev.Mol.Cell Biol. 9.3 (2008): 231-41.

Tijsterman, M., R. F. Ketting, and R. H. Plasterk. "The genetics of RNA silencing." Annu.Rev.Genet. 36 (2002): 489-519.

Tscharke, D. C., et al. "Identification of poxvirus CD8+ T cell determinants to enable rational design and characterization of smallpox vaccines." J.Exp.Med. 201.1 (2005): 95-104.

Tuschl, T. "Expanding small RNA interference." Nat Biotechnol 20.5 (2002): 446-8.

Waibler, Z., et al. "Modified vaccinia virus Ankara induces Toll-like receptor-independent type I interferon responses." J.Virol. 81.22 (2007): 12102-10.

Wasilenko, S. T., et al. "The vaccinia virus F1L protein interacts with the proapoptotic protein Bak and inhibits Bak activation." J.Virol. 79.22 (2005): 14031-43.

Wasilenko, S. T., et al. "Vaccinia virus encodes a previously uncharacterized mitochondrial-associated inhibitor of apoptosis." Proc Natl Acad Sci U S A 100.24 (2003): 14345-50.

Wittek, R. and B. Moss. "Tandem repeats within the inverted terminal repetition of vaccinia virus DNA." Cell 21.1 (1980): 277-84.

Xu, R., et al. "Cellular and humoral immunity against vaccinia virus infection of mice." J.Immunol. 172.10 (2004): 6265-71.

Erklärung

Hiermit erkläre ich, Markus Lantermann, geboren am 7. August 1977 in Groß-Gerau/Hessen, dass ich die vorliegende Arbeit selbständig und nur mit den angegebenen Hilfsmitteln und Quellen angefertigt habe. Diese Arbeit wurde bisher nicht als Prüfungsarbeit für eine andere Prüfung und ebenso nicht als Dissertation bei einer anderen Fakultät oder einem anderen Fachbereich eingereicht.

Groß-Gerau, Oktober 2009

_____
(Markus Lantermann)

Teile dieser Arbeit wurden wie folgt veröffentlicht:

Lantermann M., Schwantes A., Sliva K., Sutter G. and Schnierle B. - "Vaccinia virus double-stranded RNA-binding protein E3 does not interfere with siRNA-mediated gene silencing in mammalian cells"
Virus Research 126 (2007) 1-8

Lantermann M., Süzer Y., Schippers T., Ludwig H., Schwantes A. and Sutter G. - "Modified vaccinia virus Ankara deficient in anti-apoptotic protein F1 function efficiently provides protective immunity against lethal orthopoxvirus challenge"
In Vorbereitung